

Performance and Power Factor Improvement of Indirect Vector Controlled Cage Induction Generator in Wind Power Application

SWAGAT PATI



DEPARTMENT OF ELECTRICAL ENGINEERING
NATIONAL INSTITUTE OF TECHNOLOGY, ROURKELA
JULY 2011

Performance and Power Factor Improvement of Indirect Vector Controlled Cage Induction Generator in Wind Power Application

A Thesis Submitted in Partial Fulfillment of the Requirements for the Degree of

*Master of Technology (Research)
in
Electrical Engineering*

By

Swagat pati
Roll No: 608EE104

Under the Supervision of
Dr. K.B.Mohanty
(Associate Professor)



Department of Electrical Engineering
National Institute of Technology
Rourkela
July 2011

ABSTRACT

Wind energy is one of the most important and promising source of renewable energy all over the world, mainly because it is considered to be nonpolluting and economically viable. At the same time there has been a rapid development of related wind energy technology. The control and estimation of wind energy conversion system constitute a vast subject and are more complex than those of dc drives. Induction generators with cage type rotors have been used extensively in wind power generation systems for the variable speed applications in a wide power range. Generally, variable speed wind energy conversion system with Induction generators require both wide operating range of speed and fast torque response, regardless of any disturbances and uncertainties (turbine torque variation, parameters variation and un-modeled dynamics). This leads to more advanced control methods to meet the real demand. The recent advances in the area of field-oriented control along with the rapid development and cost reduction of power electronics devices and microprocessors have made variable speed wind energy conversion system an economical alternative for wind power applications. The complexity of wind energy conversion system increases substantially if high performances are demanded. The main reasons for this complexity are the need of variable frequency, harmonically optimum converter power supplies, the complex dynamics of ac machines, machine parameter variations etc. Various control techniques have been developed in the recent days for the control of cage induction generators. In this work a hybrid controller is developed for performance improvement of a cage induction generator used for wind power applications. The wind power generation system employs an indirect vector controlled cage induction machine as the generator. The induction generator system is evaluated separately with conventional PI-controllers, fuzzy controllers, self tuned fuzzy controllers and hybrid controllers and the performances are compared for each case. Power factor of the overall system is improved through control of grid side converter. Control circuits for PWM converter inverter system are also fabricated and tested.



**National Institute of Technology
Rourkela**

CERTIFICATE

This is to certify that the thesis entitled “Performance and Power Factor Improvement of Indirect Vector Controlled Cage Induction Generator in Wind Power Application” submitted by **Mr. Swagat Pati**, in partial fulfillment of the requirements for the award of Master of Technology (Research) in Electrical Engineering, at National Institute of Technology, Rourkela (Deemed University) is an authentic work carried out by him under my supervision and guidance.

To the best of my knowledge, the matter presented in the thesis has not been submitted to any other University/Institute for the award of any Degree or Diploma.

Date:

Place: NIT Rourkela

**Dr. K.B.Mohanty
(Associate Professor)**

Department of Electrical Engineering
National Institute of Technology
Rourkela-769008

Email: kbmohanty@nitrrkl.ac.in

ACKNOWLEDGEMENT

I have been very fortunate in having Dr. K.B.Mohanty, Associate Professor, Department of Electrical Engineering, National Institute of Technology, Rourkela as my thesis supervisor. He inspired me to develop interest in Wind Energy Systems, taught me essence and principle of research and guided me through the completion of this thesis work. Working with Prof. K.B.Mohanty is highly enjoyable, inspiring and rewarding experience. I am highly indebted to him and express my deep sense of gratitude for his guidance and support.

I humbly acknowledge the valuable suggestions and constructive criticism of Prof. B.D. Shubudhi, Prof. S. K Sahoo and Prof. S.K.Behera while scrutinizing my research results.

I am highly indebted to the authorities of NIT, Rourkela for providing me various facilities like library, computers and Internet, which have been very useful.

I express special thanks to all my friends, for being there whenever I needed them. Thank you very much Kamalesh, Srinivas, Basant, Amit and Benu.

Finally, I am forever indebted to my sister and my loving parents for their understanding and encouragement when it was most required.

I dedicate this thesis to my family and friends.

Swagat Pati

CONTENTS

<i>Abstract</i>	I
<i>Certificate</i>	II
<i>Acknowledgement</i>	III
<i>Content</i>	IV
1 INTRODUCTION	01
1.1 Background	01
1.2 Wind turbine system	02
1.2.1 Power contained in wind	02
1.2.2 Types of wind conversion devices	02
1.2.3 Working of modern wind turbines	03
1.2.4 Important terms related to wind power generation	10
1.2.5 Wind turbine characteristics	13
1.2.6 Wind turbine control system	18
1.3 Wind power conversion system	23
1.3.1 Fixed speed wind turbines	23
1.3.2 Variable speed wind turbines	24
1.4 Generators for wind power applications	25
1.4.1 Squirrel cage induction machine	25
1.4.2 Wound rotor induction machine	26
1.4.3 Permanent magnet synchronous machine	27
1.5 Self excited and line excited induction generators	27
1.5.1 Self excited induction generators	28
1.5.2 Line excited induction generators	28
1.6 Control of line excited cage induction generators	29
1.7 Motivation	32
1.8 Objectives	32
1.9 Organization of the thesis	33

2.	D-Q MODELING AND VECTOR CONTROL OF INDUCTION GENERATOR	35
2.1	Introduction	35
2.2	Axes transformation	36
2.3	D-Q model of induction machine (kron's equation)	38
2.4	Vector or field oriented control	46
2.4.1	Equivalent circuit and phasor diagram	48
2.4.2	Principle of vector control	50
2.5	Conclusion	51
3.	INDIRECT VECTOR CONTROL OF CAGE INDUCTION GENERATOR	52
3.1	Introduction	52
3.2	Indirect vector control of induction generator	53
3.3	Simulation results and discussion	56
3.3.1	Step change in turbine torque	56
3.3.2	Step change in reference speed command	59
3.4	Conclusion	62
4.	PERFORMANCE IMPROVEMENT OF FIELD ORIENTED INDUCTION GENERATOR USING MODERN CONTROLLERS	63
4.1	Introduction	63
4.2	Fuzzy controller	64
4.2.1	Introduction	64
4.2.2	Fuzzy set	64
4.2.3	Membership function	65
4.2.4	Fuzzy systems	68
4.2.5	Design of fuzzy logic controller	73
4.3	Self tuned fuzzy logic controller	79
4.3.1	Introduction	79
4.3.2	Tuning procedure	79
4.3.3	Self tuned fuzzy logic controller design	82

4.4	Hybrid controller	88
4.4.1	Introduction	88
4.4.2	Design principles for Hybrid controller	89
4.5	Result and discussion	94
4.5.1	Simulation with a step change in turbine torque	94
4.5.2	Simulation with a step change in reference speed	106
4.6	Conclusion	113
5.	VECTOR CONTROL OF GRID SIDE PWM CONVERTER FOR POWER FACTOR IMPROVEMENT	114
5.1	Introduction	114
5.2	Maximum power point tracking	114
5.3	Supply side converter control	116
5.4	Result and discussion	122
5.5	Conclusion	132
6.	FABRICATION AND TESTING OF CONTROL CIRCUIT FOR A BIDIRECTIONAL CONVERTER- INVERTER SET USED IN LINE EXCITED INDUCTION GENERATOR	133
6.1	Introduction	133
6.2	Power electronic converters	134
6.3	Control circuit for VSI	135
6.3.1	Triangular wave generator circuit	136
6.3.2	Three phase reference sine wave generator	137
6.3.3	Comparator circuit	138
6.3.4	Lockout circuit	138
6.3.5	Over current protection circuit	141
6.3.6	Gate drive circuit	141
6.4	Fabricated circuits and test results	143
6.5	Conclusion	147
7.	CONCLUSION AND SCOPE FOR FUTURE WORK	148
7.1	Conclusion	148
7.2	Scope for future work	150

8.	REFERENCES	151
9.	APPENDIX-1	154
10.	APPENDIX-2	155
11.	APPENDIX-3	157

Chapter 1

Introduction

1.1 BACKGROUND

In last 100 years, the human civilization has gone too far in exploiting the limited resources on earth, making the biosphere vulnerable to many uncertain large scale disasters. Many of such crises are due to the limited resource for the generation of electrical power. The depletion of fossil fuels such as coal and oil and rapidly increasing demand of electrical energy, has led to a world-wide interest in developing wind power plants. Wind is a free, clean, and inexhaustible energy source. It has served mankind well for many centuries by propelling ships and driving wind turbines to grind grain and pump water. Interest in wind power lagged, however, when cheap and plentiful petroleum products became available after World War II. The high capital costs and the uncertainty of the wind placed wind power at an economic disadvantageous position. In the past four decades methods of harnessing hydro and wind energy for electric power generation and the technology for such alternate systems are developed. Continuous research is going on taking into account different critical issues in this sector. Wind energy is one of the most important and promising source of renewable energy all over the world, mainly because it is considered to be nonpolluting and economically viable. At the same time there has been a rapid development of related wind energy technology. However in the last two decades,

wind power has been seriously considered to supplement the power generation by fossil fuel and nuclear methods.

1.2 WIND TURBINE SYSTEM

1.2.1 POWER CONTAINED IN WIND

The power contained in wind is given by the kinetic energy of the flowing air mass per unit time. That is,

$$P_0 = \frac{1}{2}(\text{air mass per unit time})(\text{wind velocity})^2$$

Hence
$$P_0 = \frac{1}{2}(\rho A V_\infty)(V_\infty)^2$$

$$= \frac{1}{2}\rho A V_\infty^3 \quad (1.1)$$

where P_0 is the power contained in wind(in watts), ρ is the air density ($\approx 1.225 \text{ kg/m}^3$ at 15°C and normal pressure), A is the rotor area in m^2 and V_∞ is the wind velocity (in m/sec) without rotor interference, i.e., ideally at infinite distance from the rotor.

1.2.2 TYPES OF WIND CONVERSION DEVICES

Wind energy conversion devices can be broadly categorized into two types according to their axis alignments: horizontal axis wind turbines and vertical axis wind turbines.

- *Horizontal axis wind turbines* can be further divided into three types.
 - ‘Dutch type’ grain grinding windmills
 - Multiblade water pumping windmills
 - High-speed propeller type windmills

- *Vertical axis wind turbines* come in two different designs
 - The Savonius rotor
 - The Darrieus rotor

1.2.3 WORKING OF MODERN WIND TURBINES

In recent days high speed propeller type wind turbines are mostly used as horizontal axis wind turbines due to their excellent aerodynamic efficiency. Among the vertical axis wind turbines the Darrieus rotor is more efficient than the Savonius rotor, but the major drawback of the Darrieus rotor is that it is not self starting. The Savonius rotor is simple and inexpensive, but its efficiency is less than the Darrieus rotor. Figure 1.1 shows the different types of advanced wind turbines.



(a)



(b)



(c)

Figure 1.1 *Different types of wind turbines used in recent days (a) Horizontal axis high speed propeller type wind turbine (b) Savonius rotor (c) Darrieus rotor*

1.2.3.1 High speed propeller type wind turbines

High speed propeller type wind turbines are mostly used for wind power generation. These turbines do not operate on thrust force, rather they depend mainly upon the aerodynamic forces that develop when wind flows around the blade of aerofoil design. To understand how a modern wind turbine works, first we have to understand the aerodynamics of the aerofoil design. Figure 1.2 shows the different forces acting upon the aerofoil.

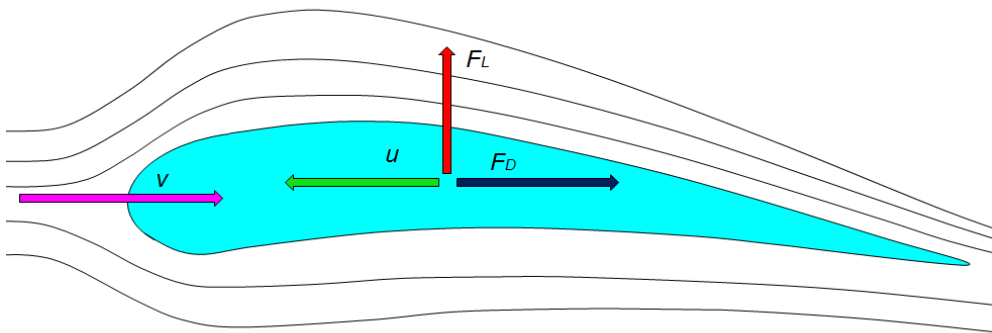


Figure 1.2 *Forces acting upon the aerofoil*

Consider an aerofoil moving in the wind stream with a velocity ' u ' and the wind velocity being ' v '. The wind stream at the top of the aerofoil has to traverse a longer path than that at the bottom, leading to a difference in velocities which gives rise to a difference in pressure from which a lift force results and comes another force called the drag force which tries to push the aerofoil back in the direction of wind. The aggregate force on the aerofoil is then determined by the resultant of these two forces.

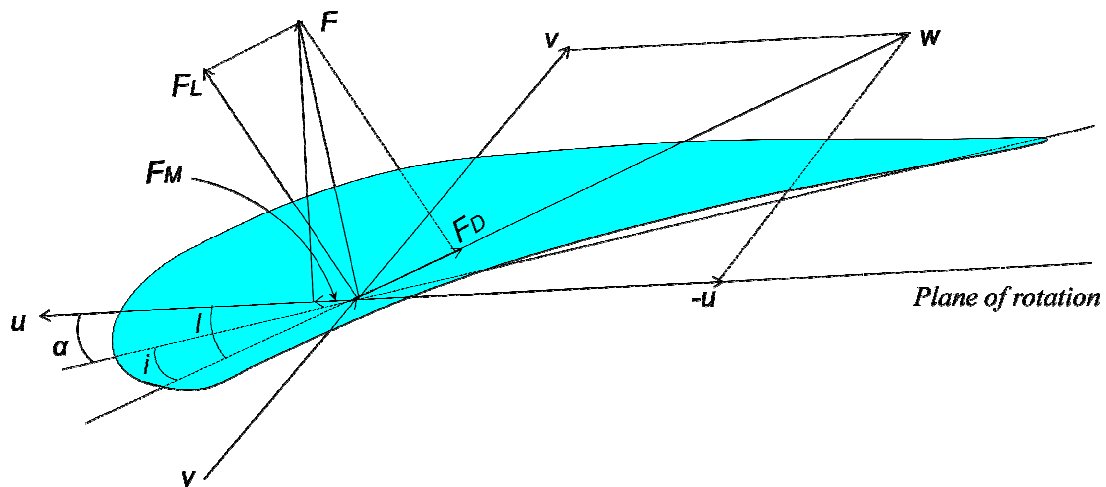


Figure 1.3 Forces acting upon the aerofoil when wind and aerofoil velocities are not along the same line

But when the aerofoil and the wind do not move along the same line then these forces are determined by the wind speed as seen by the aerofoil, called the relative wind 'w'. The relative wind is given by the vector sum of the wind velocity and the negative of the aerofoil velocity as shown in Figure 1.3. the lift force F_L will now be perpendicular to the relative wind, the drag force F_D will be parallel to it. The magnitude of these two forces will be proportional to the square of the relative wind velocity. From Figure 1.3 we can see that the lift force and the drag force have opposing components along the direction of motion. If the lift force dominates the drag, there will be a resultant force along the direction of motion, giving a positive push to it. In fact this is the force that creates the torque in the modern wind turbines. The blades are of aerofoil section, which move along the stream of wind. They are also aligned so that the drag force is minimized, and this gives the blade a net positive torque.

There will of course be another component of the two forces that is perpendicular to the direction of blade motion this force is called the thrust force. This force tries to topple the tower and is a problem at high speeds.

1.2.3.2 The Savonius rotor

The Savonius rotor is an extremely simple vertical axis device that works entirely because of the thrust force of the wind. Aerodynamically they are thrust-type devices, consisting of two or three scoops. Looking down on the rotor from above, a two-scoop machine would look like an "S" shape in cross section as shown in the Figure 1.4. Because of the curvature, the scoops experience less drag when moving against the wind than when moving with the wind. The differential drag causes the Savonius turbine to spin. Because they are drag-type devices, Savonius turbines extract much less of the wind's power than other similarly-sized lift-type turbines. Much of the swept area of a Savonius rotor is near the ground, making the overall energy extraction less effective due to lower wind speed at lower heights.

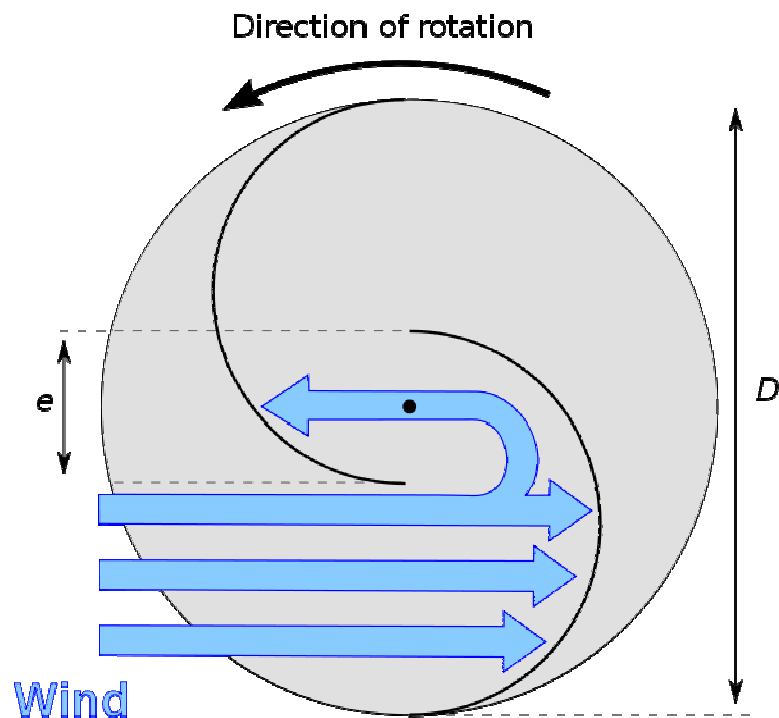


Figure 1.4 *Top view of a Savonius rotor*

The Savonius rotor is simple and inexpensive, and the material required for it is available in any rural area, enabling on site construction of such wind mills. However its utility is limited because of its relatively low efficiency.

1.2.3.3 The Darrieus rotor

In the original versions of the Darrieus design, the aerofoils are arranged so that they are symmetrical and have zero rigging angles, that is, the angle that the aerofoils are set relative to the structure on which they are mounted. This arrangement is equally effective no matter, which direction the wind is blowing in contrast to the conventional type, which must be rotated to face into the wind.

When the Darrieus rotor is spinning, the aerofoils are moving forward through the air in a circular path. Relative to the blade, this oncoming airflow is added vectorially to the wind, so that the resultant airflow creates a varying small positive angle of attack to the blade. This generates a net force pointing obliquely forward along a certain 'line-of-action'. This force can be projected inwards past the turbine axis at a certain distance, giving a positive torque to the shaft, thus helping it to rotate in the direction it is already travelling in.

As the aerofoil moves around the back of the apparatus, the angle of attack changes to the opposite sign, but the generated force is still obliquely in the direction of rotation, because the wings are symmetrical and the rigging angle is zero. The rotor spins at a rate unrelated to the wind speed, and usually many times faster. The energy arising from the torque and speed may be extracted and converted into useful power by using an electrical generator. Figure 1.5 shows the forces acting upon the blades at different blade positions.

The aeronautical terms lift and drag are, strictly speaking, forces across and along the approaching net relative airflow respectively, so they are not useful here. We really want to know the tangential force pulling the blade around, and the radial force acting against the bearings.

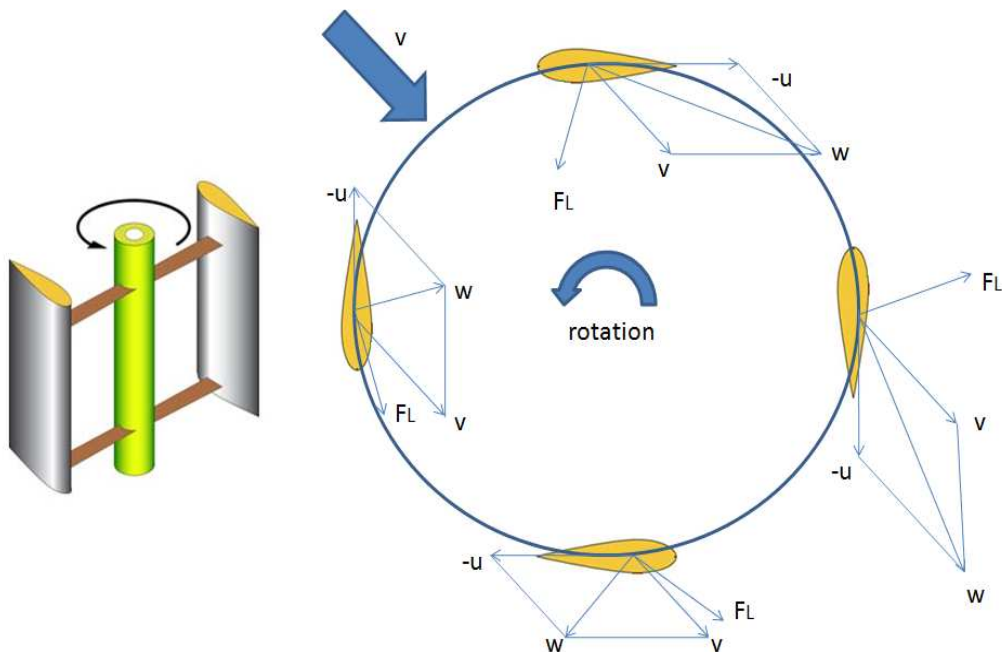


Figure 1.5 Forces acting upon the blades of Darrieus rotor at different positions

When the rotor is stationary, no net rotational force arises, even if the wind speed rises quite high the rotor must already be spinning to generate torque. Thus the design is not normally self starting. The starting torque is generally provided by an electrical machine, which initially runs as a motor, but later changes to the generator mode as the Darrieus rotor starts, generating power.

The Darrieus design is theoretically less expensive than a conventional type, as most of the stress is in the blades which provide torque to the generator located at the bottom of the turbine. The only forces that need to be balanced out vertically are the compression load due to the blades flexing outward (thus attempting to "squeeze" the tower), and the wind force trying to

blow the whole turbine over, half of which is transmitted to the bottom and the other half of which can easily be offset with guy wires.

1.2.4 IMPORTANT TERMS RELATED TO WIND POWER GENERATION

1.2.4.1 Solidity

The solidity of a wind rotor is the ratio of the projected blade area to the swept area. The projected blade area doesn't mean the actual blade area, it is the area met by the wind or projected in the direction of the wind as shown in Figure 1.6

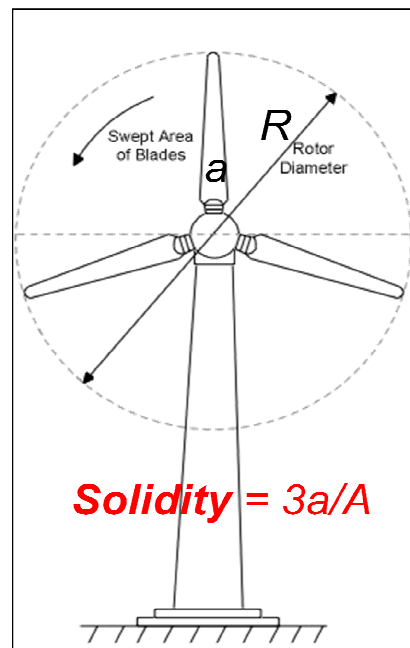


Figure 1.6 *Solidity of a horizontal wind turbine*

The solidity of Savonius rotor is unity as the wind sees no free passage through it. For Multiblade water pumping mills, it is around 0.7. for high speed horizontal axis turbines and Darrieus rotors it lies between 0.01 to 0.1.

Solidity has a direct relation with torque and speed. High solidity rotors have high torque and low speeds. On the other hand low solidity rotors have low torque and high speeds and are typically suited for electrical power generation.

1.2.4.2 Tip Speed Ratio (TSR)

Tip speed ratio of a wind turbine is defined as the ratio of the speed of the rotating blade tip to the speed of the free stream wind.

$$\lambda = \frac{2\pi RN}{V_{\infty}} = \frac{\omega_r R}{V_{\infty}} \quad (1.2)$$

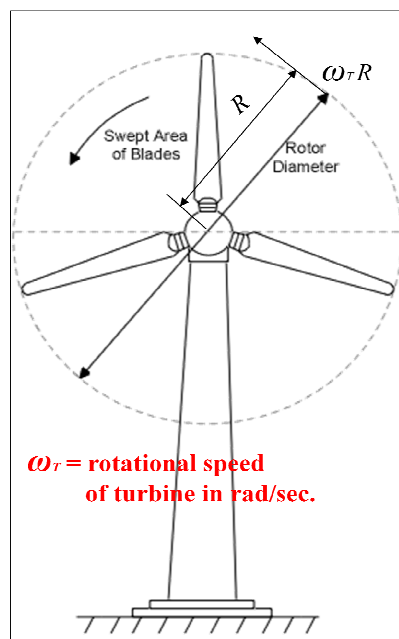


Figure 1.7 Solidity of a horizontal wind turbine

where λ is the TSR, R is the radius of the swept area in meters, N is the rotational speed in revolutions per second, and V_{∞} is the wind speed without rotor interruption in m/sec. There is an

optimum angle of attack which creates the highest lift to drag ratio. Because angle of attack is dependent on wind speed, there is an optimum tip-speed ratio.

The TSRs of the Savonius rotor and the multi-blade water pumping mills are generally low where as that of Darrieus rotors can be as high as 9. It can be said that high solidity rotors in general have low value TSRs and vice-versa.

1.2.4.3 Power coefficient (C_p)

Power coefficient of a wind energy converter is given by

$$C_p = \frac{\text{power output from the wind machine}}{\text{Power contained in wind}} \quad (1.3)$$

The power coefficient differs from the efficiency of a wind machine in the sense that the later includes the losses in the mechanical transmission, electrical generation, etc where as the former is just the efficiency of conversion of wind energy into mechanical energy of the shaft. In high speed horizontal axis machines the power coefficient is given by the Betz limit which states that all wind power cannot be captured by rotor or else air would be completely still behind rotor and not allow more wind to pass through. Theoretical limit of rotor efficiency is 59%. Most modern wind turbines are in the 35 – 45% range.

1.2.4.4 Specific Rated Capacity (SRC)

Specific rated capacity is defined as the ratio of peak power rating of the generator to the rotor swept area.

$$SRC = \frac{\text{power rating of the generator}}{\text{rotor swept area}} \quad (1.4)$$

Since the same wind turbine can produce widely varying amounts of electrical power depending on the wind speed, the SRC gives a standard procedure to specify the rating of a machine. The SRC varies between 0.2 for small rotors to 0.6 for large rotors.

1.2.5 WIND TURBINE CHARACTERISTICS

The different characteristics which define the performance of a wind turbine are

- Power coefficient versus Tip speed ratio characteristics
- Power versus speed characteristics
- Torque versus speed characteristics

1.2.5.1 Power Coefficient versus Tip Speed Ratio Characteristics

The graph of the power coefficient (C_p) against tip speed ratio (TSR) is a very important yardstick in the characterization of the wind turbine. Figure 1.8 shows the C_p vs TSR characteristics for different types of turbines.

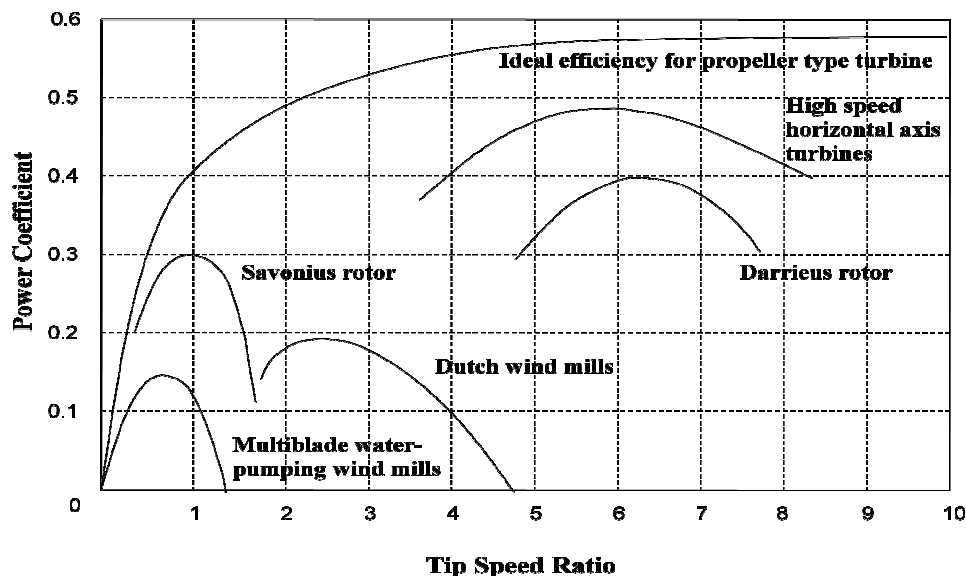


Figure 1.8 Curves of C_p versus TSR for different types of wind mills

For a given turbine, the power coefficient depends not only on the TSR but also on the blade pitch angle (α). Figure 1.9 shows the typical variation of the power coefficient with respect to the TSR (λ) with blade pitch control.

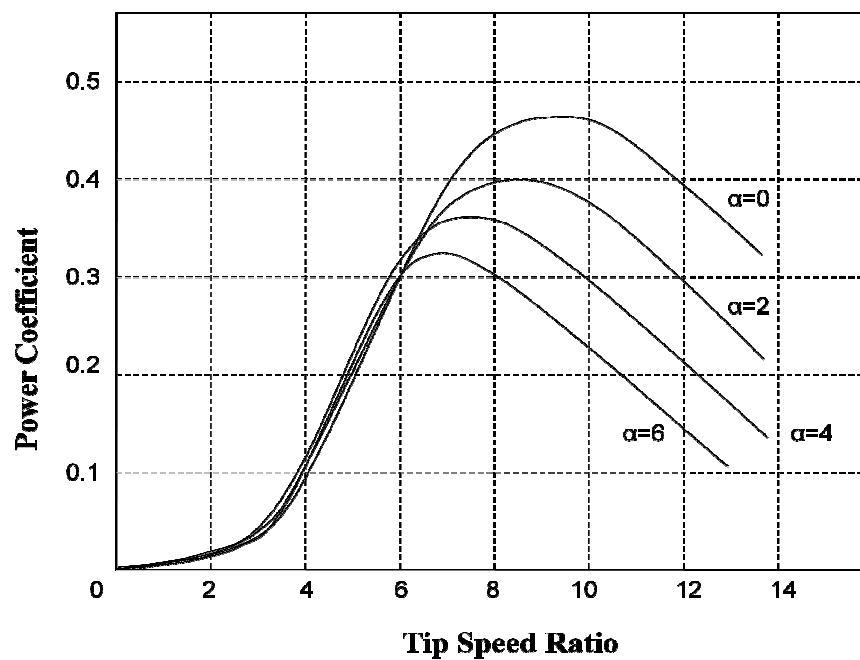


Figure 1.9 Curves of C_p versus TSR for different pitch angles α

1.2.5.2 Power versus Speed Characteristics

The wind turbine power curves shown in Figure 1.10 illustrate how the mechanical power that can be extracted from the wind depends on the rotor speed. For each wind speed there is an optimum turbine speed at which the extracted wind power at the shaft reaches its maximum. Such a family of wind turbine power curves can be represented by a single dimensionless characteristic curve, namely, the C_p - λ curve, as shown in Figure 1.9, where the power coefficient is plotted against the TSR.

From equations (1.1) and (1.3), the mechanical power transmitted to the shaft is

$$P_m = \frac{1}{2} \rho C_p A V_\infty^3 \quad (1.5)$$

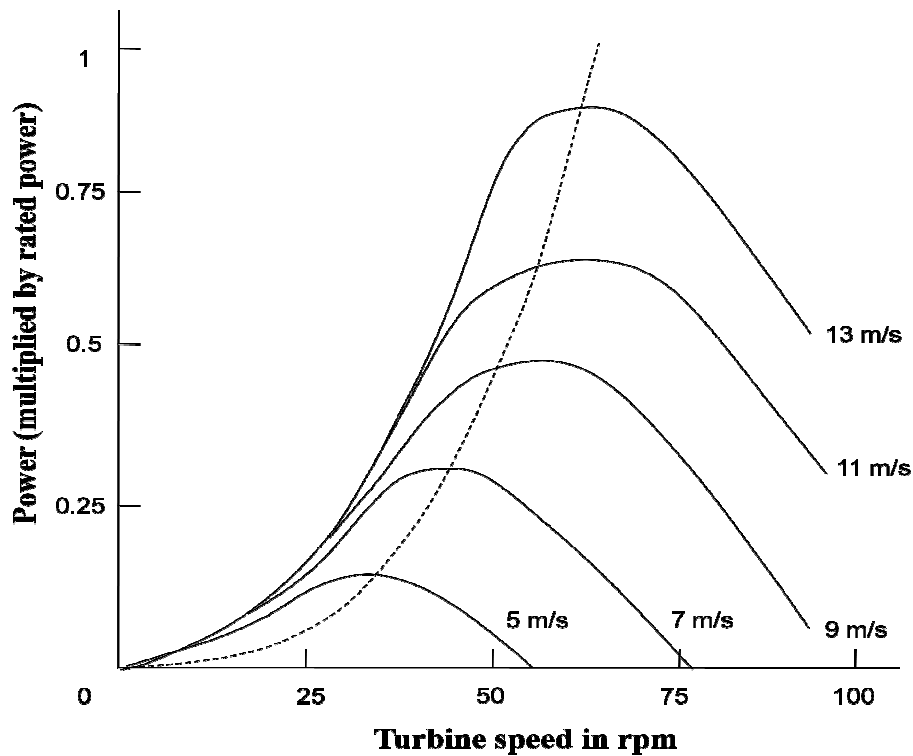


Figure 1.10 Power versus Speed characteristics of a wind turbine

Where C_p is a function of TSR (λ) and the pitch angle (α). For a wind turbine with radius R , equation (1.5) can be expressed as

$$P_m = \frac{1}{2} \rho C_p \pi R^2 V_\infty^3 \quad (1.6)$$

For a given wind speed, the power extracted from the wind is maximized if C_p is maximized. The optimum value of C_p , say $C_{p, \text{opt}}$, always occurs at a definite value of λ , say λ_{opt} , which means that for varying wind speed, the rotor speed should be adjusted proportionally to adhere always

to this value of $\lambda(=\lambda_{opt})$ for maximum mechanical power output from the turbine. Using the relation $\lambda=\omega R/V_\infty$ in equation (1.6), the maximum value of the shaft mechanical power for any wind speed can be expressed as

$$P_{max} = \frac{1}{2} C_{p,opt} \pi \left(\frac{R^5}{\lambda_{opt}^3} \right) \omega_{opt}^3 \rho \quad (1.7)$$

Thus the maximum mechanical power that can be extracted from wind is proportional to the cube of the rotor speed, i.e., $P_{max} \propto \omega^3$ this is shown by the dotted line in Figure 1.10.

1.2.5.3 Torque versus Speed Characteristics

Studying the torque versus rotational speed characteristics of any prime mover is very important for properly matching the load and insuring the stable operation of the electrical generator. The typical torque versus speed characteristics of the two- blade propeller -type wind turbine, the Darrieus rotor, and the Savonius are shown in Figures 1.11, 1.12, 1.13 respectively. The profiles of the torque – speed curves shown in Figures 1.11, 1.12 and 1.13 follow from the power curves, since torque and power are related as follows

$$T_m = \frac{P_m}{\omega} \quad (1.8)$$

From equation (1.7), at the optimum operation point ($C_{p, opt}, \lambda_{opt}$) the relation between aerodynamic torque and rotational speed is

$$T_m = \frac{1}{2} \rho C_{p,opt} \pi \left(\frac{R^5}{\lambda_{opt}^3} \right) \omega_{opt}^2 \quad (1.9)$$

It is seen that at the optimum operation point on the C_p - λ curve, the torque is quadratically related to the rotational speed.

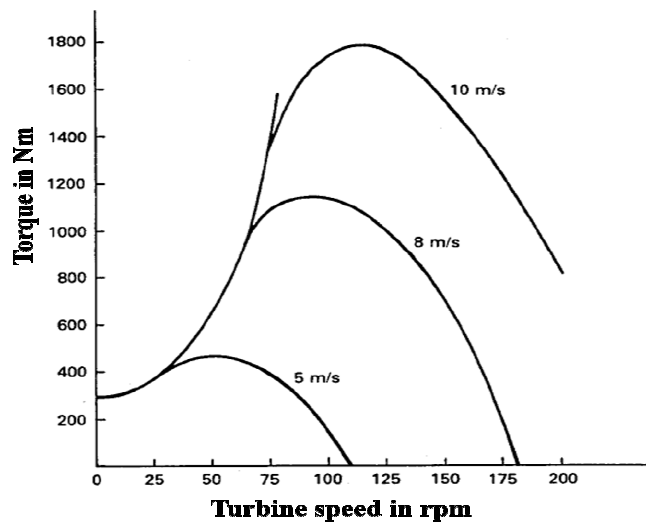


Figure 1.11 *Torque versus Speed characteristics of two blade propeller type rotor*

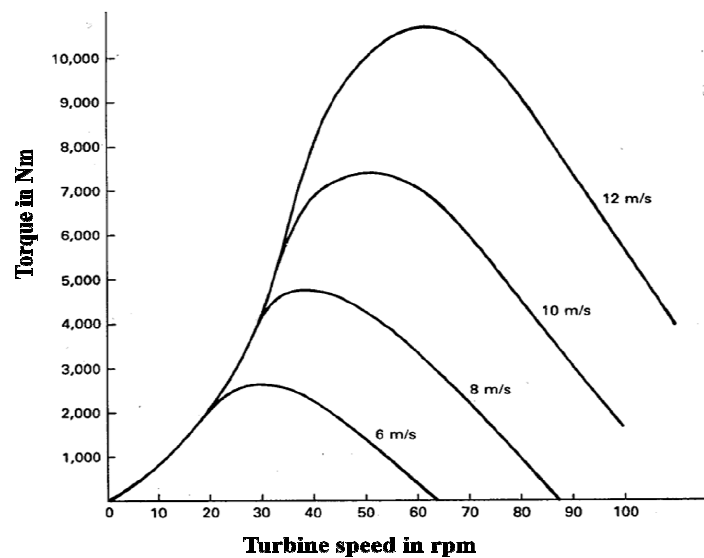


Figure 1.12 *Torque versus Speed characteristics of Darrieus rotor*

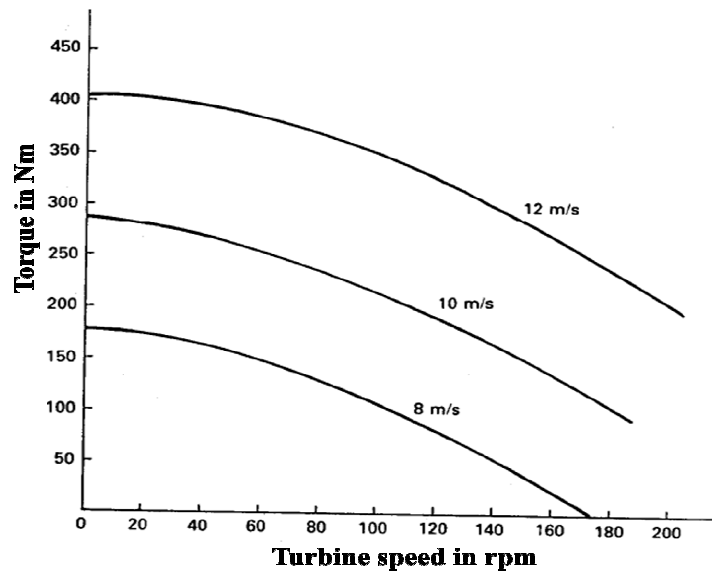


Figure 1.13 *Torque versus Speed characteristics of Savonius rotor*

The curves in the figures show that for the propeller turbine and the Darrieus rotor, for any wind speed, the torque reaches a maximum value at a specific rotational speed, and this maximum shaft torque varies approximately as the square of the rotational speed. In this case of electricity production, the load torque depends on the electrical loading, and by properly choosing the load (or power electronic interface), the torque can be made to vary as the square of the rotational speed.

1.2.6 WIND TURBINE CONTROL SYSTEMS

Control systems are required for a wind turbine for efficient power capture from wind as well as for safety of the turbine itself. When the wind speed becomes high, it becomes important to protect the generator and power electronic devices from overloading which is done by reducing the drive train load. At very high speeds the wind turbine has to be stalled. At low and medium wind speeds the turbine has to efficiently capture the power contained in the wind for which the angle of attack of the turbine blades should be accordingly adjusted. Similarly at very low speeds

the power contained in the wind becomes too low to be captured. So the turbines need to be stopped.

Along with many operating characteristics, the technical data sheet of a turbine mentions its output at a particular wind speed, generally known as the rated wind speed. This is the minimum wind speed at which the wind turbine produces its designated output power. For most of the turbines, this speed is normally between 9 and 16 m/s. The generator rating is chosen so as to best utilize the mechanical output of the turbine at the rated wind speed.

Wind turbine has four different types of control mechanisms, as discussed in the following.

1.2.6.1 Pitch Angle Control

In this type of control the pitch angle of the blades are changed according to the variation of wind speed. As the wind speed changes the pitch angle control system aligns the blade in direction of the relative wind due to which it is possible to achieve a high efficiency of power conversion.

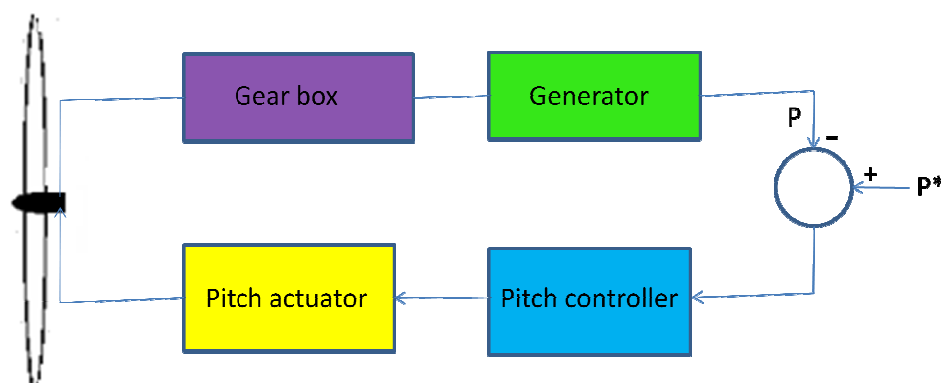


Figure 1.14 Pitch angle control block diagram

In a pitch controlled machine, as the wind speed exceeds its rated speed, the blades are gradually turned about the longitudinal axis and out of the wind to increase the pitch angle. This reduces the aerodynamic efficiency of the rotor, and rotor output power decreases. When the wind speed exceeds the safe limit for the system, the pitch angle is so changed that the power output reduces to zero and the machine shifts to the 'stall' mode. After the gust passes, the pitch angle is reset to the normal position and the turbine is restarted. At normal wind speeds, the blade pitch angle should ideally settle to a value at which the output power equals the rated power.

The pitch angle control principle is explained in Figure 1.14. The error signal which is the difference between the output electrical power and reference power is fed as the input to the pitch controller. The pitch controller operates the blade actuator to alter the pitch angle. The control system sets the blade at such an angle that maximizes the rotor efficiency while operating below the rated speed. The generator output power is accordingly adjusted such that the generator is able to absorb the mechanical power from the turbine and deliver it to the load. As continuous pitch control is relatively expensive to implement, so it is not justified to use this type of control mechanism in small wind machines. However, the stalling mechanism must be used in all types of wind turbines (large, medium and small) to prevent damage of the turbine during turbulent weather conditions.

1.2.6.2 Stall Control

- **Passive Stall Control**

Generally, stall control to limit the power output at high winds is applied to constant-pitch turbines driving induction generators connected to the network. The rotor speed is fixed by the network, allowing only 1-4% variation. Passive stall controlled wind

turbines have a simpler form of blades that are attached to the hub at a fixed angle. The rotor airfoil profile is aerodynamically designed such that when the wind speed exceeds a safe limit, the angle of attack of the airfoil to the wind stream is increased, and the laminar flow stops and is replaced by turbulence on the top side of the airfoil, due to which the lift force stops acting stalling its rotation.

- **Active Stall Control**

Large wind turbines are equipped with active stall control mechanism. In this case they use pitchable blades resembling the pitch controlled turbines. To get a large torque or turning force at low speeds, the control system pitches the blades in steps like pitch angle controlled machines at low wind speeds. But the situation becomes different when the turbine reaches its designed rated power level. At that time the stall control mechanism acts differently from a pitch control mechanism. At high speeds, to protect the generator from overloading the active stall control system pitches the blades in the opposite direction of what a pitch controlled machine would do. In this case it increases the angle of attack of the aerofoil leading a stall condition rather than decreasing the angle of attack to reduce the lift and the rotational speed of the blade.

An advantage of the active stall control is that the power output can be controlled so as to avoid overshooting the generators rated power at the start of wind gusts. A second advantage is that the generator would deliver its rated power at high wind speeds, in contrast to the passive stall controlled machines which will normally experience a drop in their electrical power output since its rotor blades experiences a deeper stall at high wind speeds.

1.2.6.3 Power Electronic Control

In a system incorporating a power electronic interface between the generator and the load (or the grid), the electrical power delivered by the generator to the load can be dynamically controlled. The instantaneous difference between mechanical power and electrical power changes the rotor speed following the equation

$$J \frac{d\omega}{dt} = \frac{P_m - P_e}{\omega} \quad (1.10)$$

Where J is the polar moment of the inertia of the rotor, ω is the angular speed of the rotor, P_m is the mechanical power produced by the turbine, and P_e is the electrical power delivered to the load. Integrating equation (1.10), we get

$$\frac{1}{2} J (\omega_2^2 - \omega_1^2) = \int_{t_1}^{t_2} (P_m - P_e) dt \quad (1.11)$$

The advantage of this method of speed control is that it does not involve any mechanical action and is smooth in operation. A disadvantage is that fast variation of speed requires a large difference between the input power and output power, which scales as the moment of inertia of the rotor. This results in a large torque and hence increased stress on the blades. Moreover, continuous control of the rotor speed by this method implies continuous fluctuation of the power output to the grid, which is usually undesirable for the power system.

1.2.6.4 Yaw Control

In this type of control the turbine continuously oriented along the direction of wind flow. In large machines this can be achieved using motorized control systems activated either by a fan-

tail (a small turbine mounted perpendicular to the main turbine) or, in case of wind farms, by a centralized instrument for the detection of the wind direction where as in small turbines this is achieved with a tail-vane. It is also possible to achieve yaw control without any additional mechanism, simply by mounting the turbine downwind so that the thrust force automatically pushes the turbine in the direction of the wind.

The yaw control mechanism can also be used for speed control— the rotor is made to face away from the wind direction at high wind speeds, thereby reducing the mechanical power. However, this method is seldom used where pitch control is available, because of the stresses it produces on the rotor blades. Yawing often produces loud noise, and it is desirable to restrict the yawing rate in large machines to reduce the noise.

1.3 WIND POWER CONVERSION SYSTEMS

Wind turbines can operate with either fixed speed (actually within a speed range about 1%) or variable speed. For fixed-speed wind turbines, the generator (induction generator) is directly connected to the grid. Since the speed is almost fixed to the grid frequency, and most certainly not controllable, it is not possible to store the turbulence of the wind in form of rotational energy. Therefore, for a fixed-speed system the turbulence of the wind will result in power variations, and thus affect the power quality of the grid. For a variable-speed wind turbine the generator is controlled by power electronic equipment, which makes it possible to control the rotor speed. In this way the power fluctuations caused by wind variations can be more or less absorbed by changing the rotor speed and thus power variations originating from the wind conversion and the drive train can be reduced. Hence, the power quality impact caused by the wind turbine can be improved compared to a fixed-speed turbine. The rotational speed of a wind turbine is fairly low and must therefore be adjusted to the electrical frequency. This can be done

in two ways: with a gearbox or with the number of pole pairs of the generator. The number of pole pairs sets the mechanical speed of the generator with respect to the electrical frequency and the gearbox adjusts the rotor speed of the turbine to the mechanical speed of the generator.

1.3.1 FIXED SPEED WIND TURBINE

For the fixed-speed wind turbine the induction generator is directly connected to the electrical grid according to Figure 1.15. The rotor speed of the fixed-speed wind turbine is in principle determined by a gearbox and the pole-pair number of the generator. The fixed-speed wind turbine system has often two fixed speeds. This is accomplished by using two generators with different ratings and pole pairs, or it can be a generator with two windings having different ratings and pole pairs. This leads to increased aerodynamic capture as well as reduced

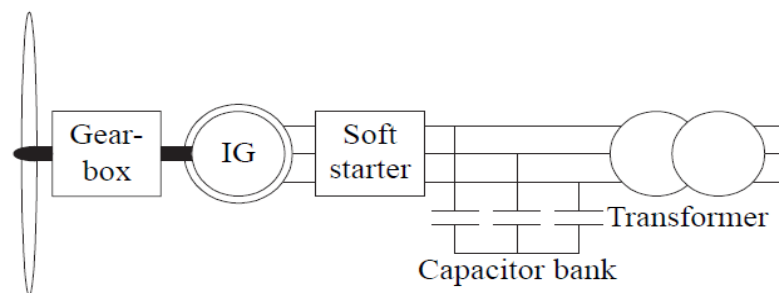


Figure 1.15 *Fixed speed wind turbine system*

magnetizing losses at low wind speeds. This system (one or two-speed) was the “conventional” concept used by many Danish manufacturers in the 1980s and 1990s.

1.3.2 VARIABLE SPEED WIND TURBINE

The system presented in Figure 1.16 consists of a wind turbine equipped with a converter connected to the stator of the generator.

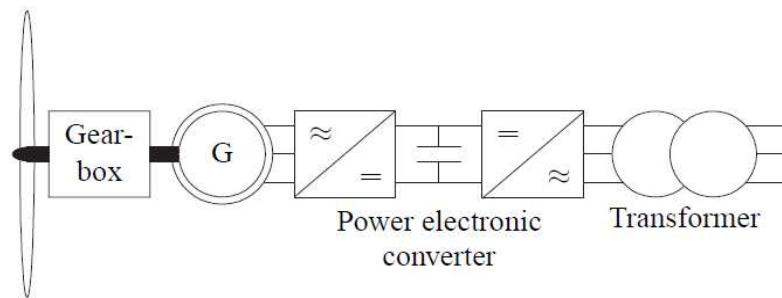


Figure 1.16 Variable speed wind turbine system

The generator could either be a cage-bar induction generator or a synchronous generator. The gearbox is designed so that maximum rotor speed corresponds to rated speed of the generator. Synchronous generators or permanent-magnet synchronous generators can be designed with multiple poles which imply that there is no need for a gearbox. Since this “full-power” converter/generator system is commonly used for other applications, one advantage with this system is its well-developed and robust control.

1.4 GENERATORS FOR WIND POWER APPLICATIONS

Generally three different types of machines are used as generators for wind power applications, those are

- Squirrel cage induction machine (SCIM)
- Wound rotor induction machine (WRIM)
- Permanent magnet synchronous machine (PMSM)

1.4.1 SQUIRREL CAGE INDUCTION MACHINE

Squirrel cage induction machines are mostly used as generators for wind power applications. These machines are robust, maintenance free and cheaper than the other types of generators used

for wind power applications. Squirrel cage machines are used as grid excited induction generators which takes the reactive power from the grid and delivers active power to the grid.

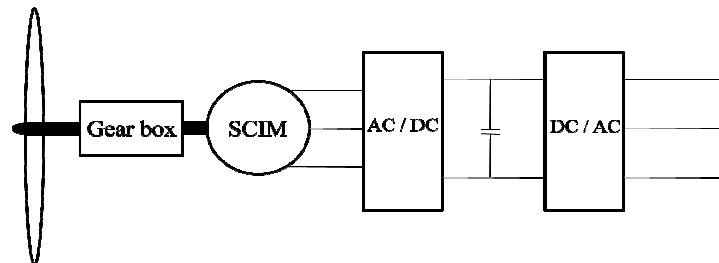


Figure 1.17 *Squirrel cage induction machine used for wind power generation*

Figure 1.17 shows the schematic diagram for a squirrel cage induction machine used for wind power generation.

1.4.2 WOUND ROTOR INDUCTION MACHINE

In recent days wound rotor induction machines have been extensively used as generators for wind power applications. These machines have attracted the interest due to their greater efficiency of power generation. These machine are supplied both from the stator and rotor side so often they are called doubly excited induction generators. In this type of system the whole control structure is connected to the rotor side, so the ratings of the control circuit components are reduced. Figure 1.18 shows the schematic diagram for a wound rotor induction machine used for wind power generation.

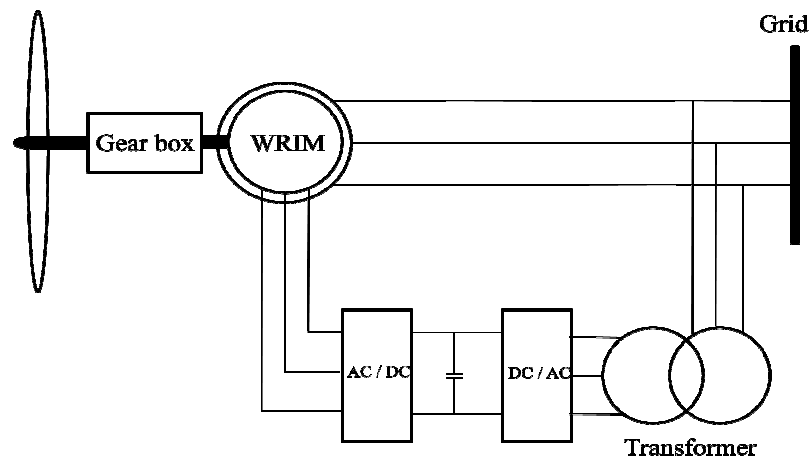


Figure 1.18 *Wound rotor induction machine used for wind power generation*

1.4.3 PERMANENT MAGNET SYNCHRONOUS MACHINE

Permanent magnet synchronous machines can also be used as generators for wind power applications. But these machines are usually not preferred for wind power generation purpose due to the fact that these machines are costly but they have an advantage of being used as direct drive generators. The scheme using permanent magnet synchronous generator is shown in Figure 1.19.

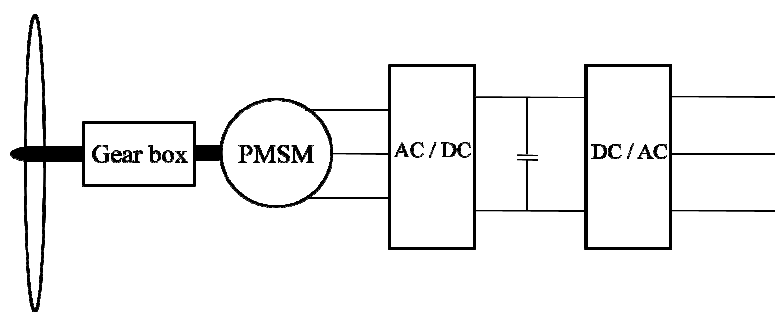


Figure 1.19 *Permanent magnet synchronous machine used for wind power generation*

This work is extensively done upon wind power generation using squirrel cage induction machines as generators.

1.5 SELF EXCITED AND LINE EXCITED INDUCTION GENERATORS

The squirrel cage induction generators are basically used in two different configurations for wind power generation purpose.

- Self excited induction generators
- Line excited induction generators

1.5.1 SELF EXCITED INDUCTION GENERATORS

Self excited induction generators are basically used for stand-alone wind power systems. In this scheme a capacitor bank is connected to the system to supply the required reactive power to the induction generator. The self excited induction generator scheme is shown in the Figure 1.20

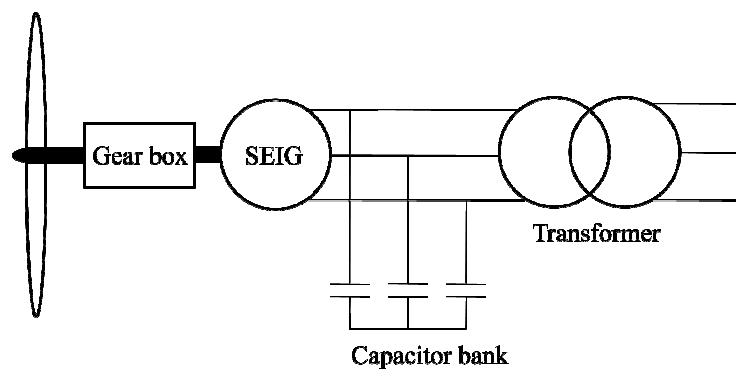


Figure 1.20 *Self excited induction generator scheme*

1.5.2 LINE EXCITED INDUCTION GENERATORS

Squirrel cage induction machines are most often used as line excited induction generators for wind power applications. In this scheme the induction generators are connected to the grid through a bidirectional converter-inverter set. The induction generator takes the required reactive

power from the generator side inverter and generates active power which is then fed to the grid. For the fact that the induction generator takes the reactive power and delivers active power, it has a poor power factor at the generation end. But by the vector control of the line side converter the power factor at the grid end can be maintained perfectly at unity, which will be described in details in chapter 6. Figure 1.21 shows the line excited induction generator scheme for wind power applications.

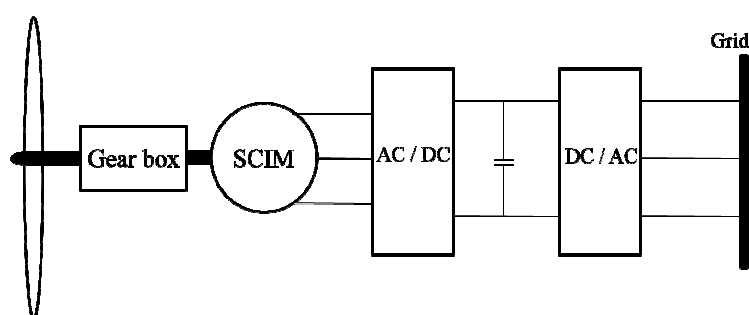


Figure 1.21 *Line excited induction generator scheme*

1.6 CONTROL OF LINE EXCITED CAGE INDUCTION GENERATORS

Line excited cage induction generators are most commonly used for wind power applications. These generators are robust, cheaper than its counter parts and need less maintenance, which make these machines suitable for wind power generation. Cage induction generators have drawback that, due to the coupling effect between active and reactive power the transient response becomes sluggish and the control becomes difficult and complex. Because of this there arises stability problem when the system is connected with the grid. A lot of research has been done in recent past to improve the transient characteristics of induction machines. When induction machines are operated using vector control techniques, fast dynamic response and accurate torque control are obtained. All of these characteristics are advantageous in variable

speed wind energy conversion systems (WECS). Squirrel cage generators with shunt passive or active VAR (volt ampere reactive) generators was proposed in [1], which generate constant frequency power through a diode rectifier and line commutated thyristor inverter. A comparative study of fixed speed and DFIG during power system disturbances such as network voltage sags and three phase faults, as well as the possibility of network voltage instability is investigated in [2]. The performance of a DFIG driven by a wind turbine connected to large power systems is studied in [3], where as in [4] a doubly excited induction generator is studied as an alternative to line excited cage induction generators for variable speed wind power generation. In this paper a feed forward vector control scheme is also developed for the performance improvement of the doubly fed induction generator system. A comparative study is done in [5] between fixed speed wind turbines, variable speed wind turbines employing line excited cage generators and variable speed wind turbines using doubly excited induction generators. Self excited induction generator system using cage induction machine is described in [6], and in [7] the operation of several self excited induction generators connected to a common bus is analyzed. The field oriented control of induction generator for variable speed wind energy applications are discussed in [8]-[12]. A sensor-less vector control scheme based on a model reference adaptive system (MRAS) observer used to estimate the rotational speed, which is suitable to control cage induction generators for wind power applications is discussed in [8] In this paper a separate estimation of the speed is obtained from the rotor slot harmonics using an algorithm for spectral analysis in order to tune the MRAS observer and compensate for the parameter variation and uncertainties. In [9] a doubly fed induction machine is considered while it is connected to the grid and operating in sub synchronous as well as super synchronous speeds. In order to decouple the active and reactive powers generated by the machines, stator flux oriented vector control is applied in this paper. A

new control scheme using non-linear controller and FLC is employed for a variable speed grid connected wind energy system in [10] where as a vector control scheme for both supply side and machine converters is discussed and the independent control of active and reactive power is done in [11]. In [4] and [8] -[11] the vector control schemes employ PI controllers for the control purpose. In [12] a cage induction machine is considered and a fuzzy control system is used to drive the wind energy conversion system to the point of maximum energy capture for a given wind velocity. A FLC based speed control scheme is described in [13] employing feed-forward vector control scheme for performance improvement of an induction motor drive system. Again in [14] fuzzy logic is used to develop an advanced and intelligent control strategy for a line excited cage generator system used for wind power applications. A detailed approach on fuzzy logic controllers is given in [15]. In this paper different aspects of fuzzy controller tuning such as effect of membership functions on fuzzy controller tuning, tuning of fuzzy controller using the input and output normalizing factors, effect of fuzzy rules on tuning etc. are discussed in a very detailed manner. In [16] methods for improving the performance of a fuzzy logic controller especially when used for control of higher order systems are discussed. In this paper two different schemes for improvising the performance of a fuzzy logic controller are given. In [17] a self tuned fuzzy logic controller is implemented for the performance improvement of a field oriented control of an induction motor drive. In this paper another fuzzy logic controller is used to tune the normalization factors of the main fuzzy logic controller. In [18] a similar strategy has been adopted to tune the output normalization factor of the fuzzy logic controller. The output normalization factor tuning scheme works taking the error and change of error of the system into account. Several other self tuned fuzzy logic controller schemes are given in [19] – [23]. In [24] and [25] hybrid controllers are described. In [24] the hybrid controller is a hybrid of PI controller

and fuzzy logic controller where as in [25] the hybrid controller is a combination of a PI controller and a sliding mode controller.

1.7 MOTIVATION

Generation of pollution free power has become the main aim of the researchers in the field of electrical power generation. The depletion of fossil fuels, such as coal and oil, also aid to the importance of switching to renewable and non-polluting energy sources such as solar, tidal and wind energy etc., among which wind energy is the most cost efficient and wide spread source of energy. From the recent scenario it is also evident that wind energy is drawing a great deal of interest in the power generation sector. If the wind energy could be effectively captured it could solve the problems such as environmental pollution and unavailability of fossil fuel in future. The above fact gives the motivation for development of a wind power generation system which would have better performance and efficiency.

1.8 OBJECTIVES

Wind energy has been utilized by human for centuries but in the last four decades serious research has been done for the generation of electrical power from wind. As the research area is not so old, many developments are yet to be done in this field. A number of wind power conversion systems have been developed using different types of machines such as, cage induction machines, wound rotor induction machines and permanent magnet synchronous machines, as generators. This work employs a cage induction machine as electrical power generator due to the fact that cage induction machines are cheaper than their counterparts and also need less maintenance. A lot of research has been done in improving the transient and steady state performances of the induction generator system by using different control strategies

such as direct and indirect vector control, sensor-less vector control, direct torque control etc. But most of the control strategies employed the conventional PI controller and some employed fuzzy logic controllers for the control of the induction machine. Again the power factor of the induction generator system becomes a big issue, because induction generators have low power factors as they take the reactive power from the grid and supply active power to the grid.

In this work the main objectives are

- Development and Implementation of new controllers for transient and steady state performance improvement of the line excited induction generator system.
- Power factor improvement of the wind energy conversion system.
- Fabrication of a control circuit for control of PWM converter- inverter set which could be interfaced with PC.

1.9 ORGANISATION OF THE THESIS

The thesis includes six chapters among which chapter-1 gives a brief description of wind power and wind electrical systems. In chapter-2 the d-q modeling of induction generator is done and the vector control strategy for induction machine is described. Chapter-3 includes the description and simulation results of an indirect vector controlled cage induction generator. The indirect vector control strategy described in this chapter employs conventional PI controllers. The simulation results are taken for both turbine torque and reference speed variations. In chapter-4 three controllers are designed and implemented for the performance improvement of the indirect vector controlled cage induction generator system. Among the three controllers the first is the fuzzy logic controller. Then a second controller is designed which is the self tuned fuzzy logic controller. The third controller is a hybrid controller which employs both conventional PI

controller and the self tuned fuzzy logic controller. The improvement in the performance of the cage induction generator system is shown in the simulations later in that chapter. In chapter-5 a control scheme for the grid side PWM converter is described and simulated. The control of grid side converter is done to improve the power factor of the wind power generation system. Chapter-6 contains the details of the fabrication of the control circuit for control of PWM converter- inverter set. The outputs of the fabricated circuits are shown later in that chapter.

The main contributions of the thesis are:-

1. Performance improvement of indirect vector controlled induction generator using:
 - i. Fuzzy logic controller.
 - ii. Self turned fuzzy logic controller.
 - iii. A novel hybrid controller combining P-I controller and self tuned fuzzy logic controller.
2. Performance comparison of the indirect vector control scheme with different controllers .
3. Power factor improvement of wind power generation system through control of grid side converter.
4. Fabrication and testing of control circuit for PWM-converter-inverter system.

Chapter 2

D-Q Modeling And Vector Control of Induction Generator

2.1 INTRODUCTION

In many applications, the dynamic behavior of the induction machine has an important effect upon the overall performance of the system of which it is a part. A machine is a complex structure electrically, mechanically and thermally. The dynamic performance of an ac machine is complex because the three phase rotor windings move with respect to the three phase stator windings. The machine model can be described by differential equations with time varying mutual inductances, but such a model tends to be very complex. The three phase machine can be represented by an equivalent two-phase machine i.e. $a-b-c$ to $d-q$ transformation. In the 1920s, to overcome the problem of time varying parameters, R.H. Park proposed a new theory of electrical machine analysis. He transformed or referred the stator variables (voltages, currents and flux linkages) to a synchronously rotating reference frame fixed in the rotor. Later, in the 1930s, H.C. Stanley showed that time varying inductances in the voltage equations of an induction machine due to electric circuits in relative motion can be eliminated by transforming

the rotor variables to variables associated with fictitious stationary windings. Later, G. Kron proposed a transformation of both stator and rotor variables to a synchronously rotating reference frame that moves with the rotating magnetic field. A proper model for the three phase induction machine is essential to simulate and study the complete drive system.

2.2 AXES TRANSFORMATION

Consider a symmetrical three-phase induction machine with stationary $as-bs-cs$ axes at $2\pi/3$ -angle apart as shown in Figure 2.1 . We have to transform the three phase stationary reference frame ($as-bs-cs$) variables into two-phase stationary reference frame (d^s-q^s) variables and then transform these to synchronously rotating reference frame (d^e-q^e), and vice versa. Assuming that the d^s-q^s axes are oriented at θ angle, as shown in Figure 2.1, the voltages v_{ds}^s and v_{qs}^s can be resolved into $as-bs-cs$ components and can be represented in the matrix form as

$$\begin{bmatrix} v_{as} \\ v_{bs} \\ v_{cs} \end{bmatrix} = \begin{bmatrix} \cos \theta & \sin \theta & 1 \\ \cos(\theta - 120^\circ) & \sin(\theta - 120^\circ) & 1 \\ \cos(\theta + 120^\circ) & \sin(\theta + 120^\circ) & 1 \end{bmatrix} \begin{bmatrix} v_{qs}^s \\ v_{ds}^s \\ v_{os}^s \end{bmatrix} \quad (2.1)$$

The corresponding inverse relation is

$$\begin{bmatrix} v_{qs}^s \\ v_{ds}^s \\ v_{os}^s \end{bmatrix} = \frac{2}{3} \begin{bmatrix} \cos \theta & \cos(\theta - 120^\circ) & \cos(\theta + 120^\circ) \\ \sin \theta & \sin(\theta - 120^\circ) & \sin(\theta + 120^\circ) \\ 0.5 & 0.5 & 0.5 \end{bmatrix} \begin{bmatrix} v_{as} \\ v_{bs} \\ v_{cs} \end{bmatrix} \quad (2.2)$$

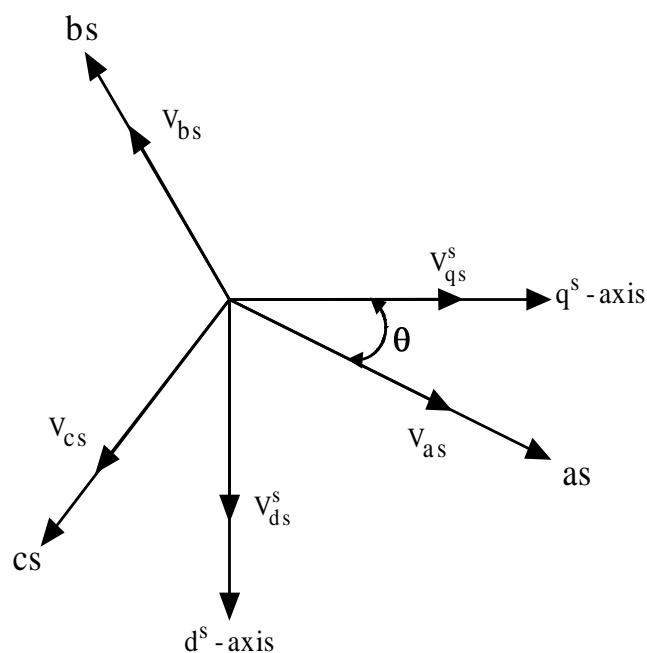


Figure 2.1 Stationary frame $a-b-c$ to $d^s - q^s$ axes transformation

where v_{os}^s is added as the zero sequence component, which may or may not be present. We have considered voltage as variable. The current and flux linkages can be transformed by similar equations. Figure 2.2 shows the synchronously rotating $d^e - q^e$ axes, which rotate at synchronous speed ω_e with respect to the $d^s - q^s$ axes and the angle $\theta_e = \omega_e t$.

The two-phase $d^s - q^s$ windings are transformed into the hypothetical windings mounted on the $d^e - q^e$ axes. The voltages v_{ds}^s and v_{qs}^s can be resolved into $d^e - q^e$ components and can be represented in matrix form as

$$\begin{bmatrix} v_{qs} \\ v_{ds} \end{bmatrix} = \begin{bmatrix} \cos \theta_e & -\sin \theta_e \\ \sin \theta_e & \cos \theta_e \end{bmatrix} \begin{bmatrix} v_{qs}^s \\ v_{ds}^s \end{bmatrix} \quad (2.3)$$

For convenience, the superscript 'e' has been dropped from the synchronously rotating frame parameters. The corresponding inverse relation is

$$\begin{bmatrix} v_{qs}^s \\ v_{ds}^s \end{bmatrix} = \begin{bmatrix} \cos \theta_e & \sin \theta_e \\ -\sin \theta_e & \cos \theta_e \end{bmatrix} \begin{bmatrix} v_{qs}^e \\ v_{ds}^e \end{bmatrix} \quad (2.4)$$

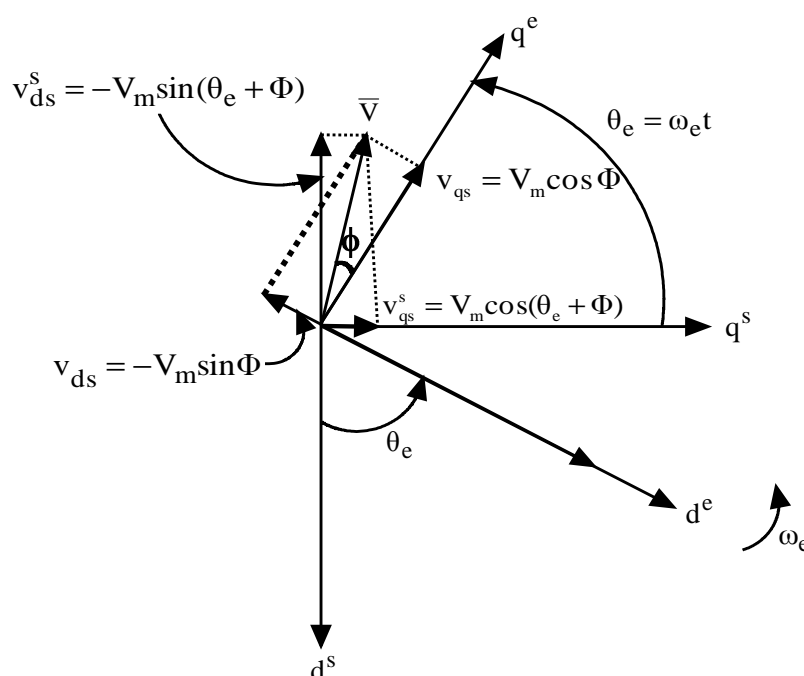


Figure 2.2 Stationary frame $d^s - q^s$ to synchronously rotating frame $d^e - q^e$ transformation

2.3 D-Q MODEL OF INDUCTION MACHINE (KRON'S EQUATION)

G. Kron introduced a change of variables that eliminated the position or time-varying mutual inductances of a symmetrical induction machine by transforming both the stator variables and the rotor variables to a reference frame rotating in synchronism with the rotating magnetic field. This reference frame is commonly referred to as the synchronously rotating reference frame. Consider the two-phase machine shown in Figure 2.3, we need to represent both $d^s - q^s$ and $d^r - q^r$ circuits and their variables in a synchronously rotating $d^e - q^e$ frame. For simplicity, the following assumptions about the induction machine are made:

- Symmetrical two-pole, three phase windings.

- The slotting effects are neglected.
- Mutual inductances are equal.
- The flux density is radial in the air gap and saturation of the magnetic circuit is neglected.
- The stator and the rotor windings are simplified as a single, multi-turn full pitch coil situated on the two sides of the air gap.
- The harmonics in voltages and currents are neglected.
- Hysteresis and eddy current losses and skin effects are neglected.

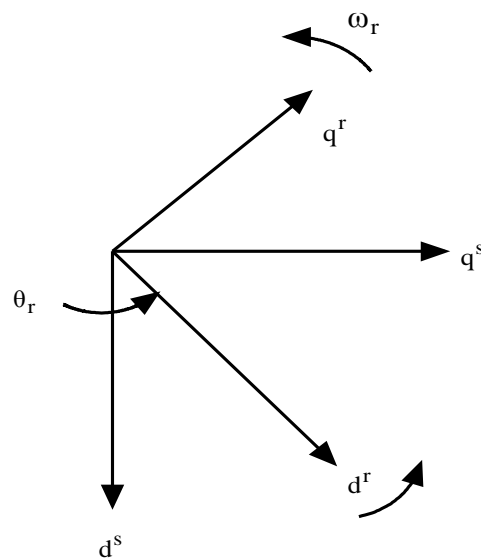


Figure 2.3 *Equivalent two-phase transformation*

The stator circuit equations can be written as

$$v_{qs}^s = R_s i_{qs}^s + \frac{d}{dt} \Psi_{qs}^s \quad (2.5)$$

$$v_{ds}^s = R_s i_{ds}^s + \frac{d}{dt} \Psi_{ds}^s \quad (2.6)$$

where Ψ_{qs}^s and Ψ_{ds}^s are q -axis and d -axis stator flux linkages, respectively. When these equations are converted to $d^e - q^e$ frame, the following equation can be written:

$$v_{qs} = R_s i_{qs} + \frac{d}{dt} \Psi_{qs} + \omega_e \Psi_{ds} \quad (2.7)$$

$$v_{ds} = R_s i_{ds} + \frac{d}{dt} \Psi_{ds} - \omega_e \Psi_{qs} \quad (2.8)$$

If the rotor is not moving, that is, $\omega_r=0$, the rotor equations for a doubly-fed wound-rotor machine will be

$$v_{qr} = R_r i_{qr} + \frac{d}{dt} \Psi_{qr} + \omega_e \Psi_{dr} \quad (2.9)$$

$$v_{dr} = R_r i_{dr} + \frac{d}{dt} \Psi_{dr} - \omega_e \Psi_{qr} \quad (2.10)$$

where all the variables and parameters are referred to the stator. Since the rotor actually moves at speed ω_r , the d - q axes fixed on the rotor move at a speed $\omega_e - \omega_r$ relative to the synchronously rotating frame. Therefore, in $d^e - q^e$ frame, the rotor equations should be modified as

$$v_{qr} = R_r i_{qr} + \frac{d}{dt} \Psi_{qr} + (\omega_e - \omega_r) \Psi_{dr} \quad (2.11)$$

$$v_{dr} = R_r i_{dr} + \frac{d}{dt} \Psi_{dr} - (\omega_e - \omega_r) \Psi_{qr} \quad (2.12)$$

The $d^e - q^e$ dynamic model equivalent circuits are shown in Figure 2.21 that satisfies equations (2.7)-(2.8) and (2.11)-(2.12). The advantage of the $d^e - q^e$ dynamic model of the machine is that all the sinusoidal variables in stationary frame appear as dc quantities in synchronous frame.

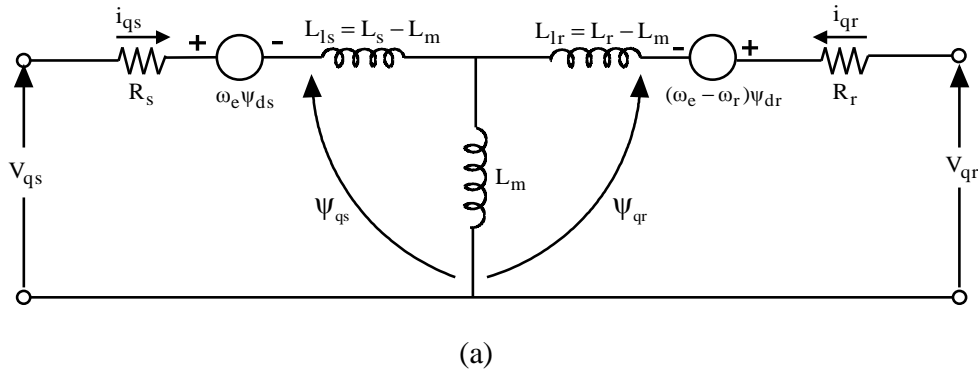


Figure 2.4 Dynamic $d^e - q^e$ equivalent circuits of machine (a) $q^e -$ axis circuit

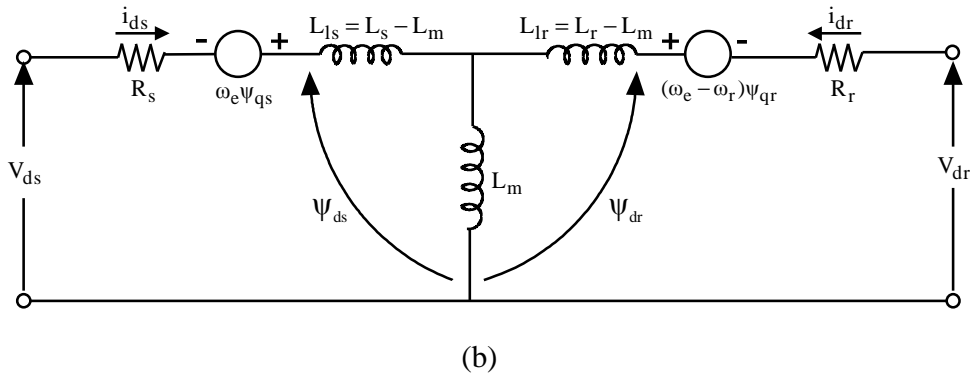


Figure 2.4 Dynamic $d^e - q^e$ equivalent circuits of machine (b) $d^e -$ axis circuit

The flux linkage expressions in terms of the currents can be written from Figure 2.4 as:

$$\Psi_{qs} = L_{ls} i_{qs} + L_m (i_{qs} + i_{qr}) \quad (2.13)$$

$$\Psi_{qr} = L_{lr} i_{qr} + L_m (i_{qs} + i_{qr}) \quad (2.14)$$

$$\Psi_{qm} = L_m (i_{qs} + i_{qr}) \quad (2.15)$$

$$\Psi_{ds} = L_{ls} i_{ds} + L_m (i_{ds} + i_{dr}) \quad (2.16)$$

$$\Psi_{dr} = L_{lr} i_{dr} + L_m (i_{ds} + i_{dr}) \quad (2.17)$$

$$\Psi_{dm} = L_m (i_{ds} + i_{dr}) \quad (2.18)$$

Combining the above expressions, the electrical transient model in terms of voltages and currents can be given in matrix form as

$$\begin{bmatrix} v_{ds} \\ v_{qs} \\ v_{dr} \\ v_{qr} \end{bmatrix} = \begin{bmatrix} R_s + sL_s & -\omega_e L_s & sL_m & -\omega_e L_m \\ \omega_e L_s & R_s + sL_s & \omega_e L_m & sL_m \\ sL_m & -(\omega_e - \omega_r)L_m & R_r + sL_r & -(\omega_e - \omega_r)L_r \\ (\omega_e - \omega_r)L_m & sL_m & (\omega_e - \omega_r)L_r & R_r + sL_r \end{bmatrix} \begin{bmatrix} i_{ds} \\ i_{qs} \\ i_{dr} \\ i_{qr} \end{bmatrix} \quad (2.19)$$

where s is the Laplace operator. For singly-fed machine, such as a cage motor, $v_{qr}=v_{dr}=0$.

Now splitting equation (2.19) such that the differential terms become separate and rewriting the equation we get

$$\begin{bmatrix} V_{ds} \\ V_{qs} \\ V_{dr} \\ V_{qr} \end{bmatrix} = \begin{bmatrix} R_s & -\omega_e L_s & 0 & -\omega_e L_m \\ \omega_e L_s & R_s & \omega_e L_m & 0 \\ 0 & -(\omega_e - \omega_r)L_m & R_r & -(\omega_e - \omega_r)L_r \\ (\omega_e - \omega_r)L_m & 0 & (\omega_e - \omega_r)L_r & R_r \end{bmatrix} \begin{bmatrix} i_{ds} \\ i_{qs} \\ i_{dr} \\ i_{qr} \end{bmatrix} + \begin{bmatrix} L_s & 0 & L_m & 0 \\ 0 & L_s & 0 & L_m \\ L_m & 0 & L_r & 0 \\ 0 & L_m & 0 & L_r \end{bmatrix} \begin{bmatrix} si_{ds} \\ si_{qs} \\ si_{dr} \\ si_{qr} \end{bmatrix} \quad (2.20)$$

where

$$\begin{bmatrix} V_{ds} \\ V_{qs} \\ V_{dr} \\ V_{qr} \end{bmatrix} = U, \quad \begin{bmatrix} si_{ds} \\ si_{qs} \\ si_{dr} \\ si_{qr} \end{bmatrix} = \dot{X}, \quad \begin{bmatrix} i_{ds} \\ i_{qs} \\ i_{dr} \\ i_{qr} \end{bmatrix} = X$$

$$\begin{bmatrix} R_s & -\omega_e L_s & 0 & -\omega_e L_m \\ \omega_e L_s & R_s & \omega_e L_m & 0 \\ 0 & -(\omega_e - \omega_r) L_m & R_r & -(\omega_e - \omega_r) L_r \\ (\omega_e - \omega_r) L_m & 0 & (\omega_e - \omega_r) L_r & R_r \end{bmatrix} = A_I$$

and

$$\begin{bmatrix} L_s & 0 & L_m & 0 \\ 0 & L_s & 0 & L_m \\ L_m & 0 & L_r & 0 \\ 0 & L_m & 0 & L_r \end{bmatrix} = A_2$$

So we have the equation as

$$U = A_I X + A_2 \dot{X} \quad (2.21)$$

Rearranging we get

$$\dot{X} = -A_2^{-1} A_I X + A_2^{-1} I U \quad (2.22)$$

Where

$$A_2^{-1} = \frac{1}{L_s L_r - L_m^2} \begin{bmatrix} L_r & 0 & -L_m & 0 \\ 0 & L_r & 0 & -L_m \\ -L_m & 0 & L_s & 0 \\ 0 & -L_m & 0 & L_s \end{bmatrix}$$

and ' I ' is the identity matrix.

Substituting the values of A_1 , A_2^{-1} and I in equation (2.21) we get our state equation in the form

$$\dot{X} = AX + BU \quad (2.23)$$

Where

$$A = -A_2^{-1}A_1$$

and

$$B = A_2^{-1}I$$

The matrix 'A' has some values which are constants and some values which are functions of ' ω_r '. Now separating out the ' ω_r ' dependent terms from the matrix 'A' and rewriting the equation we get the equation in the form of

$$\dot{X} = A'X + A''X + BU \quad (2.24)$$

Where matrix ' A' ' is a constant matrix which is independent of ' ω_r ', but the matrix ' A'' ' is dependent on ' ω_r ' and can be written as

$$A'' = \omega_r * A'''$$

Where ' A''' ' is a constant matrix.

Hence the final equation is of the form given below

$$\dot{X} = A'X + \omega_r * A'''X + BU \quad (2.25)$$

And is given by the equation 2.26

$$\begin{aligned}
 \begin{bmatrix} s\dot{i}_{ds} \\ s\dot{i}_{qs} \\ s\dot{i}_{dr} \\ s\dot{i}_{qr} \end{bmatrix} &= \begin{bmatrix} \frac{-L_r R_s}{L_s L_r - L_m^2} & \omega_e & \frac{L_m R_r}{L_s L_r - L_m^2} & 0 \\ -\omega_e & \frac{-L_r R_s}{L_s L_r - L_m^2} & 0 & \frac{L_m R_r}{L_s L_r - L_m^2} \\ \frac{L_m R_s}{L_s L_r - L_m^2} & 0 & \frac{-L_s R_r}{L_s L_r - L_m^2} & \omega_e \\ 0 & \frac{L_m R_s}{L_s L_r - L_m^2} & -\omega_e & \frac{-L_s R_r}{L_s L_r - L_m^2} \end{bmatrix} \begin{bmatrix} i_{ds} \\ i_{qs} \\ i_{dr} \\ i_{qr} \end{bmatrix} \\
 + \omega_r &\begin{bmatrix} 0 & \frac{L_m^2}{L_s L_r - L_m^2} & 0 & \frac{L_m L_r}{L_s L_r - L_m^2} \\ -\frac{L_m^2}{L_s L_r - L_m^2} & 0 & -\frac{L_m L_r}{L_s L_r - L_m^2} & 0 \\ 0 & -\frac{L_m L_s}{L_s L_r - L_m^2} & 0 & -\frac{L_s L_r}{L_s L_r - L_m^2} \\ \frac{L_m L_s}{L_s L_r - L_m^2} & 0 & \frac{L_s L_r}{L_s L_r - L_m^2} & 0 \end{bmatrix} \begin{bmatrix} i_{ds} \\ i_{qs} \\ i_{dr} \\ i_{qr} \end{bmatrix} \\
 + &\begin{bmatrix} \frac{L_r}{L_s L_r - L_m^2} & 0 & \frac{-L_m}{L_s L_r - L_m^2} & 0 \\ 0 & \frac{L_r}{L_s L_r - L_m^2} & 0 & \frac{-L_m}{L_s L_r - L_m^2} \\ \frac{-L_m}{L_s L_r - L_m^2} & 0 & \frac{L_s}{L_s L_r - L_m^2} & 0 \\ 0 & \frac{-L_m}{L_s L_r - L_m^2} & 0 & \frac{L_s}{L_s L_r - L_m^2} \end{bmatrix} \begin{bmatrix} V_{ds} \\ V_{qs} \\ V_{dr} \\ V_{qr} \end{bmatrix}
 \end{aligned} \tag{2.26}$$

The torque equation for motor can be given as

$$T_e = T_L + J \frac{d\omega_m}{dt} + B\omega_m \tag{2.27}$$

And the torque equation for generator can be given as

$$T_e + T_{turbine} = J \frac{d\omega_m}{dt} + B\omega_m \quad (2.28)$$

where T_L =load torque, $T_{turbine}$ = turbine torque, J =rotor inertia, ω_m =mechanical speed = $2/p \omega_r$, ω_r = is the electrical speed of the rotor and P = pole pares of the machine.

The expression for the developed torque can be derived as

$$\begin{aligned} T_e &= \frac{3}{2} \frac{P}{2} (\Psi_{dm} i_{qs} - \Psi_{qm} i_{ds}) \\ &= \frac{3}{2} \frac{P}{2} (\Psi_{ds} i_{qs} - \Psi_{qs} i_{ds}) \\ &= \frac{3}{2} \frac{P}{2} (\Psi_{dr} i_{qr} - \Psi_{qr} i_{dr}) \\ &= \frac{3}{2} \frac{P}{2} (\Psi_{dm} i_{qr} - \Psi_{qm} i_{dr}) \\ &= \frac{3}{2} \frac{P}{2} L_m (i_{qs} i_{dr} - i_{ds} i_{qr}) \end{aligned} \quad (2.29)$$

Equations (2.26), (2.27),(2.28) and (2.29) give the complete model of the electro-mechanical dynamics of an induction machine in synchronous frame.

2.4 VECTOR OR FIELD ORIENTED CONTROL

The scalar control techniques is simple to implement, but due to inherent coupling effect i.e. both torque and flux are functions of voltage or current and frequency, gives sluggish response due to which the system becomes easily prone to instability because of higher order system effect. This problem can be solved by vector or field-oriented control. By this control technique the induction machine can be controlled like a separately excited dc machine. Because

of dc machine-like performance, vector control is also known as decoupling, orthogonal, or transvector control. Vector control is applicable to both induction and synchronous machine drives.

Consider the separately excited dc machine as shown in Figure 2.5. The developed torque is given by

$$T_e = K_t I_a I_f \quad (2.30)$$

where I_a = armature current and I_f = field current. The construction of dc machine is such that the field flux ψ_f produced by current I_f is perpendicular to the armature flux ψ_a , which is produced by armature current I_a . These space vectors, which are stationary in space are orthogonal or decoupled in nature. This means that when torque is controlled by controlling the current I_a , the flux ψ_f is not affected.

DC machine-like performance can also be extended to an induction motor if the machine control is considered in a synchronously rotating reference frame ($d^e - q^e$), where the sinusoidal variables appear as dc quantities in steady state. Figure 2.6 shows the induction machine with the inverter and vector control with the two control current inputs, i_{ds}^* and i_{qs}^* . With vector control, i_{ds} is analogous to field current I_f and i_{qs} is analogous to armature current I_a of a dc machine. Therefore, the torque equation can be expressed as

$$T_e = K_t \hat{\psi}_r i_{qs} \quad (2.31)$$

or

$$T_e = K_t i_{ds} i_{qs} \quad (2.32)$$

The dc machine like performance is only possible if the i_{ds} is aligned in the direction of $\hat{\psi}_r$ and i_{qs} is established perpendicular to it. This means that when i_{qs}^* is controlled, it affects the actual

i_{qs} current only, but does not affect the flux $\hat{\Psi}_r$. Similarly, when i_{ds}^* is controlled, it controls the flux only and does not affect the i_{qs} component of current.

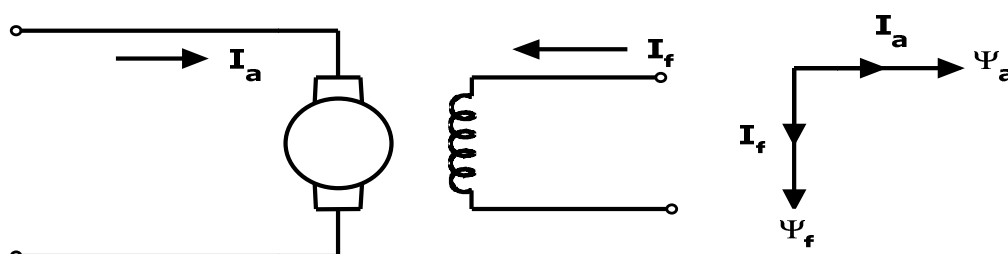


Figure 2.5 Separately excited dc machine

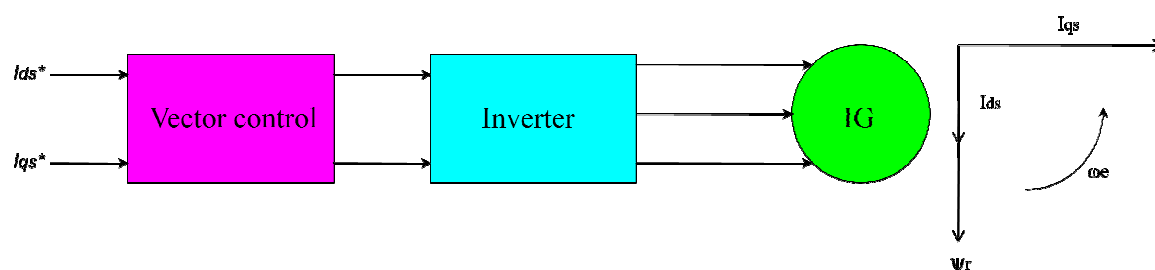


Figure 2.6 Vector-controlled induction machine

2.4.1 EQUIVALENT CIRCUIT AND PHASOR DIAGRAM

Consider the $d^e - q^e$ equivalent circuit diagram of induction machine under steady state condition as shown in Figure 2.7. The rotor leakage inductance L_{lr} is neglected for simplicity, which makes the rotor flux $\hat{\Psi}_r$ the same as the air gap flux $\hat{\Psi}_m$. The stator current \hat{I}_s can be expressed as

$$\hat{I}_s = \sqrt{i_{ds}^2 + i_{qs}^2} \quad (2.33)$$

where i_{ds} = magnetizing component of stator current flowing through the inductance L_m and i_{qs} = torque component of stator current flowing in the rotor circuit. Figure 2.8 and Figure 2.9 shows phasor diagrams in $d^e - q^e$ frame with peak value of sinusoids and air gap voltage \hat{V}_m aligned on

the q^e axis. The in-phase or torque component of current i_{qs} contributes the active power across the air gap, whereas the reactive or flux component of current i_{ds} contributes only reactive power. Figure 2.8 indicates an increase of the i_{qs} component of stator current to increase the torque while maintaining the flux Ψ_r constant, whereas Figure 2.9 indicates a weakening of the flux by reducing the i_{ds} component.

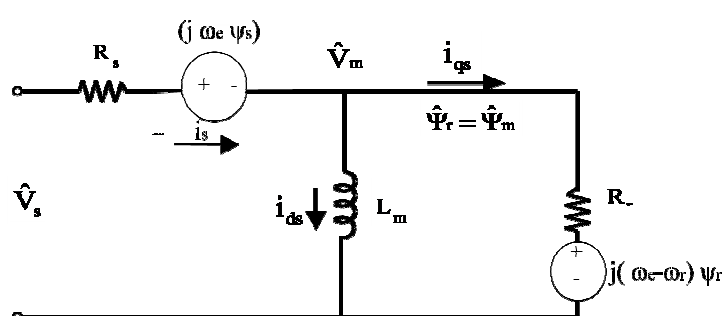


Figure 2.7 Complex (qds) equivalent circuit in steady state

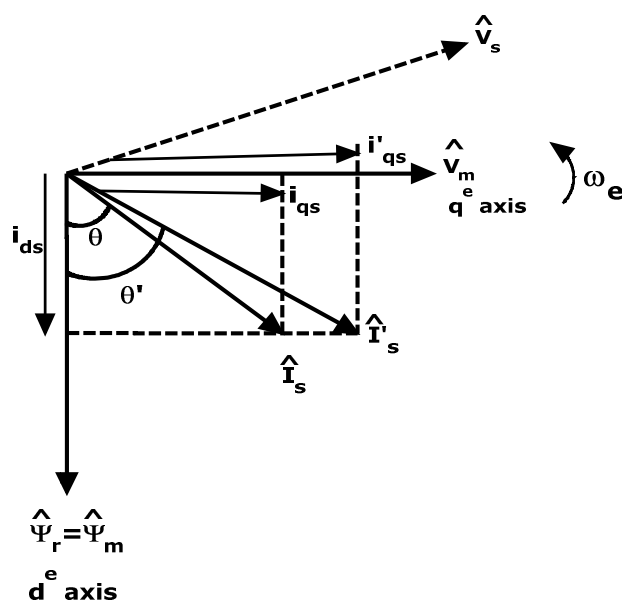


Figure 2.8 Steady-state phasor diagram with increase of torque component of current

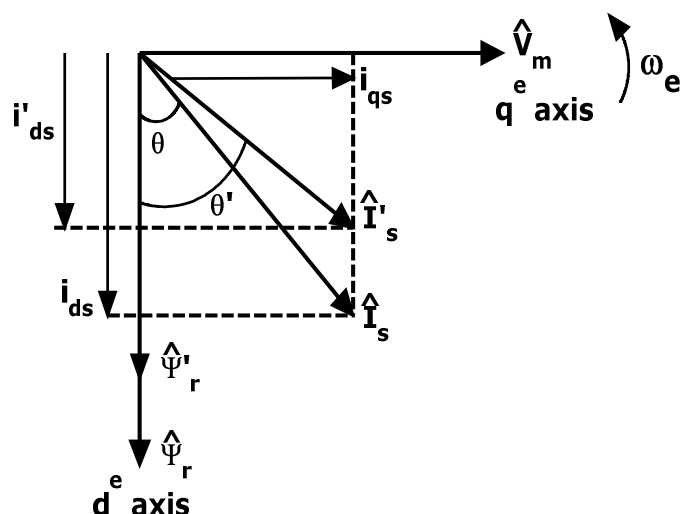


Figure 2.9 Steady-state phasor diagram with increase of flux component of current

2.4.2 PRINCIPLE OF VECTOR CONTROL

The fundamental of vector control implementation can be explained with the help of Figure 2.10, where the machine model is represented in a synchronously rotating reference frame. The inverter is omitted from the figure, assuming that it has unity current gain, that is,

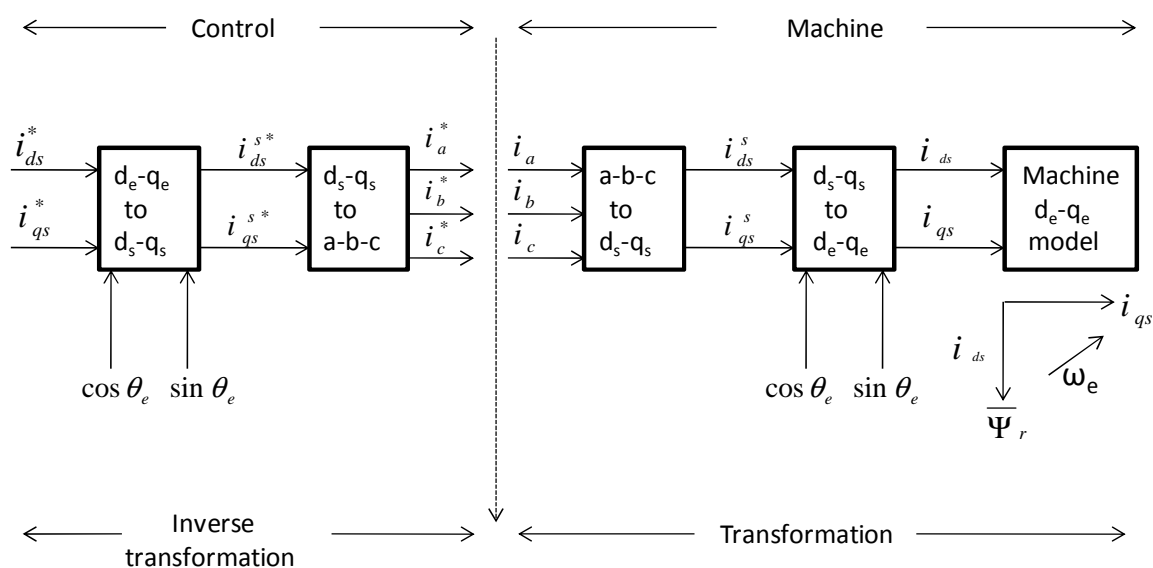


Figure 2.10 Vector control implementation principle with machine $d^e - q^e$ model

it generates currents i_a, i_b , and i_c as dictated by the corresponding command currents i_a^*, i_b^* , and i_c^* from the controller. A machine model with internal conversion is shown on the right. The machine terminal phase currents i_a, i_b , and i_c are converted to i_{ds}^s and i_{qs}^s components by $3\Phi/2\Phi$ transformation. These are then converted to synchronously rotating frame by the unit vector components $\cos\theta_e$ and $\sin\theta_e$ before applying them to the $d^e - q^e$ machine model as shown. The controller makes two stages of inverse transformation, so that the control currents i_{ds}^* and i_{qs}^* correspond to the machine currents i_{ds} and i_{qs} respectively. In addition, the unit vector assures correct alignment of i_{ds} current with the flux vector Ψ_r and i_{qs} perpendicular to it.

There are essentially two general methods of vector control. One, called the direct or feedback method, was invented by Blaschke and the other known as the indirect or feed-forward method was invented by Hasse. These two methods are different essentially by how the unit vector is generated for the control.

2.5 CONCLUSION

In this chapter the voltage and flux equations of the induction machine are discussed. The induction machine is modeled in the synchronously rotating reference frame and the final equation of the induction machine is represented in state space using d and q-axis stator and rotor currents as variables. The vector control strategy is also discussed in the chapter. The vector control technique and the state space equation of the induction machine are used in the coming chapters for simulation of the induction generator system.

Chapter 3

Indirect vector control of cage induction generator

3.1 INTRODUCTION

The control and estimation of wind energy conversion system constitute a vast subject and are more complex than those of dc drives. Induction generators with cage type rotors have been used extensively in wind power generation systems for the variable speed applications in a wide power range. Generally, variable speed wind energy conversion system with Induction generators require both wide operating range of speed and fast torque response, regardless of any disturbances and uncertainties (turbine torque variation, parameters variation and un-modelled dynamics). This leads to more advanced control methods to meet the real demand. The recent advances in the area of field-oriented control along with the rapid development and cost reduction of power electronics devices and microprocessors have made variable speed wind energy conversion system an economical alternative for wind power applications. The complexity of wind energy conversion system increases substantially if high performances are demanded. The main reasons for this complexity are the need of variable frequency, harmonically optimum converter power supplies, the complex dynamics of ac machines, machine parameter variations, and the difficulties of processing feedback signals in the presence of harmonics. The objective of this chapter is to illustrate the indirect vector control technique for induction generator in wind power applications.

3.2 INDIRECT VECTOR CONTROL OF INDUCTION GENERATOR

The indirect vector control method is essentially the same as the direct vector control, except that the rotor angle θ_e is generated in an indirect manner (estimation) using the measured speed ω_r and the slip speed ω_{sl} . Figure 3.1 explains the fundamental principle of indirect vector control with the help of phasor diagram. The $d^s - q^s$ axes are fixed on the stator, but the $d^r - q^r$ axes, which are fixed on the rotor, are moving at speed ω_r , as shown. Synchronously rotating axes $d^e - q^e$ are rotating ahead of the $d^r - q^r$ axes by the positive slip angle θ_{sl} corresponding to slip frequency ω_{sl} . Since the rotor pole is directed on the d^e axis and $\omega_e = \omega_r + \omega_{sl}$, so we have

$$\theta_e = \int \omega_e dt = \int (\omega_r + \omega_{sl}) dt = \theta_r + \theta_{sl} \quad (3.1)$$

The phasor diagram suggests that for decoupling control, the stator flux component of current i_{ds} should be aligned on the d^e axis, and the torque component of current i_{qs} should be on the q^e axis as shown in Figure 3.1.

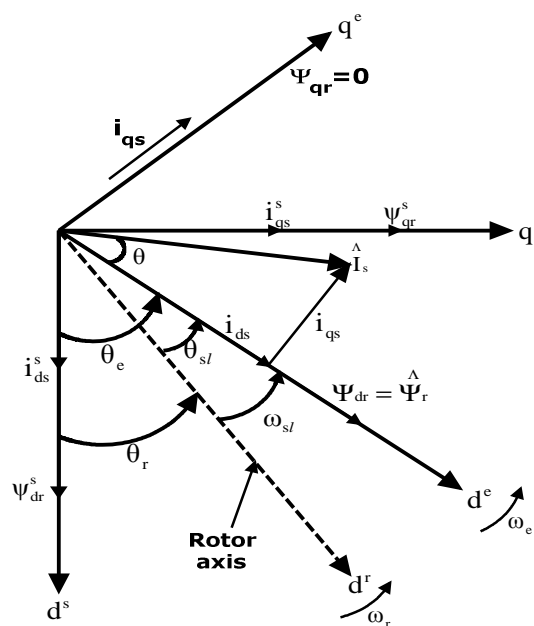


Figure 3.1 Phasor diagram explaining indirect vector control

The rotor circuit equations can be written as

$$\frac{d\Psi_{dr}}{dt} + R_r i_{dr} - (\omega_e - \omega_r) \Psi_{qr} = 0 \quad (3.2)$$

$$\frac{d\Psi_{qr}}{dt} + R_r i_{qr} + (\omega_e - \omega_r) \Psi_{dr} = 0 \quad (3.3)$$

By eliminating rotor currents which are inaccessible, we have

$$\frac{d\Psi_{dr}}{dt} + \frac{R_r}{L_r} \Psi_{dr} - \frac{L_m}{L_r} R_r i_{ds} - \omega_{sl} \Psi_{qr} = 0 \quad (3.4)$$

$$\frac{d\Psi_{qr}}{dt} + \frac{R_r}{L_r} \Psi_{qr} - \frac{L_m}{L_r} R_r i_{qs} + \omega_{sl} \Psi_{dr} = 0 \quad (3.5)$$

For decoupling control

$$\Psi_{qr} = 0 \quad (3.6)$$

and,

$$\frac{d\Psi_{qr}}{dt} = 0 \quad (3.7)$$

So we have

$$\frac{L_r}{R_r} \frac{d\psi_r}{dt} + \psi_r = L_m i_{ds} \quad (3.8)$$

And the slip frequency for decoupling control is given as:

$$\omega_{sl} = \frac{L_m R_r}{\psi_r L_r} i_{qs} = \frac{R_r i_{qs}}{L_r i_{ds}} \quad (3.9)$$

If the rotor flux $\hat{\Psi}_r = \text{constant}$, we have

$$\hat{\Psi}_r = L_m i_{ds} \quad (3.10)$$

The block diagram of indirect vector control scheme for induction machine drive is shown in

Figure 3.2. The PWM inverters are not modelled and simulated in this work. The inverters are considered to have instantaneous response with fixed gain.

The speed and current controllers may be PI controllers, Fuzzy controllers or any controller which is used to improve the transient as well as steady state performance of the induction machine drive. The simulation results of this drive system with PI- controllers is discussed in this chapter. The performance comparison of the drive system incorporating different controllers is done in the next chapter. (*Chapter-5.*)

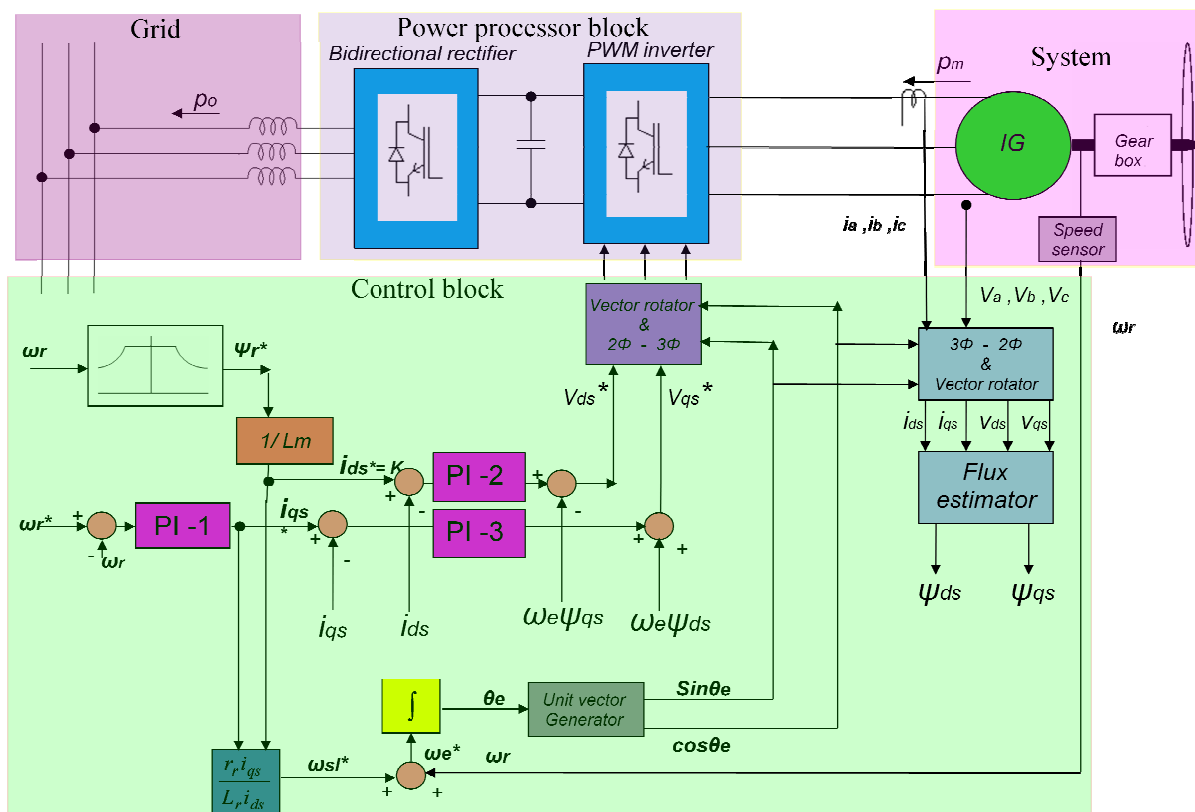


Figure 3.2 Block diagram of indirect vector controlled induction generator system

In the above given scheme the whole control structure consists of a speed control loop and two current control loops. In the speed control loop the rotor speed is compared with the reference speed and the speed error is then fed to the PI-controller (PI-1) which generates the reference current command i_{qs}^* . Then in the current control loop the current error is generated by comparing the current i_{qs} with its reference value and the error is then given to a

PI controller (PI-3) . The output of PI-3 after CEMF compensation gives the reference quadrature axis voltage command v_{qs}^* . Similarly for the direct axis current control loop the reference value for rotor flux is generated from the rotor speed signal through a flux limiter. According to equation (3.10) we get the reference command i_{ds}^* . The direct axis current error is generated by comparing i_{ds} with its reference value and the error is then fed to a PI controller (PI-2). The output of controller PI-2 after CEMF compensation gives the reference direct axis voltage command V_{ds}^* . In this control scheme the control loop consisting of PI-1 and PI-3 controls the active power of the induction generator where as the control loop consisting of PI-2 controls the reactive power flowing to the induction generator.

3.3 SIMULATION RESULTS AND DISCUSSION

The drive system is simulated with PI controllers with different operating conditions such as step change in the reference speed and step change in turbine torque and some sample results are presented in the following section.

3.3.1 STEP CHANGE IN TURBINE TORQUE

A step change in command for turbine torque from 10 Nm to 15 Nm is given at $t = 2.5s$ which continues for 0.5s and again returns to the previous value. The electromagnetic torque response of the induction generator with PI controllers is shown in Figure 3.3. With PI control it takes approximately 0.3s to achieve steady state which can be seen clearly from Figure 3.3. From Figure 3.3 it can be seen that there is an overshoot of 4% which is within the allowable range.

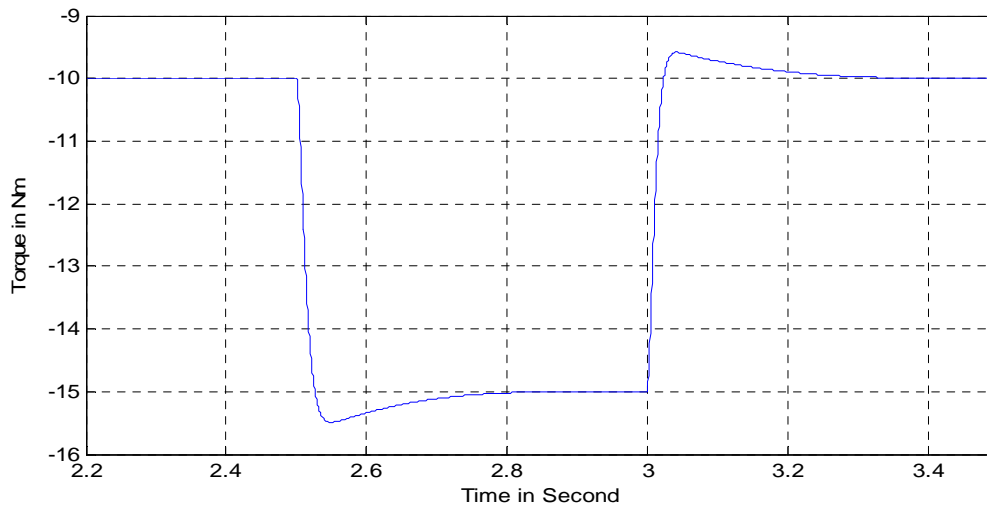


Figure 3.3 *Electromagnetic torque response*

Figure 3.4 shows the speed response of the induction generator during change in the turbine torque. From this figure it can be observed that during the prime mover torque change even if the reference speed command is 1880 rpm, the actual speed changes for a transient period and then settles to 1880 rpm again.

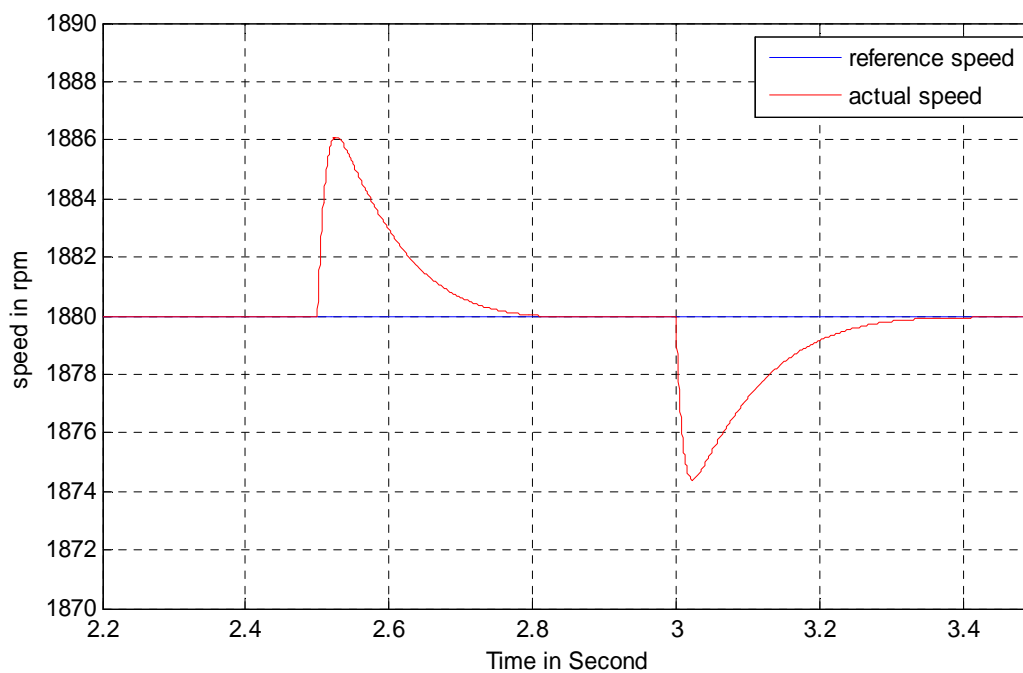


Figure 3.4 *Speed response*

The active and reactive power responses are given in Figure 3.5. In the Figure 3.6 the direct and quadrature axis current responses are given. From Figure 3.6 it is clear that due to change in turbine torque the quadrature axis current or the torque component of current changes whereas the flux component or the direct axis current almost remains unchanged, which is due to the effect of vector control strategy. The rotor flux ' ψ_r ', and flux component of stator current ' i_{ds} ', are maintained constant through vector control. As the speed increases temporarily, due to the increase in turbine torque, both generated voltage V_{ph} , and frequency f , increase by the same factor. Thus reactive power, which is given by $\frac{V^2}{X_m}$, increases by the same factor. The magnitude of the active power increases, as the input power increases.

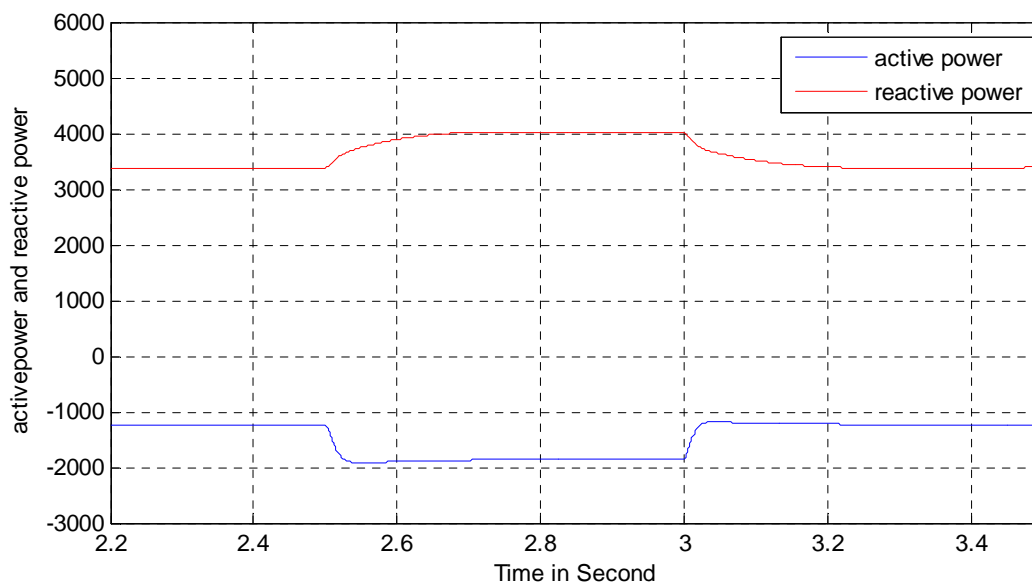


Figure 3.5 Active and reactive power responses

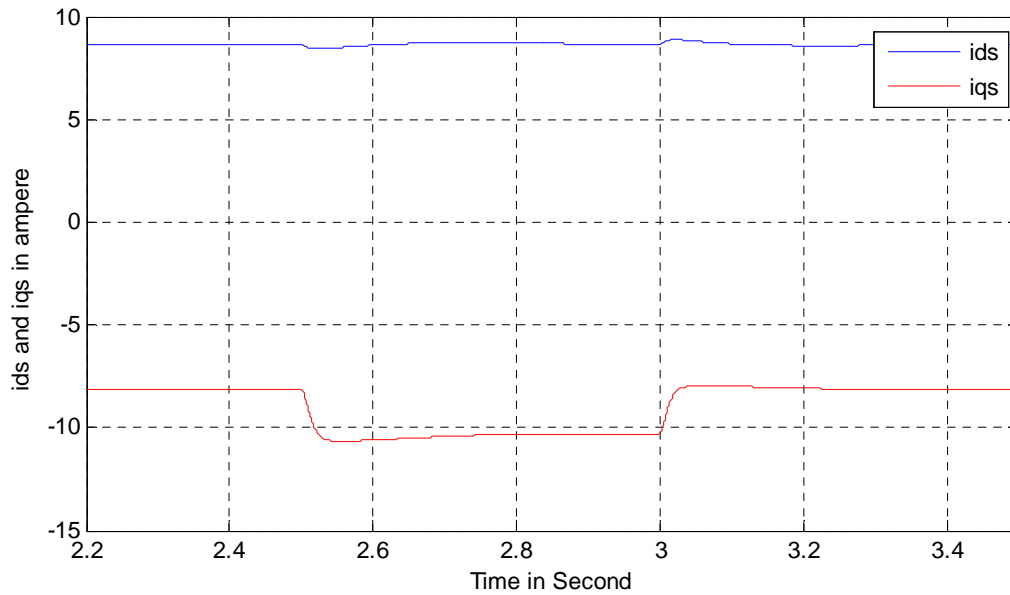


Figure 3.6 *Direct and quadrature axis current responses*

The power factor response is given in Figure 3.7, which shows that as the turbine torque change from 10 Nm to 15 Nm the power factor increases from 0.342 to 0.42. Figure 3.8 shows the generated phase current response.

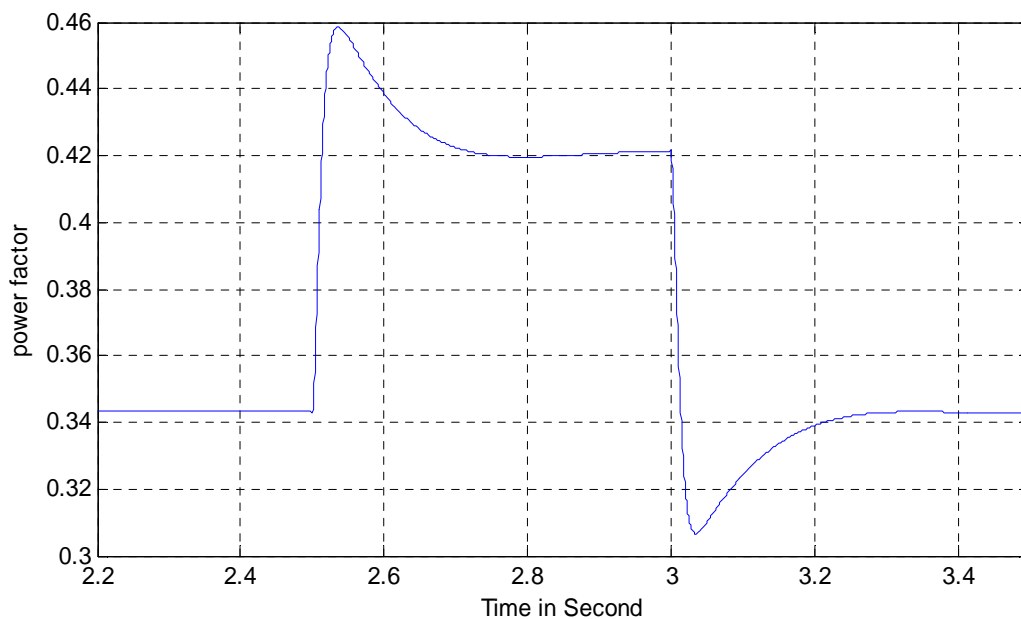


Figure 3.7 *Power factor*

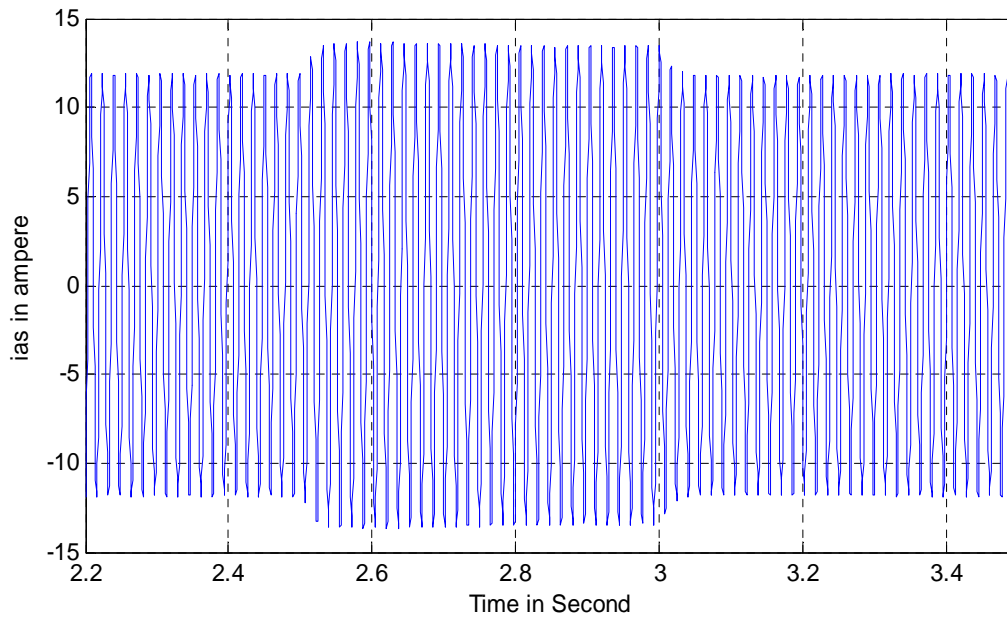
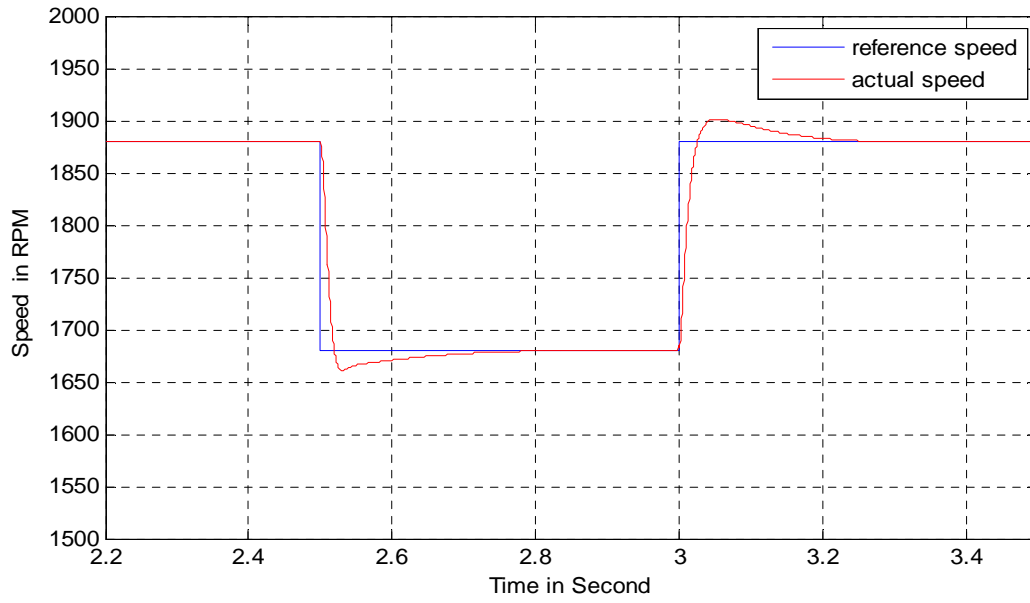
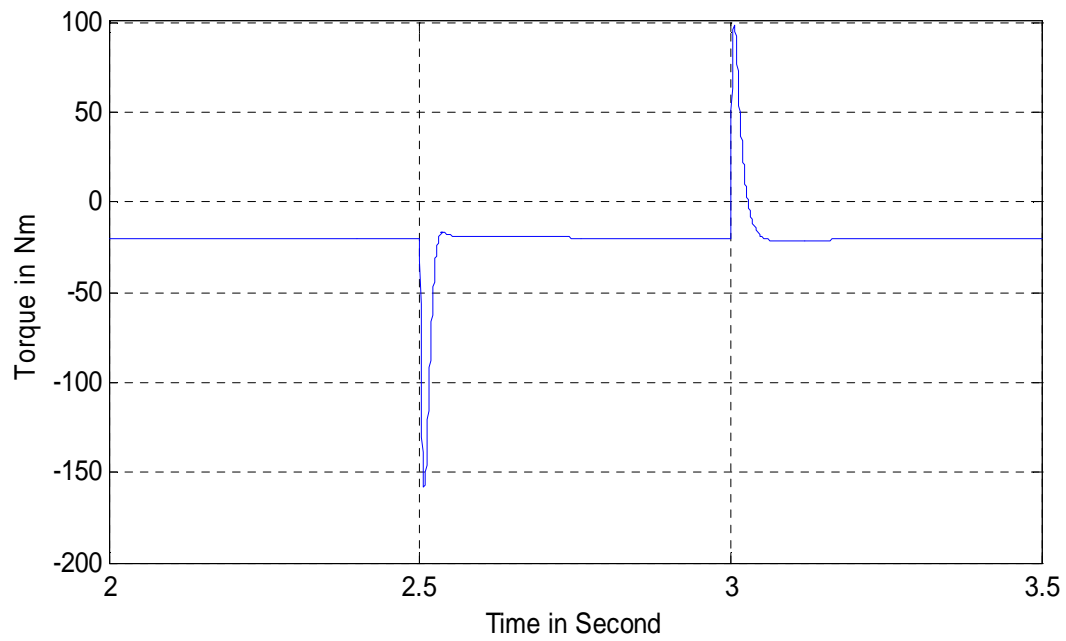


Figure 3.8 *Phase current*

3.3.2 STEP CHANGE IN REFERENCE SPEED COMMAND

The performance of the drive system is again evaluated by subjecting the system to a step change in the reference speed. A step decrease of 200 rpm, from 1880 rpm to 1680 rpm is given to the reference speed and the speed response of the vector controlled induction generator is given in Figure 3.9. Figure 3.10 shows the torque response of the induction generator. As there is no change in the input torque, the electromagnetic torque of the machine changes for a transient period and then returns to the initial value.

Figure 3.9 *Speed response*Figure 3.10 *Electromagnetic torque response*

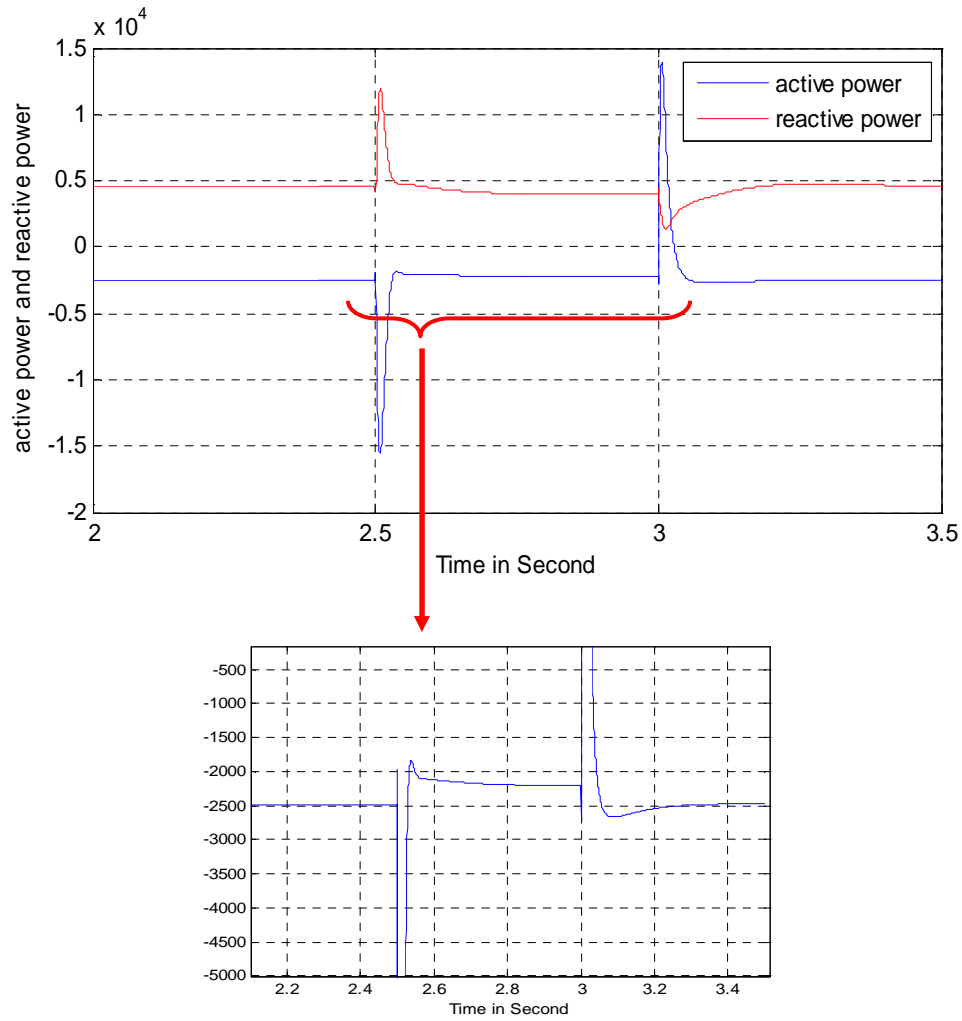


Figure 3.11 Active and reactive power response

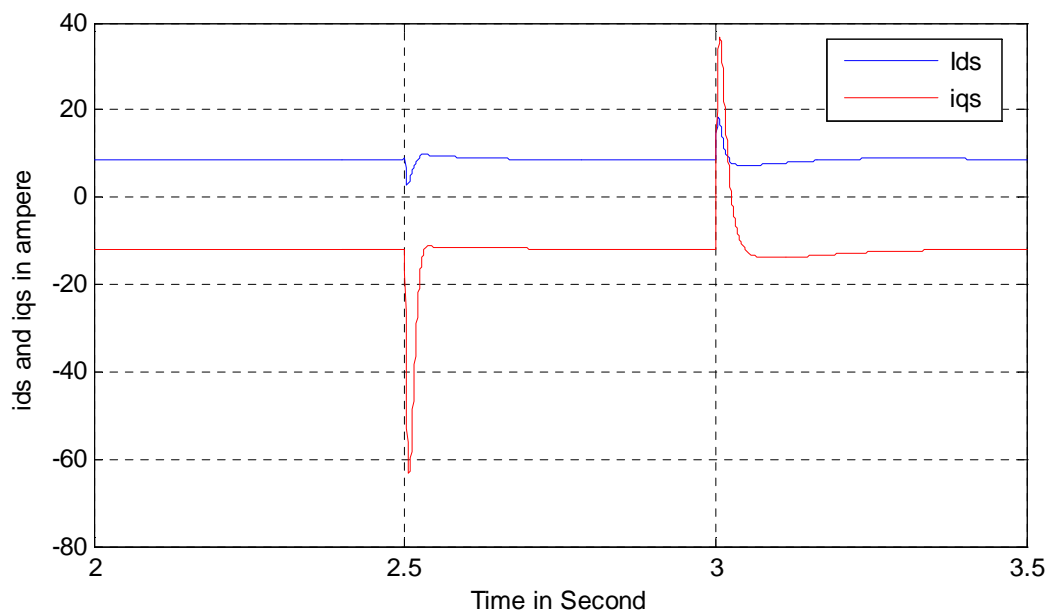


Figure 3.12 Direct and quadrature axis current response

Figure 3.11 shows the active and reactive power response of the induction generator. In this figure it can be seen that the active power is reduced with the reduction in speed due to the fact that the power input to the machine is reduced. The Figure 3.12 shows the direct and quadrature axis current response of the machine when a change in reference speed command is given.

3.4 CONCLUSION

Thus with indirect vector control using PI controllers the performance of the wind energy conversion system using induction generator is improved. The induction machine shows a dc machine like performance due to the indirect vector control. The transient as well as the steady state performances of the drive system are improved. The active power, reactive power and line current values change for a very short transient time or else remain constant thus improving the stability of the system.

Chapter 4

Performance improvement of field oriented induction generator using modern controllers

4.1 INTRODUCTION

In the previous section we have studied the performance of a field oriented induction generator used for wind power applications. The vector control scheme in the previous section was done employing PI controllers due to which the performance of the machine in transient period was improved but could not be made optimum. In this section some advanced controllers will be employed in place of the PI controllers to further improve the transient performance of the induction generator system. In this section first we will study the induction generator system using fuzzy controller. Then a self tuned fuzzy controller will be developed for the induction generator system. Then the performance of the induction generator system employing a hybrid controller will be studied and the performances of each controller will be compared.

4.2 FUZZY CONTROLLER

4.2.1 INTRODUCTION

In 1965, Lotfi A. Zadeh of the University of California at Berkeley published "Fuzzy Sets," which laid out the mathematics of fuzzy set theory and, by extension, fuzzy logic. Zadeh had observed that conventional computer logic couldn't manipulate data that represented subjective or vague ideas, so he created fuzzy logic to allow computers to determine the distinctions among data with shades of gray, similar to the process of human reasoning. Fuzzy logic, as its name suggests, is the logic underlying modes of reasoning which are approximate rather than exact. The importance of fuzzy logic derives from the fact that most modes of human reasoning and especially common sense reasoning are approximate in nature. In doing so, the fuzzy logic approach allows the designer to handle efficiently very complex closed-loop control problems. There are many artificial intelligence techniques that have been employed in modern power systems, but fuzzy logic has emerged as the powerful tool for solving challenging problems. As compared to the conventional PI, PID controllers, and their adaptive versions, the FLC has some advantages such as:

- 1) it does not need any exact system mathematical model.
- 2) it can handle nonlinearity of arbitrary complexity.
- 3) it is based on the linguistic rules with an IF-THEN general structure, which is the basis of human logic.

4.2.2 FUZZY SETS

Fuzzy set, as the name implies, is a set without a crisp boundary. The transition from "belong to a set" to "not belong to a set" is gradual, and this smooth transition is characterized by membership functions. The fuzzy set theory is based on fuzzy logic, where a particular object

has a degree of membership in a given set that may be anywhere in the range of 0 to 1. On the other hand, classical set theory is based on Boolean logic, where a particular object or variable is either a member of a given set (logic 1), or it is not (logic 0).

4.2.3 MEMBERSHIP FUNCTIONS

A membership function is a curve that defines how the values of a fuzzy variable in a certain region are mapped to a membership value μ (or degree of membership) between 0 and 1. If X is a collection of objects denoted generically by x , then a fuzzy set A in X is defined as a set of ordered pairs:

$$A = \{(x, \mu_A(x)) / x \in X\}, \quad (4.1)$$

where $\mu_A(x)$ is called the membership function for the set A . There exist different shapes of membership functions. The shapes could be triangular, trapezoidal, curved or their variations.

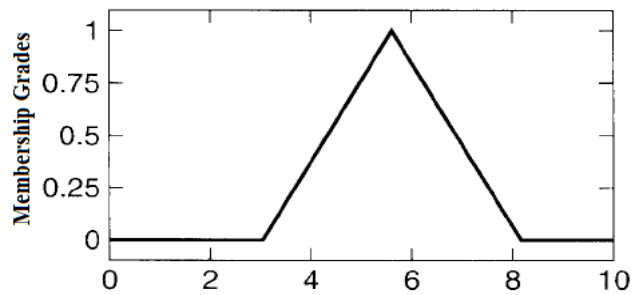
The various types of membership functions are given below.

4.2.3.1 Triangular Membership Functions

A triangular Membership Function is specified by three parameters $\{a, b, c\}$ as follows:

$$\text{triangle}(x; a, b, c) = \begin{cases} 0, & x \leq a. \\ \frac{x-a}{b-a}, & a \leq x \leq b. \\ \frac{c-x}{c-b}, & b \leq x \leq c. \\ 0, & c \leq x. \end{cases} \quad (4.2)$$

For example the triangular membership function $\text{triangle}(x; 3, 5.8, 8.1)$ can be illustrated as shown in Figure 4.1.

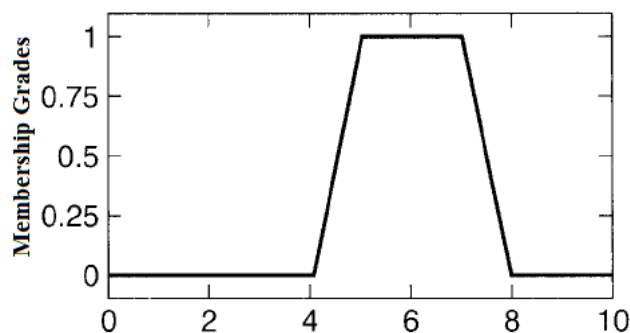
Fig 4.1 *Triangular Membership Function*

4.2.3.2 Trapezoidal Membership Functions

A trapezoidal membership function is specified by four parameters $\{a, b, c, d\}$:

$$\text{trapezoid}(x; a, b, c, d) = \begin{cases} 0, & x \leq a. \\ \frac{x-a}{b-a}, & a \leq x \leq b. \\ 1, & b \leq x \leq c. \\ \frac{d-x}{d-c}, & c \leq x \leq d. \\ 0, & d \leq x. \end{cases} \quad (4.3)$$

For example the trapezoidal membership function $\text{trapezoid}(x; 4, 5, 7, 8)$ can be illustrated as shown in Figure 4.2.

Figure 4.2 *Trapezoidal Membership Function*

In real time implementation, both the triangle membership functions and trapezoidal membership functions have been used extensively due to their simple formulas and computational efficiency. These two membership functions can have symmetrical or unsymmetrical shape.

4.2.3.3 Gaussian Membership Functions

A Gaussian membership function is specified by two parameters $\{c, \sigma\}$:

$$\text{gaussian}(x; c, \sigma) = e^{-\frac{1}{2} \left(\frac{x-c}{\sigma} \right)^2} \quad (4.4)$$

A Gaussian membership function is determined completely by c and σ ; c represents the membership functions centre and σ determines the membership functions width. Figure 4.3 plots a Gaussian membership function defined by $\text{gaussian}(x; 5, 2)$.

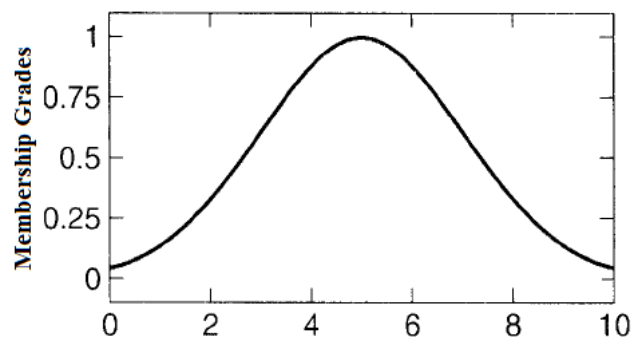


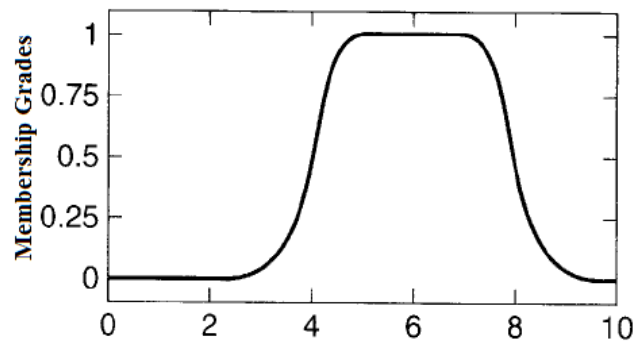
Figure 4.3 *Gaussian Membership Function*

4.2.3.4 Generalized bell Membership Functions

A generalized bell membership function is specified by three parameters $\{a, b, c\}$:

$$\text{bell}(x; a, b, c) = \frac{1}{1 + \left| \frac{x-c}{a} \right|^{2b}} \quad (4.5)$$

where the parameter b is usually positive. If b is negative, the shape of this membership function becomes an upside-down bell. Figure 4.4 plots a Generalized bell membership function defined by $\text{bell}(x; 3, 0.4, 5)$.

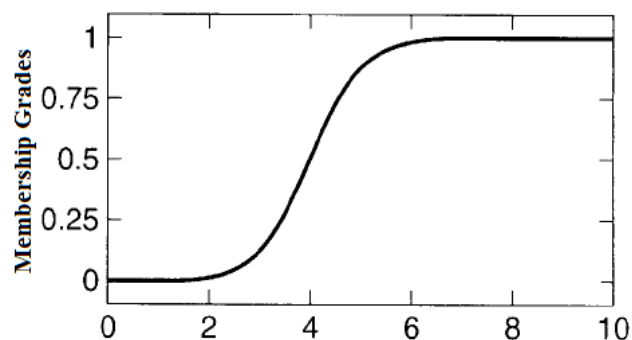
Figure 4.4 *Generalized bell Membership Function*

4.2.3.5 Sigmoidal Membership Functions

A sigmoidal membership function is defined by:

$$\text{sig}(x; a, c) = \frac{1}{1 + \exp[-a(x - c)]} \quad (4.6)$$

where a controls the slope at the crossover point $x=c$. Depending on the sign of the parameter a , a sigmoidal membership function is inherently open right or left. Figure 4.5 plots a Sigmoidal membership function defined by $\text{sig}(x; 1, -5)$.

Figure 4.5 *Sigmoidal Membership Function*

4.2.4. FUZZY SYSTEMS

The fuzzy inference system or fuzzy system is a popular computing framework based on the concept of fuzzy set theory, fuzzy if-then rules, and fuzzy reasoning. The fuzzy inference system basically consists of a formulation of the mapping from a given input set to an output set

using FL as shown in Figure 4.6. The mapping process provides the basis from which the inference or conclusion can be made. The basic structure of fuzzy inference system consists of three conceptual components: *a rule base*, which contains a selection of fuzzy rules; *a data base*, which defines the membership functions used in the fuzzy rules; and *a reasoning mechanism* which performs the inference procedure upon the rules and given facts to derive a reasonable output or conclusion.

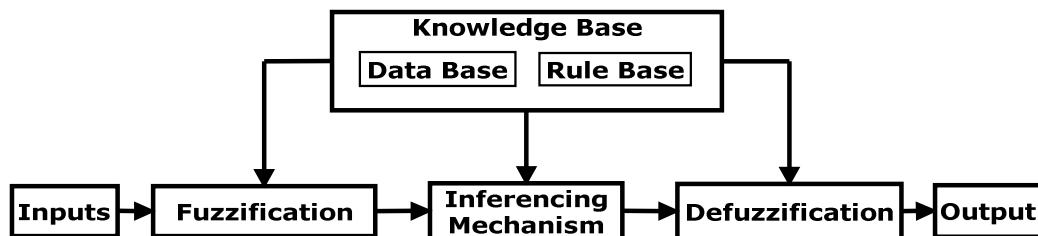


Figure 4.6 *Fuzzy Inference System*

The basic inference process consists of the following five steps:

- Step 1: Fuzzification of input variables
- Step 2: Application of fuzzy operator (AND, OR, NOT) in the IF (antecedent) part of the rule.
- Step 3: Implication from the antecedent to the consequent THEN part of the rule
- Step 4: Aggregation of the consequents across the rules
- Step 5: Defuzzification

4.2.4.1 Implication Methods

There are number of implication methods to fuzzy logic but only two widely used methods are discussed here. Those are Mamdani type fuzzy model and Sugeno type fuzzy model.

4.2.4.1.1 Mamdani fuzzy model

Mamdani fuzzy rule for a fuzzy controller involving three input variables and two output variables can be described as follows:

IF x_1 is A AND x_2 is B AND x_3 is C THEN z_1 is D , z_2 is E

where x_1 , x_2 , and x_3 are input variables (e.g., error, its first derivative and its second derivative), and z_1 and z_2 are output variables. In theory, these variables can be either continuous or discrete; practically speaking, they should be discrete because virtually all fuzzy controllers and models are implemented using digital computers. A , B , C , D and E are fuzzy sets. "IF x_1 is A AND x_2 is B AND x_3 is C " is called the rule antecedent, whereas the remaining part is named the rule consequent.

The structure of Mamdani fuzzy rules for fuzzy modelling is the same. The variables involved, however, are different. An example of a Mamdani fuzzy rule for fuzzy modelling is:

IF $y(t)$ is A AND $y(t - 1)$ is B AND $y(t - 2)$ is C AND $u(t)$ is D AND $u(t - 1)$ is E
THEN $y(t + 1)$ is F

where A , B , C , D , E , and F are fuzzy sets, $y(t)$, $y(t - 1)$, and $y(t - 2)$ are the output of the system to be modelled at sampling time t , $t - 1$ and $t - 2$, respectively. And, $u(t)$ and $u(t - 1)$ are system input at time t and $t - 1$, respectively; $y(t + 1)$ is system output at the next sampling time, $t + 1$.

Obviously, a general Mamdani fuzzy rule, for either fuzzy control or fuzzy modelling, can be expressed as

IF x_1 is A_1 AND x_2 is A_2 AND ... AND x_k is A_k THEN z_1 is B_1 , z_2 is B_2 ..., z_m is B_m

where x_i is the input variable, $i = 1, 2, \dots, k$ and z_j is the output variable, $j = 1, 2, \dots, m$. A_k is the input fuzzy set and B_m is the output fuzzy set.

4.2.4.1.2 Sugeno fuzzy model

The Sugeno fuzzy model or TSK fuzzy model was proposed by Takagi, Sugeno, and Kang and was introduced in 1985. A typical fuzzy rule in a Sugeno fuzzy model has the form

$$\text{If } x \text{ is } A \text{ and } y \text{ is } B \text{ then } z = f(x, y),$$

where A and B are fuzzy sets in the antecedent, while $z = f(x, y)$ is a crisp function in the consequent. Usually $z = f(x, y)$ is a polynomial in the input variables x and y , but it can be any function as long as it can appropriately describe the output of the model within the fuzzy region specified by the antecedent of the rule. When $z = f(x, y)$ is a first-order polynomial, the resulting fuzzy inference system is called a first-order Sugeno fuzzy model. When f is a constant, we then have a zero-order Sugeno fuzzy model.

4.2.4.2 Defuzzification Methods

Defuzzification refers to the way a crisp value is extracted from a fuzzy set as a representative value. Several methods are available for defuzzification. Here, a few of the widely used methods namely centroid method, centre of sums and mean of maximum are discussed.

4.2.4.2.1 Centroid Method

Centroid method is also known as centre of gravity method, it obtains the centre of area z^* occupied by the fuzzy set A of universe of discourse Z . It is given by the expression

$$z^* = \frac{\int_Z \mu_A(z)z \, dz}{\int_Z \mu_A(z) \, dz} \quad (4.7)$$

for a continuous membership function,

and

$$z^* = \frac{\sum_{i=1}^n z_i \mu(z_i)}{\sum_{i=1}^n \mu(z_i)} \quad (4.8)$$

for a discrete membership function.

Where $\mu_A(z)$ is the aggregated output MF. This is the most widely adopted defuzzification strategy, which is reminiscent of the calculation of expected values of probability distributions.

4.2.4.2.2 Centre of Sums (COS) Method

In the centroid method, the overlapping area is counted once whereas in centre of sums, the overlapping area is counted twice. COS builds the resultant membership function by taking the algebraic sum of outputs from each of the contributing fuzzy sets A_1, A_2, A_3, \dots , etc. The defuzzified value z^* is given by

$$z^* = \frac{\sum_{i=1}^N z_i \sum_{k=1}^n \mu_{A_k}(z_i)}{\sum_{i=1}^N \sum_{k=1}^n \mu_{A_k}(z_i)} \quad (4.9)$$

where n is the number of fuzzy sets and N is the number of fuzzy variables.

4.2.4.2.3 Mean of Maxima (MOM) Defuzzification

MOM is the average of the maximizing z^* at which the MF reach maximum μ^* . In symbols,

$$z^* = \frac{\sum_{z_i \in M} z_i}{|M|} \quad (4.10)$$

where $M = \{ z_i | \mu(z_i) \text{ is the height of the fuzzy set} \}$ and $|M|$ is the cardinality of the set M .

4.2.5 DESIGN OF FUZZY LOGIC CONTROLLER

The basic structure of the fuzzy logic controller is given in Figure 4.7, where the inputs to the fuzzy logic controller are the normalized values of error ' e ' and change of error ' ce '. Normalization is done to limit the universe of discourse of the inputs between -1 to 1 such that the controller can be successfully operated within a wide range of input variation. Here ' K_e ' and ' K_{ce} ' are the normalization factors for error input and change of error input respectively. For this fuzzy logic controller design, the normalization factors are taken as constants. The output of the fuzzy logic controller is then multiplied with a gain ' K_o ' to give the appropriate control signal ' U '. The output gain is also taken as a constant for this fuzzy logic controller. K_e is taken to be the synchronous speed because when the machine is used as a generator the slip remains below 8% (-ve). So for any variation in reference speed the speed error remains below unity. Similarly K_{ce} is chosen to be the maximum value of change that can occur in speed error. K_{ce} is chosen by trial and error method.

Basically, the fuzzy logic controller consists of four blocks i.e. fuzzification, fuzzy inferencing engine, knowledge base and a defuzzification block.

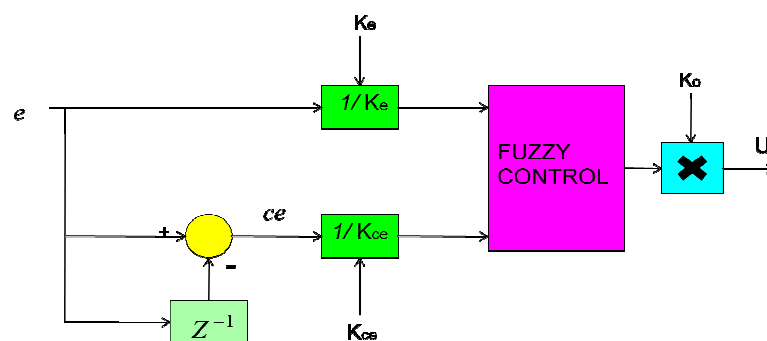


Figure 4.7 Structure of fuzzy logic controller

4.2.5.1 Input/output Variables

The design starts with assigning the mapped variables Inputs/output of the FLC. In this work, the first controller to be designed is the fuzzy logic controller used for speed control in the active power control loop. The first input variable to the speed controller FLC-1 is the speed error “ e_ω ” and the second is the change in the speed error “ ce_ω ” at the k^{th} sampling time “ kt_s ”. The two input variables $e_\omega(kt_s)$ and $ce_\omega(kt_s)$ are calculated at every sampling time as:

$$e_\omega(kt_s) = \omega_r^*(kt_s) - \omega_r(kt_s) \quad (4.11)$$

$$ce_\omega(kt_s) = e_\omega(kt_s) - e_\omega((k-1)t_s) \quad (4.12)$$

where ‘ $\omega_r(kt_s)$ ’ is the actual rotor speed, ‘ $\omega_r^*(kt_s)$ ’ is the reference speed and ‘ $e_\omega((k-1)t_s)$ ’ is the value of error at a previous sampling time. The output variable of FLC-1 is the reference value of torque component of current ‘ i_{qs}^* ’. Next controller to be designed is the current controller in the active power control loop. The current controller FLC-3 takes the normalized values of error in ‘ i_{qs} ’ and the change of error in ‘ i_{qs} ’ as inputs. The output of the controller after gain multiplication and CEMF compensation gives the quadrature axis control voltage V_{qs}^* which controls the active power of the induction generator.

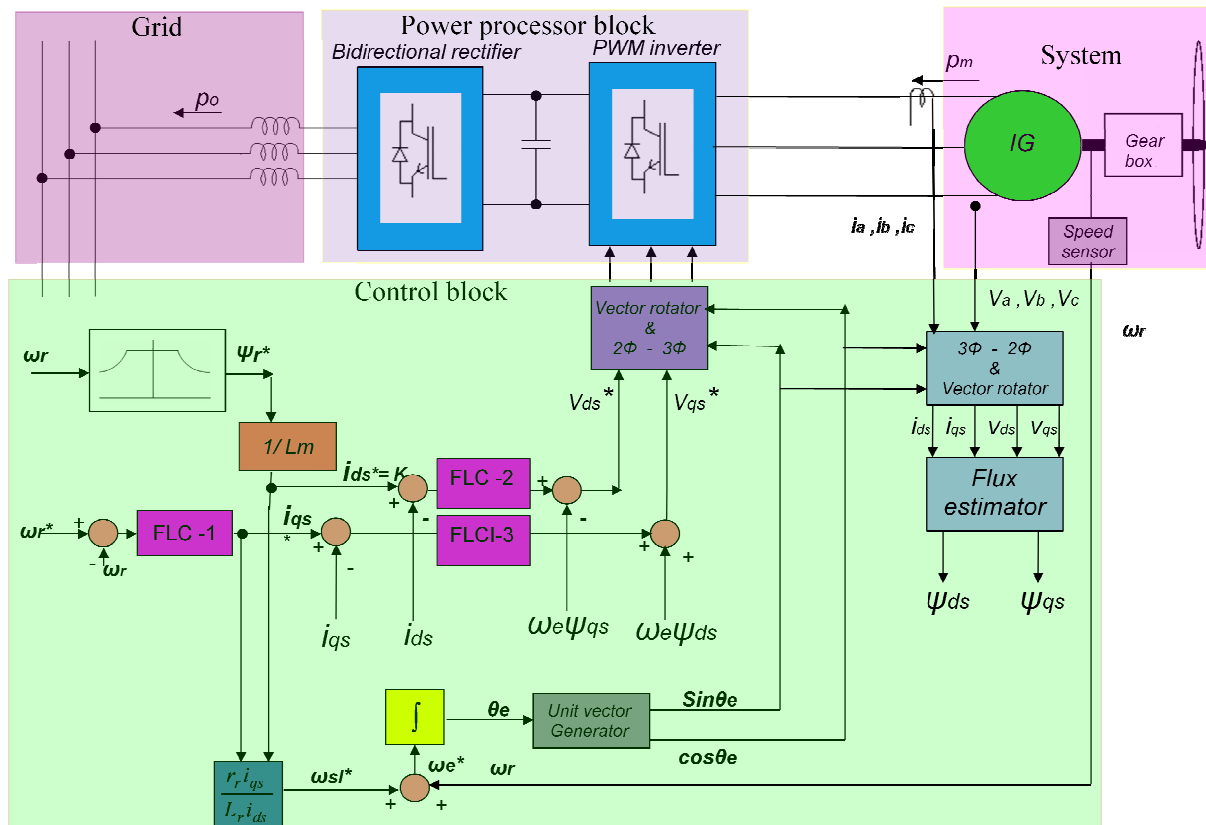


Figure 4.8 Control scheme using fuzzy logic controllers

After the design of the FLC's in the active power control loop, comes the design of the FLC in the reactive power control loop. The reference flux signal is generated from the speed command through a function generator implementing flux weakening controller. The reference flux is then divided by ' L_m ', the mutual inductance of the induction generator to get the reference command for the flux component of current ' i_{ds}^* '. FLC-2, the current controller in the reactive power control loop is then fed with the normalized values of error in ' i_{ds} ' and the change of error in ' i_{ds} ' as the inputs. The output of the controller 'FLC-2' after gain multiplication and CEMF compensation gives the direct axis control voltage V_{ds}^* which controls the reactive power of the induction generator. The whole control scheme using fuzzy logic controllers is given in Figure 4.8.

The input error membership functions are shown in Figure 4.9. The input error fuzzy sets use both triangular and trapezoidal membership functions, which are found to be optimum. Triangular membership functions as shown in Figure 4.10 are used for change of error input. The output membership functions are shown in Figure 4.11. All the membership functions are chosen to be triangular or trapezoidal in nature to reduce the computational burden on the computer and to make the controllers more suitable for real time applications. The output membership functions are chosen by a trial and error basis such that the controller gives optimum results i.e. faster response with low steady state error. For this reason some unsymmetry can be seen in the output membership functions which is clear from Figure 4.11. It can be seen that the membership functions are crowded towards 'zero' which is done to make the steady state error zero. This also increases the speed of response of the system.

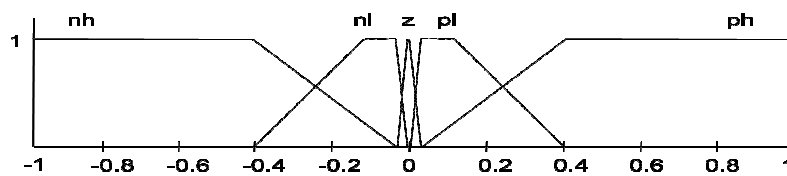


Figure 4.9 Membership function for input variable 'e'

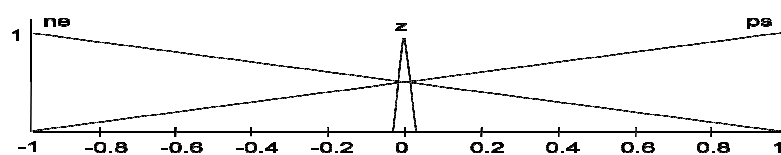


Figure 4.10 Membership function for input variable 'ce'

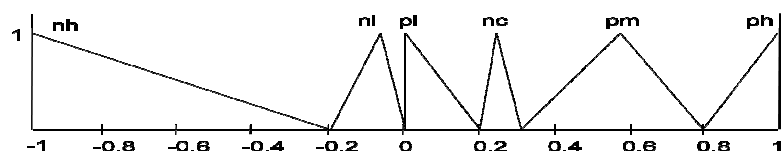


Figure 4.11 Membership function for output variable

4.2.5.2 Fuzzification

In this stage the crisp variables of the inputs ' e ' and ' ce ' are converted into fuzzy variables that can be identified by the levels of membership in the fuzzy set. Each fuzzy variable is a member of the subsets with a degree of membership ' μ ' varying between 0 (non-member) to 1. The fuzzy sets for error input are defined as z = Zero, pl = Positive low, ph = Positive high, nl = Negative low, nh = Negative high. The fuzzy sets for change of error input are defined as ne = Negative, z = Zero and ps = Positive. The output fuzzy sets are given as nh = Negative high, nl = Negative low, nc = No change, pl = Positive low, pm = Positive medium and ph = Positive high.

The universe of discourse of all the variables, covering the whole region, is expressed in per unit values. All membership functions have asymmetrical shape with more crowding near the origin. This permits higher precision at steady state.

4.2.5.3 Knowledge Base and Inferencing

Knowledge base involves defining the rules represented as IF-THEN rules statements governing the relationship between inputs and output variables in terms of membership functions. In this stage the input variables ' e ' and ' ce ' are processed by the inference engine that executes 5×3 rules represented in rule Table 4.1. A typical rule can be written as follows.

If e is a_k and ce is b_k then output is c_k

where a_k , b_k , c_k are the labels of linguistic variables of error (e), change of error (ce) and output (U) respectively. Inferencing stage also includes application of fuzzy operator AND, OR, NOT,

implication and aggregation. By definition of AND, evaluation of rule results in a minimum of $\mu_{ak}(x)$, $\mu_{bk}(x)$ allocated to $\mu_{ck}(x)$.

Table 4.1

<i>ce</i> \ <i>e</i>	nh	nl	ze	pl	ph
ne	nh	nl	nc	pm	ph
ze	nh	nl	nc	pm	ph
ps	nh	nl	pl	pm	ph

4.2.5.4 Defuzzification

In defuzzification stage the fuzzy variables are converted into a crisp variable. This stage introduces different inference methods that can be used to produce the fuzzy set value for the output fuzzy variable U . In this, the centre of gravity (COA) or centroid method is used to calculate the final fuzzy value.

Defuzzification using COA method means that the crisp output of U is obtained by using the centre of gravity, in which the crisp U variable is taken to be the geometric centre of the output fuzzy variable value $\mu_{out}(U)$ area, where $\mu_{out}(U)$ is formed by taking the union of all the contributions of rules with the degree of fulfilment greater than 0. Then the COA expression with a discretized universe of discourse can be written as follows:

$$U^* = \frac{\sum_{k=1}^n U_k \mu_{out}(U_k)}{\sum_{k=1}^n \mu_{out}(U_k)} \quad (4.13)$$

4.3 SELF TUNED FUZZY LOGIC CONTROLLER

4.3.1 INTRODUCTION

Recently many successful applications of fuzzy control have been reported in the field of power systems and electric drives. The performance of a controller is closely related to its tuning. If the tuning of the controller is optimum then the controller will give best results. Since the well known fact remains that the tuning of a fuzzy controller is more difficult than tuning a conventional controller. Most of the times the tuning of the fuzzy controller is done on the basis of 'hit and trial' and are arbitrarily chosen. But in very rare cases the tuning is optimum. Many researchers have investigated different methods of tuning a fuzzy controller. The optimum values of a controller always depend upon the specific model of the process that has to be controlled. So tuning of the controller must be done based on the knowledge of the controlled plant. In most of the cases the tuning parameters are taken as constants, due to which the control action remains the same in for any nonlinearity such as dead time or parameter variation. Due to which despite of optimum tuning parameters the controller fails to give optimum results. To avoid this kind of drawback a self tuned fuzzy logic controller scheme has been developed in this work.

Before proceeding to the self tuning process it is important to have an idea about the different tuning parameters and their effect on the performance of the controller.

4.3.2 TUNING PROCEDURE

4.3.2.1 Tuning parameters

Let us consider a fuzzy logic controller with triangular membership functions. The parameters of the fuzzy logic controller that can be tuned are given below.

- Scaling factors of IF/ THEN part fuzzy variables:

We define scaling factor as the maximum peak value, which defines the universe of discourse of the fuzzy variable.

- Peak value

Peak value is defined as the value at which the membership function is 1.

- Rules
- Width value

Width value is given as the interval from the peak value to the point at which membership becomes 0.

4.3.2.2 Effect of parameter changes

Here we consider how each parameter affects the performance of a fuzzy control system.

- **Scaling factor:** when a scaling factor of a fuzzy variable is changed, we assume the definition of each membership function will change by the same ratio. Hence, changing of any scaling factor can change the meaning of one part, i.e., the IF part or the THEN part, in any rule. So we can say that a change of scaling factor may affect all of the control rules in the rule table as shown by the shaded areas in Table 4.2

Table 4.2

<i>ce</i> \ <i>e</i>	nh	nl	ze	pl	ph
ne	nh	nl	nc	pm	ph
ze	nh	nl	nc	pm	ph
ps	nh	nl	pl	pm	ph

Effect of change of a scaling factor

- **Peak value:** When peak value is changed the definition of only one fuzzy label is changed. Hence, changing a peak value can affect only the rules which use the changed fuzzy label. The Table 4.3 shows the affected rules when changing a peak value of an IF part variable.

Table 4.3

<i>ce</i> \ <i>e</i>	nh	nl	ze	pl	ph
ne	nh	nl	nc	pm	ph
ze	nh	nl	nc	pm	ph
ps	nh	nl	pl	pm	ph

Effect of change of a peak value

- **Rules :** When a rule changes it affects only the rule involved as shown in the Table 4.4

Table 4.4

<i>ce</i> \ <i>e</i>	nh	nl	ze	pl	ph
ne	nh	nl	nc	pm	ph
ze	nh	nl	nc	pm	ph
ps	nh	nl	pl	pm	ph

Effect of change of a rule

- **Width value:** Changing the width value affects the interpolation between two peak values. If the width values are equal to the interval between two adjacent peak values, then its output changes continuously and smoothly as the input changes. But as the width value goes on reducing, the degree of crisp of the output goes on increasing.

4.2.3 SELF TUNED FUZZY LOGIC CONTROLLER DESIGN

An FLC has a fixed set of control rules, usually derived from experts' knowledge. The membership functions (MF's) of the associated input and output linguistic variables are generally predefined on a common universe of discourse. For the successful design of FLC's proper selection of input and output scaling factors (SF's) and/or tuning of the other controller parameters are crucial jobs, which in many cases are done through trial and error or based on some training data. Of the various tunable parameters, SF's have the highest priority due to their global effect on the control performance. However, relative importance of the input and output SF's to the performance of a fuzzy logic control system is yet to be fully established.

Unlike conventional control, which is based on mathematical model of a plant, a FLC usually embeds the intuition and experience of a human operator and sometimes those of designers and researchers. While controlling a plant, a skilled human operator manipulates the *process input* (i.e., controller output) based on the knowledge of error and change of error with a view to minimize the error within the shortest possible time. Fuzzy logic control is a knowledge-based system. By analogy with the human operator, the output SF should be considered a very important parameter of the FLC since its function is similar to that of the controller gain. Moreover, it is directly related to the stability of the control system. So the output SF should be determined very carefully for the successful implementation of a FLC.

Here, we have concentrated only on the tuning of output SF, considering that it is equivalent to the controller gain. Tuning of the output SF has been given the highest priority because of its strong influence on the performance and stability of the system. In this scheme, the

FLC is tuned on-line (while the controller is in operation) by dynamically adjusting its output SF by a gain updating factor ' α '.

In this scheme a tuning FLC (TFLC) is used to tune the output gain of the main FLC. The inputs to both the main FLC and the TFLC are normalized values of error and change of error. The output of the TFLC is the gain updating factor α which has a value between 0 and 1. When α is multiplied with ' K_o ' gives the output gain of the STFLC. The main FLC is similar to the FLC as discussed in the previous subsection. The gain tuning mechanism of the STFLC is shown in Figure 4.12. In the TFLC triangular membership functions are used for all input as well as output fuzzy sets. With a view to improve the overall control performance, we use the rule base in Table-4.5 for computation of α .

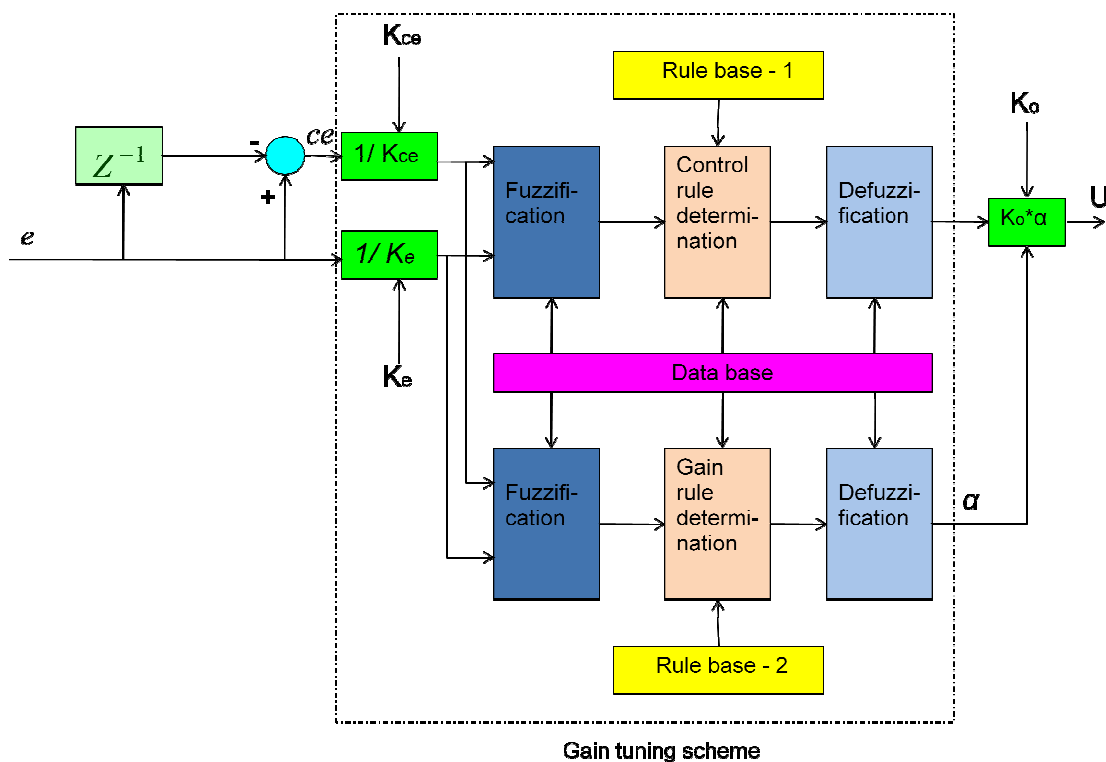


Figure 4.12 *STFLC gain tuning scheme*

Some of the important considerations that have been taken into account for determining the rules are as follows.

- 1) To make the controller produce a lower overshoot and reduce the settling time (but not at the cost of increased rise time) the controller gain is set at a small value when the error is big (it may be -ve or +ve), but 'e' and 'ce' are of opposite signs. For example, If 'e' is positive big (pb) and 'ce' is negative small (ns) then ' α ' is very small (vs) or if 'e' is negative medium (nm) and 'ce' is positive medium (pm) then ' α ' is small (s). Observe that when the error is big but 'e' and 'ce' are of the same sign (i.e., the process is now not only far away from the set point but also it is moving farther away from it), the gain should be made very large to prevent from further worsening the situation. This has been realized by rules of the form: If 'e' is 'pb'(positive big) and 'ce' is 'ps'(positive small) then ' α ' is 'vb'(very big) or If 'e' is 'nm' and 'ce' is 'nm' then ' α ' is 'vb'.
- 2) Depending on the process trend, there should be a wide variation of the gain around the set point (i.e., when 'e' is small) to avoid large overshoot and undershoot. For example, overshoot will be reduced by the rule If 'e' is 'ze'(zero) and 'ce' is 'nm'(negative medium) then ' α ' is 'b'(big). This rule indicates that the process has just reached the set point, but it is moving away upward from the set point rapidly. In this situation, large gain will prevent its upward motion more severely resulting in a smaller overshoot. Similarly, a large undershoot can be avoided using the rules of the form: If 'e' is 'ns' and 'ce' is 'ps'(positive small) then ' α ' is 'vs'(very small). This type of gain variation around the set point will also prevent excessive oscillation and as a result the convergence rate of the process to the set point will be increased. Note that unlike conventional FLC's, here the gain of the proposed controller around the set point may

vary considerably depending on the trend of the controlled process. Such a variation further justifies the need for variable scaling factors.

- 3) Practical processes or systems are often subjected to load disturbances. A good controller should provide regulation against changes in load; in other words, it should bring the system to the stable state within a short time in the event of load disturbance. This is accomplished by making the gain of the controller as high as possible. Hence, to improve the control performance under load disturbance, the gain should be sufficiently large around the steady-state condition. For example If ' e ' is 'ps' and ' ce ' is 'pm' then ' α ' is 'b' or If ' e ' is 'ns' and ' ce ' is 'nm' then ' α ' is 'b'. Note that immediately after a large load disturbance ' e ' may be small but ' ce ' will be sufficiently large and they both will be of the same sign and in that case, ' α ' is needed to be large to increase the gain. At steady state controller gain should be very small to avoid chattering problem around the set point.

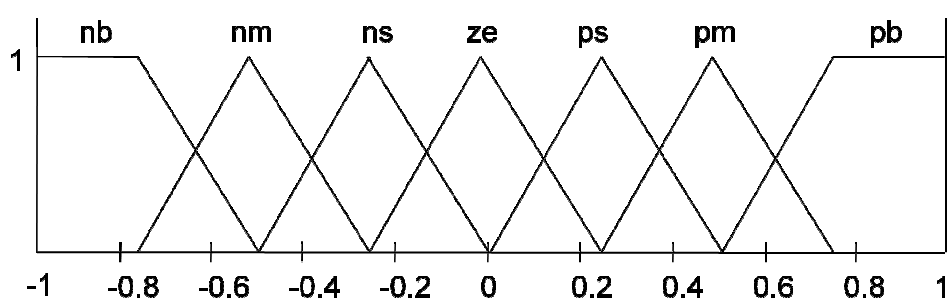
Further modification of the rule base for ' α ' may be required, depending on the type of response the control system designer wishes to achieve. It is very important to note that the rule base for computation of ' α ' will always be dependent on the choice of the rule base for the controller. Any significant change in the controller rule base may call for changes in the rule base for ' α ' accordingly.

Table 4.5

$ce \backslash e$	nb	nm	ns	ze	ps	pm	pb
nb	vb	vb	vb	b	sb	s	ze
nm	vb	vb	b	b	mb	s	vs
ns	vb	mb	b	vb	vs	s	vs
ze	s	sb	mb	ze	mb	sb	s
ps	vs	s	vs	vb	b	mb	vb
pm	vs	s	mb	b	b	vb	vb
pb	ze	s	sb	b	vb	vb	vb

Rule table

The input and output membership functions for the TFLC are given in Figure 4.13 and Figure 4.14 respectively. For designing of the TFLC, Mamdani type fuzzy inferencing is used. The values of membership functions, fuzzy sets for input and output variables, and the rules used in the study are chosen to be the same as those of a general fuzzy controller. In this study the centroid method of defuzzification is used.

Figure 4.13 *Input membership functions for TFLC*

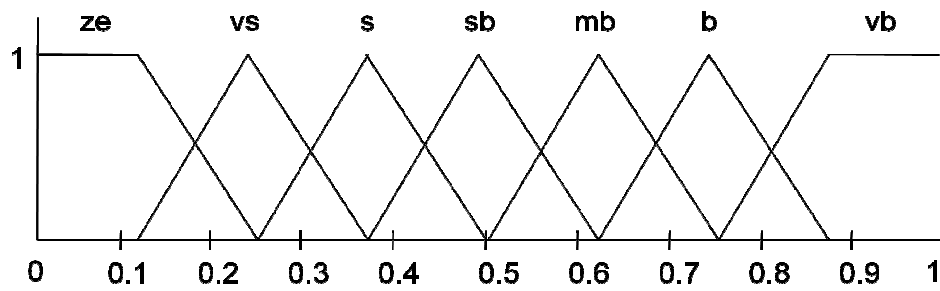


Figure 4.14 *Output membership functions for TFLC*

The whole indirect vector control scheme is same as the scheme in the previous subsection. The three fuzzy logic controllers are replaced by three self tuned fuzzy logic controllers and the performance of the system is evaluated.

4.4 HYBRID CONTROLLER

4.4.1 INTRODUCTION

The cage induction machine is one of the most robust machines, which is often used for wind power generation purpose. There are many techniques to control the speed of the induction machine such as stator voltage control and frequency control etc. For achieving variable speed operation, the frequency control method of the cage machine is the best method among all the methods, of the speed control. Vector control of the cage machine, is considered as a fast response and high performance method to achieve variable speeds. In vector control method the induction machine can be operated like a separately excited compensated DC motor for high performance applications. In the last decade, many closed loop speed control techniques have been developed to provide high level performance. However, the desired drive specifications are still to be perfectly satisfied and /or their algorithms are too complex.

However in vector control of cage induction machine the controller plays the most significant role. The performance of the drive is determined by the accuracy and robustness of the controller. The most common and widely used controller is the PI controller. The PI controller gives very accurate performance i.e. the steady state error is very less and most of the times zero steady state error can be achieved. With PI controllers the computational time is also very less so it is best suited for real time applications. At steady state the noise is also negligible with PI controller. But despite of these advantages the major drawback of this type of controller is that the transient performance of the controller is poor and the controller also sometimes suffers from stability problems. Despite of perfect tuning the controller cannot give optimum performance due to parameter variation of the induction machine. Due to this fact PI controllers are not capable of giving high performance.

On the other hand the fuzzy logic approach has got an increasing interest and has found application in many domains of control problem. The main feature is the construction of the fuzzy logic controller (FLC), which utilizes the linguistic imprecise knowledge of human experts. The main advantage of fuzzy logic control method as compared to conventional control techniques resides in fact that no mathematical modelling is required for controller design and also it does not suffer from the stability problem. In variable speed control problem, fuzzy logic can be considered as an alternative approach to conventional control. It has been recently demonstrated that dynamic performance of electric drives as well as robustness with regards to parameter variations can be improved by adapting the non linear speed control techniques. Fuzzy logic is a non linear control and it allows the design of optimized non linear controllers to improve the dynamic performance of the conventional controllers. The fuzzy logic controller has very good transient performance but introduces noise at the set reference speed and shows steady state error during load. The computational burden of this type of controller is also very high.

In this section the application of hybrid control to an indirect vector controlled cage induction machine drive is investigated.

4.4.2 DESIGN PRINCIPLES FOR HYBRID CONTROLLER

The hybrid controller is the combination of PI controller and self tuned fuzzy controller. The control law switches between the self tuned fuzzy controller and the PI control. The hybrid controller is designed to have all the advantages of PI controller as well as the fuzzy controller. The hybrid controller is stable and it also gives accurate performance at steady state. This controller has less computational burden so it is also well suited for real time applications. The transient performance is also very good which makes it a very suitable controller for high performance drives.

4.4.2.1 Design of the PI controller

The most popular speed control used in conventional machine control is PI control because the PI control is simple and accurate. As the computational burden for this controller is less it is reliable to implement. The PI controller used here is a conventional controller given by the equation

$$U(t) = K_p * e(t) + K_i * \int e(t)dt$$

Where K_p and K_i are the proportional and integral gains respectively. These gains are determined by trial and error process to give the best performance.

However, since the variation and high uncertainty of induction machine internal parameters, the tuning of PI control gains becomes a challenging problem. This problem again becomes more serious when the system's states are far from their steady state values. At this condition the PI controller often shows stability problems. Again the transient performance of this type of controller is also not up to mark. Due to these draw backs the PI controller is not considered as a robust controller and is not suitable for very high performance drive applications.

4.4.2.2 Design of the SELF TUNED FUZZY controller

The self tuned fuzzy controller design is described in the previous subsection. This controller doesn't have any stability problem. Due to this advantage the self tuned fuzzy controller is made active when the system's states are far from their steady state values. This controller is robust and gives appreciable performance during parameter variations. But during load changes the controller introduces some steady state error and with this controller some noise is also introduced during steady state. The computational burden is also very high in this controller so it is not well suited for real time applications.

4.4.2.3 Design of the HYBRID controller

This design approach combines both self tuned fuzzy control and a PI control into an integrated one. The control law switches between the self tuned fuzzy control and the PI control. It is important to know the switch conditions between both. The idea is as follows. When the system states are far from their steady state values, the controller used is the self tuned fuzzy controller. This self tuned fuzzy controller drives the system states towards their steady state, even under unknown system uncertainties. When the system states are about to approach their steady state, the PI controller starts to work and ensures that the system states eventually reach the equilibrium point under the system parametric variations and disturbances, as illustrated in Figure 4.15.

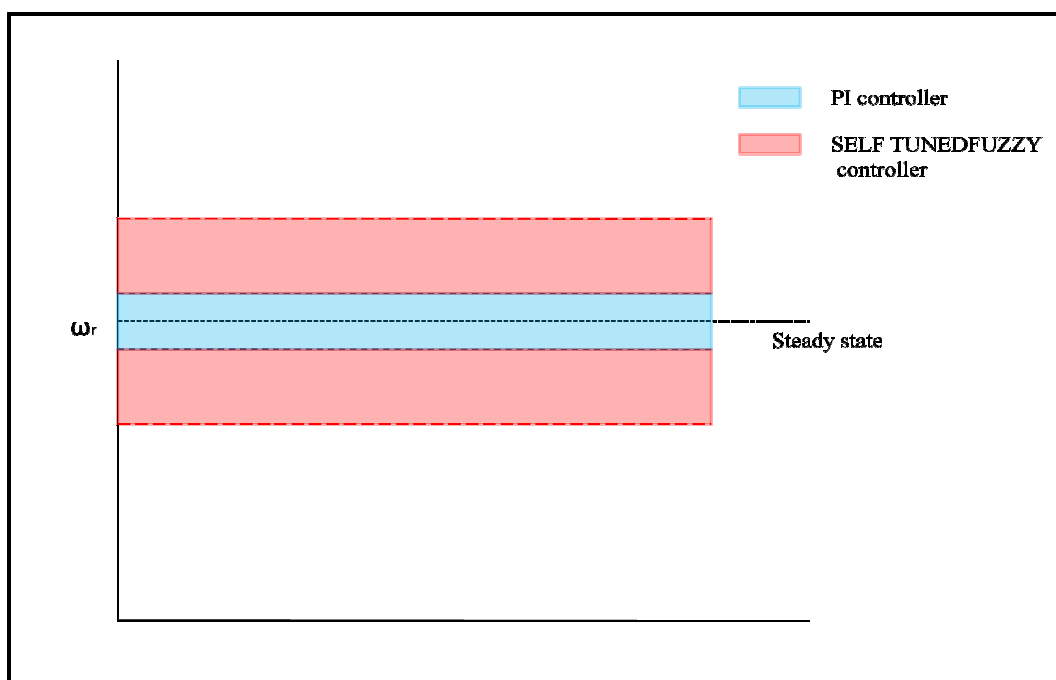


Figure 4.15 *Principle of hybrid controller*

The output 'Y' of the induction generator is compared with the reference input 'R' and the error 'e' is fed to the block which decides the switching logic as shown in Figure 4.16. The switching logic is developed on the fact that when the system's states are far from their steady

state values they may cause instability with PI controller, so in that condition the self tuned fuzzy logic controller is made on which drives the system towards steady state. When the system comes to the range where PI controller is stable the switch position is changed to PI controller which takes the system to steady state. The self tuned fuzzy logic controller has a good transient performance so it drives the system states quickly towards steady state, so the transient time is reduced, enhancing the stability of the system. On the other hand during low error values the PI controller drives the system to steady state giving zero steady state error and minimum noise at steady state. As the PI controller is active throughout the steady state the computational burden is also reduced which makes the controller suitable for real time applications.

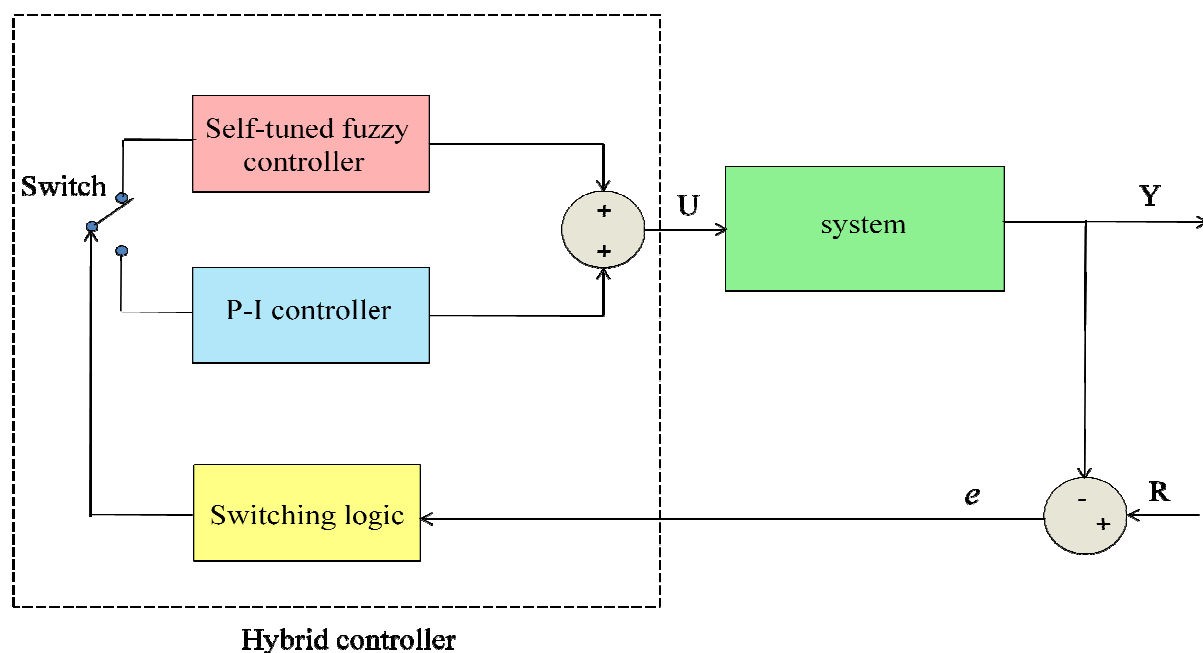


Figure 4.16 Block diagram of hybrid controller

Figure 4.17 shows the switching between the two controllers. The pink area shows the working region of the PI controller where the yellow area is the working region of the self tuned fuzzy logic controller. The self tuned fuzzy logic controller works till 2.55 seconds and after 2.55 seconds the PI controller comes into action and the speed reaches steady state at 2.57 seconds.

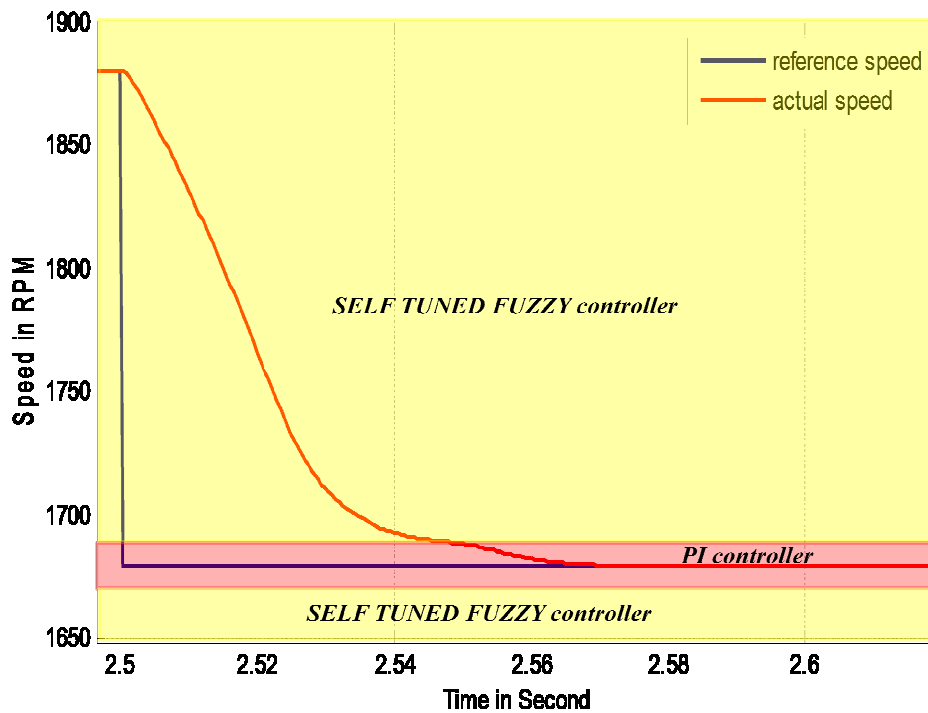


Figure 4.17. Working regions of PI controller and SELF TUNED FUZZY LOGIC controller

The performance of the hybrid controller is tested by using it in the indirect vector control scheme of induction generator which is same as the scheme in the previous subsection 4.2. The three fuzzy logic controllers are replaced by three hybrid controllers and the performance of the system is evaluated.

4.5 RESULTS AND DISCUSSION

4.5.1 SIMULATIONS WITH A STEP CHANGE IN TURBINE TORQUE

Initially the turbine torque is set at 10 Nm. A step increment of 5Nm in turbine torque is given at 2.5 s. At 3 s the turbine torque again comes to 10Nm.

4.5.1.1 Speed Responses

Figures 4.18, 4.19 and 4.20 show the speed responses of the induction generator with fuzzy controller, self tuned fuzzy controller and hybrid controller respectively. With fuzzy controller a steady state error is introduced in speed which increases with the change in the turbine torque. From Figure 4.18 it can be seen that the steady state error with fuzzy controller is 3 rpm, but when the turbine torque is increased from 10Nm to 15Nm the steady state error increases to 8 rpm. But the steady state error with self tuned fuzzy controller is less than that in fuzzy controller, i.e. the steady state error is 1.5 rpm for turbine torque of 10Nm and it increases to 2.6 rpm for turbine of 15Nm which can be seen from Figure 4.19. With hybrid controller the steady state error is zero.

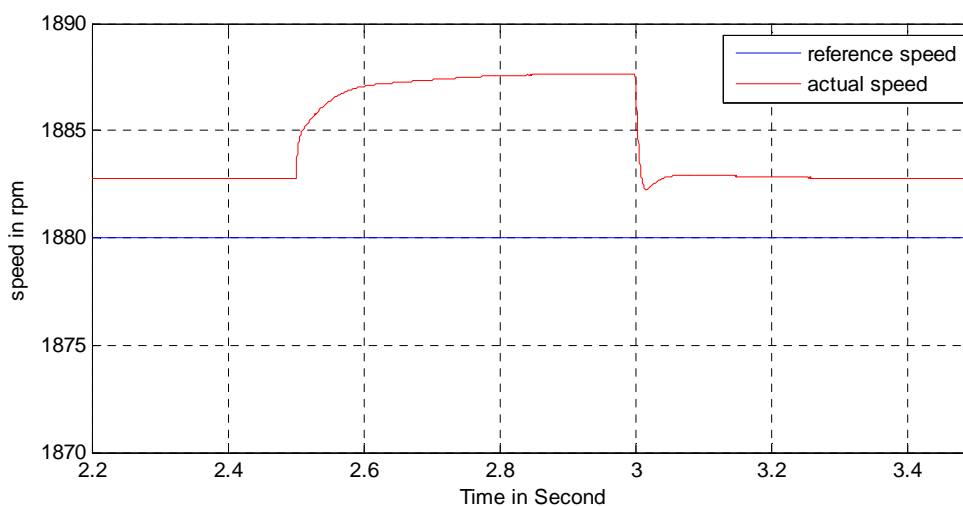


Figure 4.18 *Speed response with fuzzy controller*

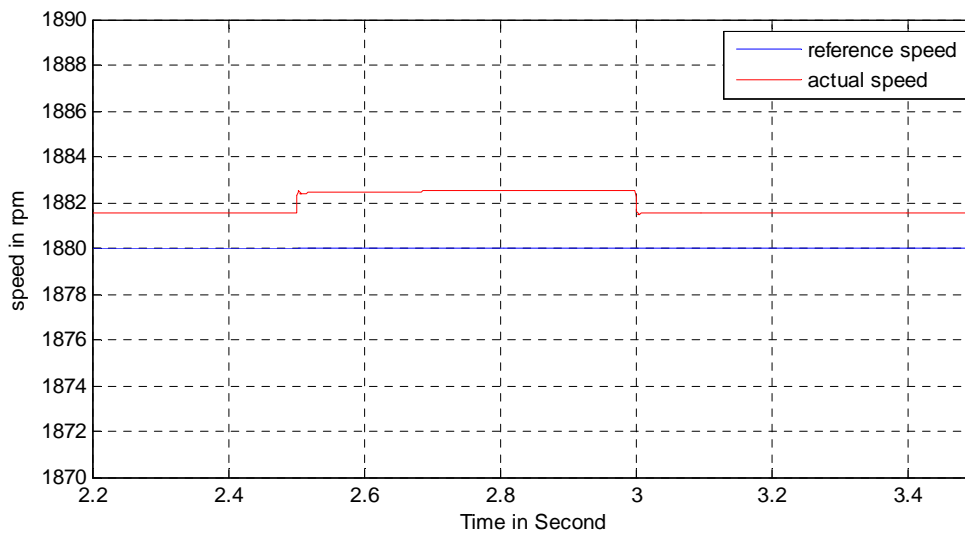


Figure 4.19 *Speed response with self tuned fuzzy controller*

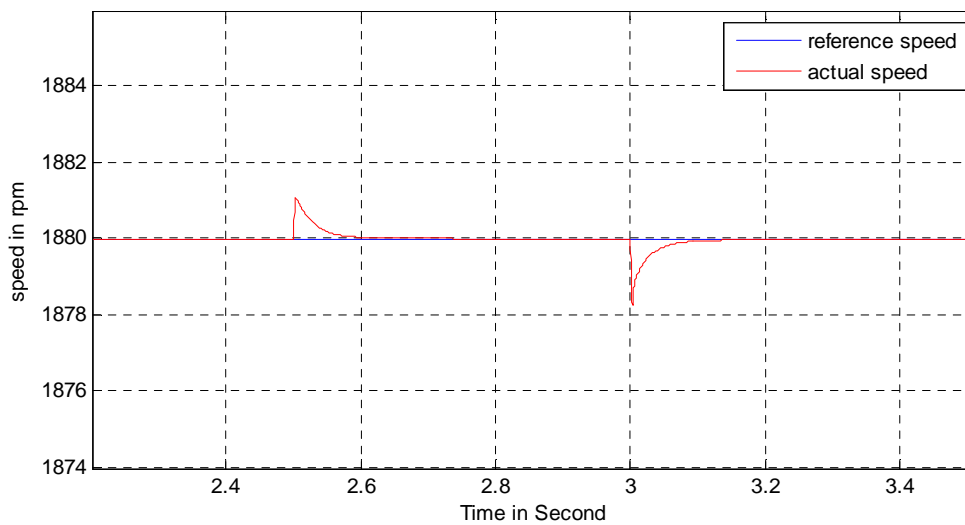


Figure 4.20 *Speed response with hybrid controller*

4.5.1.2 Torque Responses

Figures 4.21, 4.22 and 4.23 show the electromagnetic torque response of the induction generator with fuzzy controller, self tuned fuzzy controller and hybrid controller respectively. From these figures it is clear that the response time is the minimum with the self tuned fuzzy controllers and

with the hybrid controller the performance is as faster as that with self tuned fuzzy controllers but the hybrid control has other advantages such that it gives a noise free performance and has much less computational burden than fuzzy and self tuned fuzzy controllers.

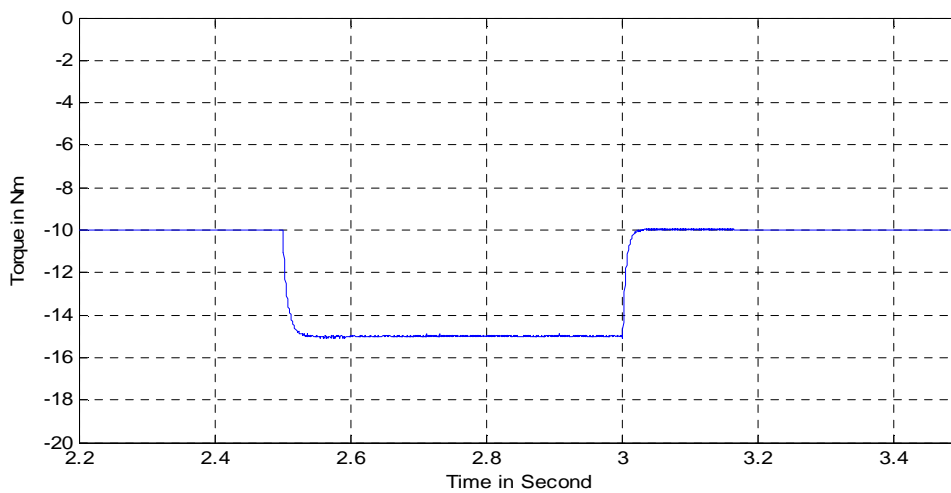


Figure 4.21 *Torque response with fuzzy controller*

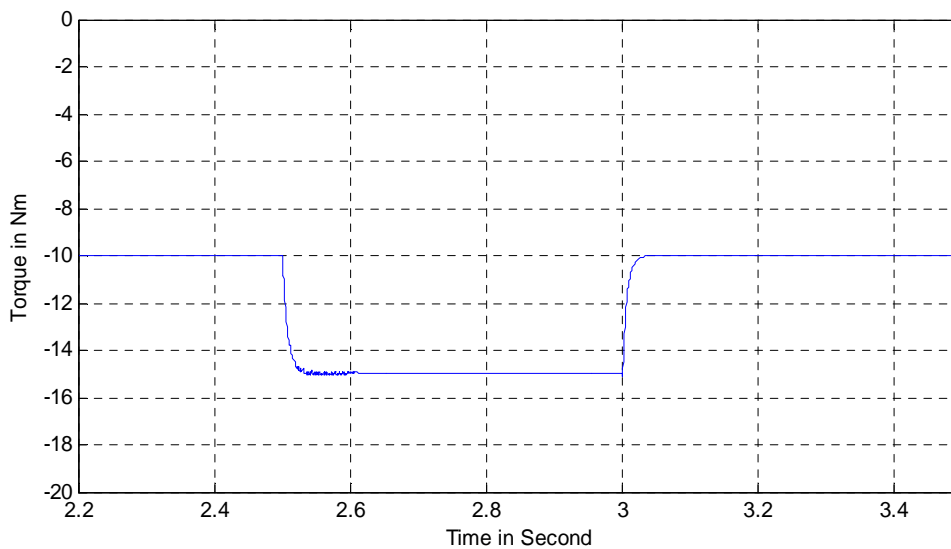


Figure 4.22 *Torque response with self tuned fuzzy controller*

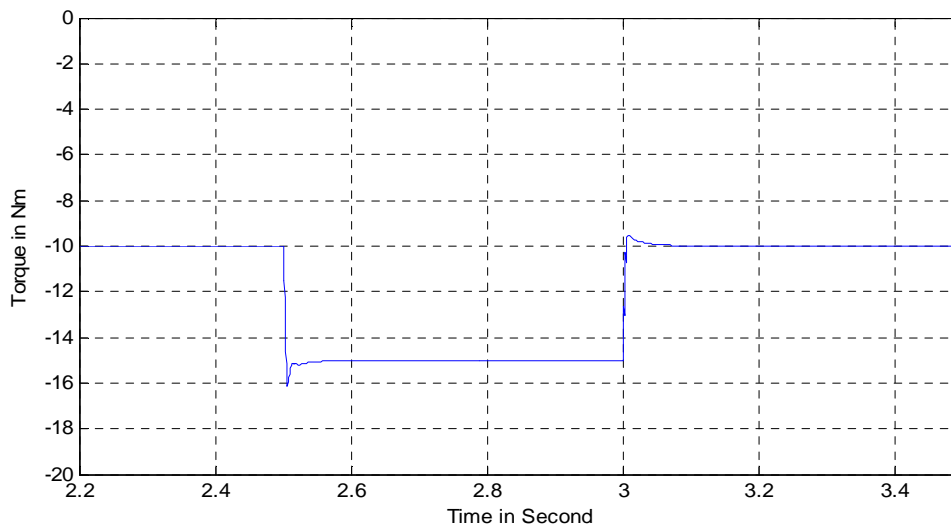


Figure 4.23 Torque response with hybrid controller

4.5.1.3 Active and Reactive Power Responses

The active and reactive power responses for fuzzy controller, self tuned fuzzy controller and hybrid controller are given in Figures 4.24, 4.25 and 4.26 respectively. From the figures it can be seen that when there is an increase in the turbine torque at 2.5 seconds the active power increases in the negative direction. The negative sign is due to the convention that power fed to the machine is taken as positive, but in case of induction generator active power is fed to the grid where as the machine takes reactive power from the grid. For that reason the active power is negative where as the reactive power is positive.

Due to vector control the reactive power variation is very less as compared to the active power variation. For fuzzy controller the reactive power varies from 1655 Var to 1750 Var giving 5.74% variation whereas for self tuned fuzzy controller the reactive power variation is from 1567 Var to 1615 Var giving 3.06% variation. The active power varies from 1240 Watts to 1834 Watts in case of both the fuzzy and self tuned fuzzy controller.

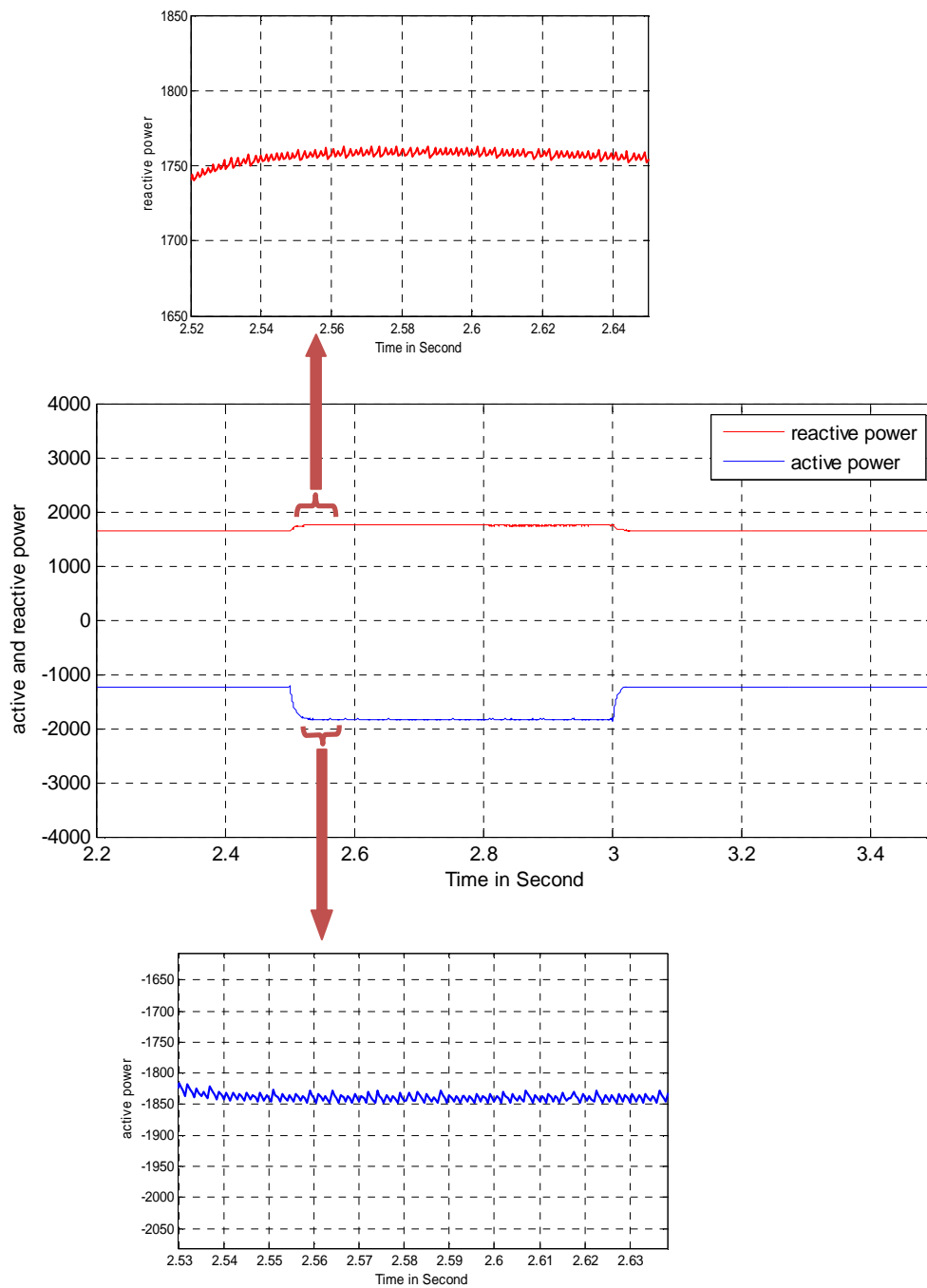


Figure 4.24 Active and reactive power response with fuzzy controller

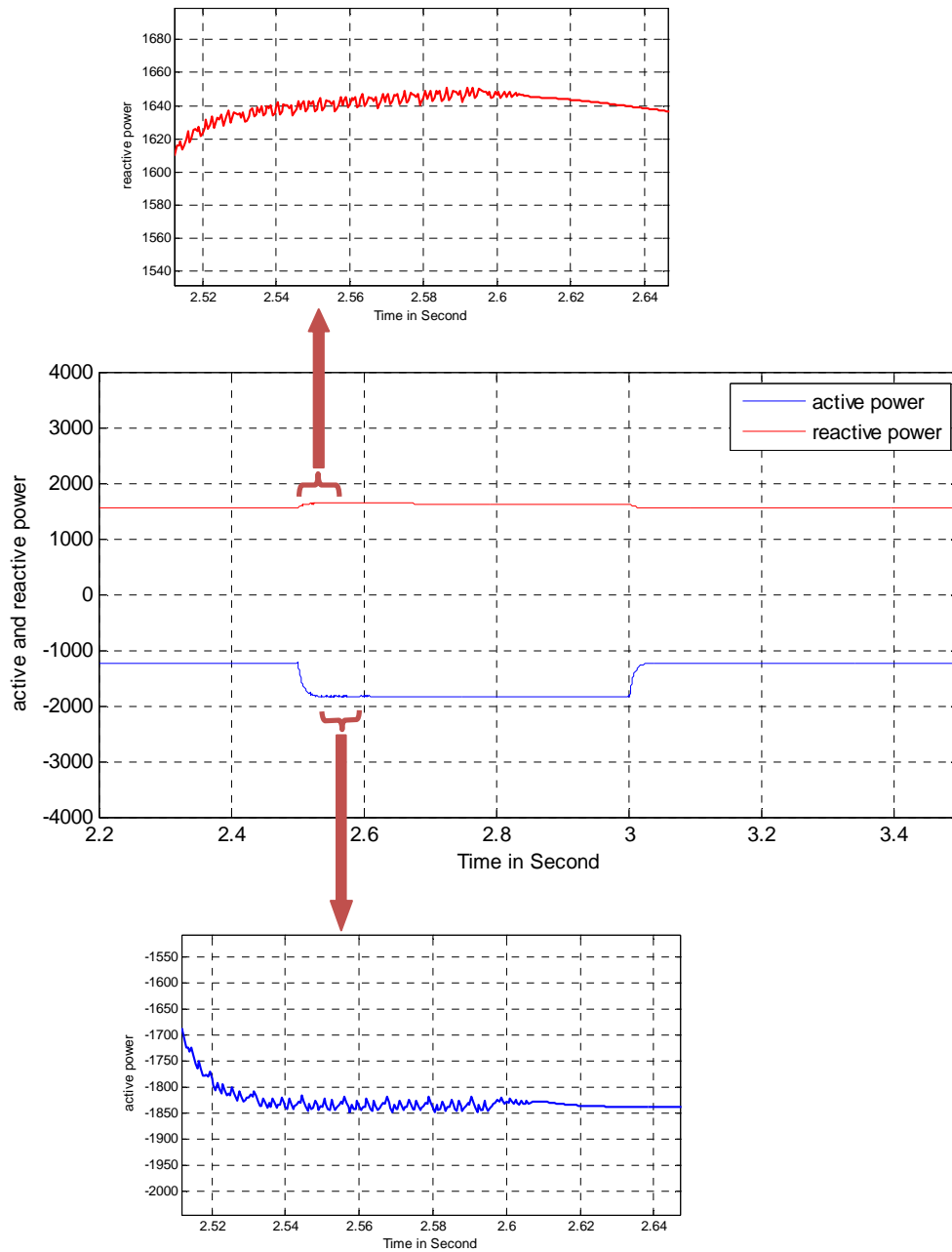


Figure 4.25 Active and reactive power response with self tuned fuzzy controller

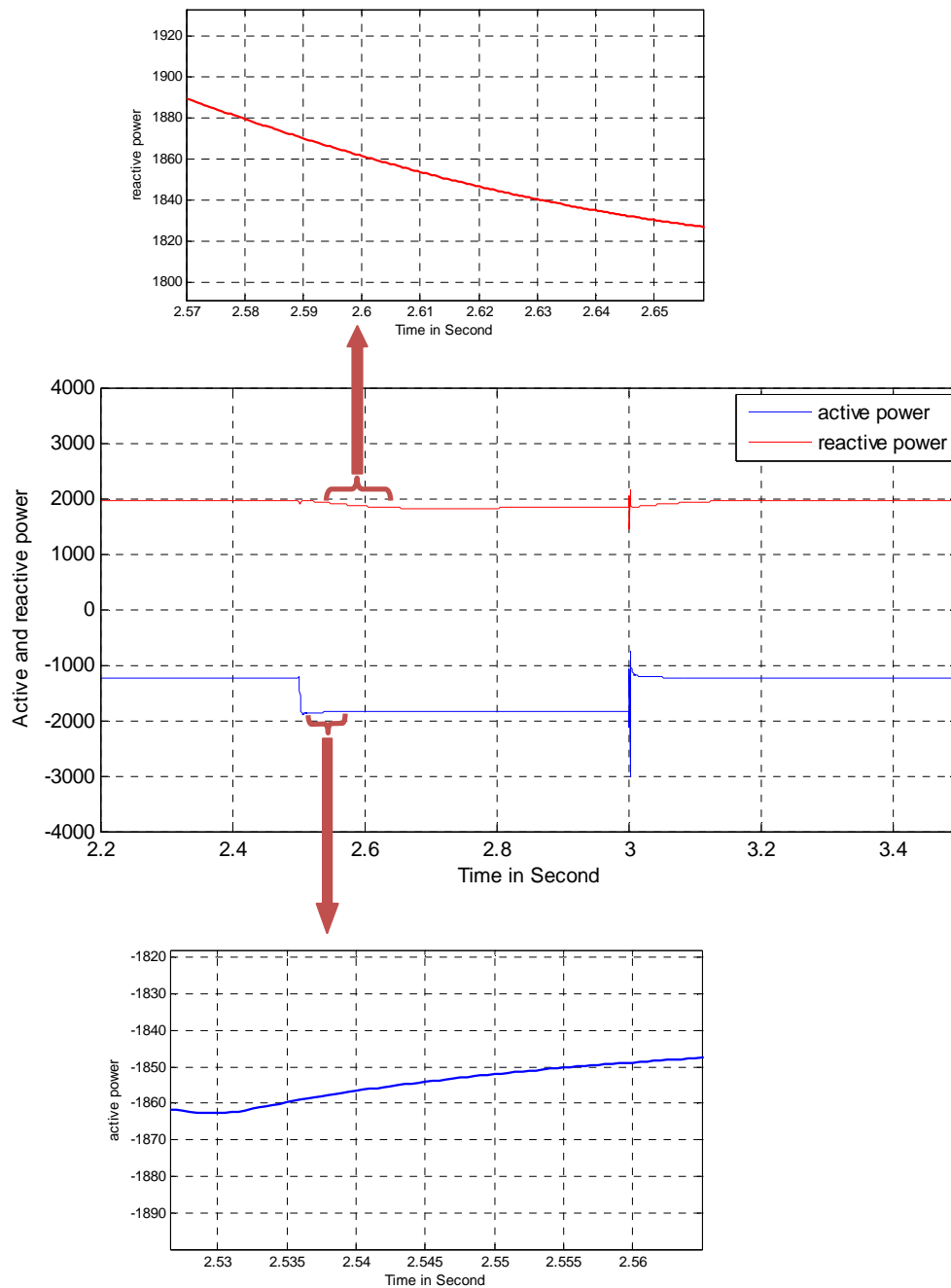


Figure 4.26 Active and reactive power response with hybrid controller

With hybrid controller the active power varies from 1240 Watts to 1834 Watts but the reactive power is higher than both fuzzy and self tuned fuzzy controller. This compromise is due

to the PI controller part of the hybrid controller. The reactive power varies from 1945 Var to 1850 Var, giving 5.13% variation.

At steady state both fuzzy and self tuned fuzzy controllers introduce noise in active as well as reactive power which can be clearly seen from Figures 4.24 and 4.25. The noise content of the self tuned fuzzy controller is less in steady state compared to the fuzzy controller, but with hybrid controller there is no noise content at all in active and reactive power, which becomes a strong advantage of the hybrid controller. The signs of change in the reactive power are different. With self tuned fuzzy controller, the reactive power remains almost unchanged. With P-I and fuzzy controllers, it increases. But with hybrid controller (Fig. 4.26) the reactive power is reduced. This may be due to the switching back and forth between P-I controller and the self tuned fuzzy controller.

4.5.1.4 Current Responses

In Figures 4.27, 4.28 and 4.29 the variations in torque component and flux component of current are shown.

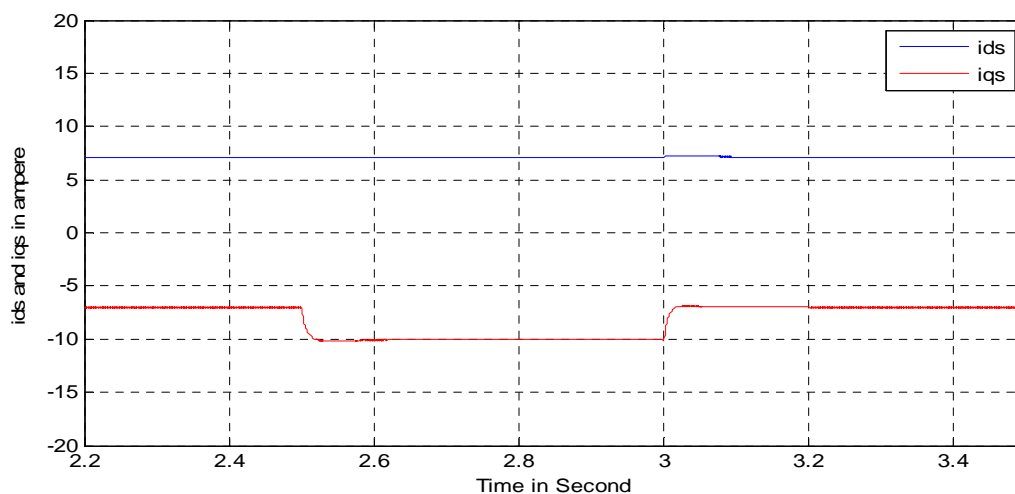


Figure 4.27 *Direct and quadrature axis current response with fuzzy controller*

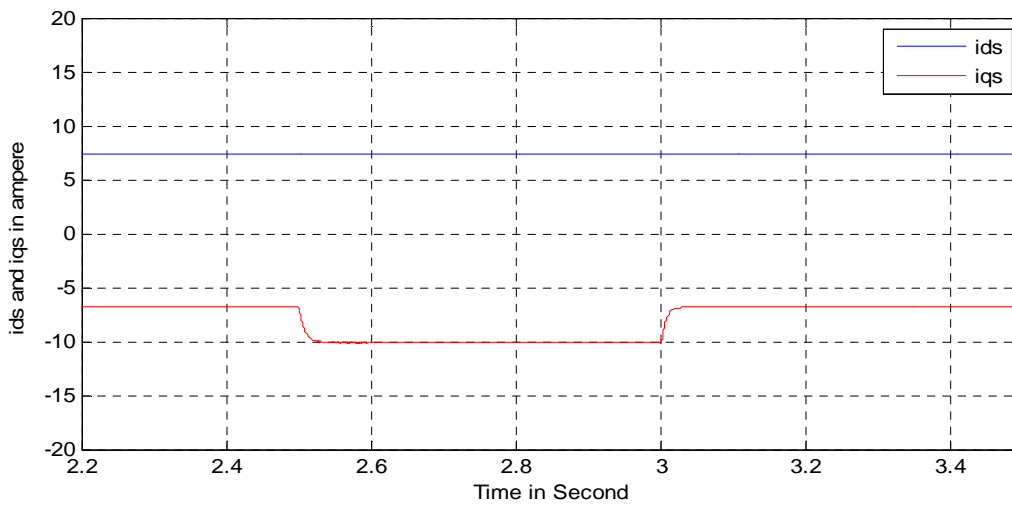


Figure 4.28 *Direct and quadrature axis current response with self tuned fuzzy controller*

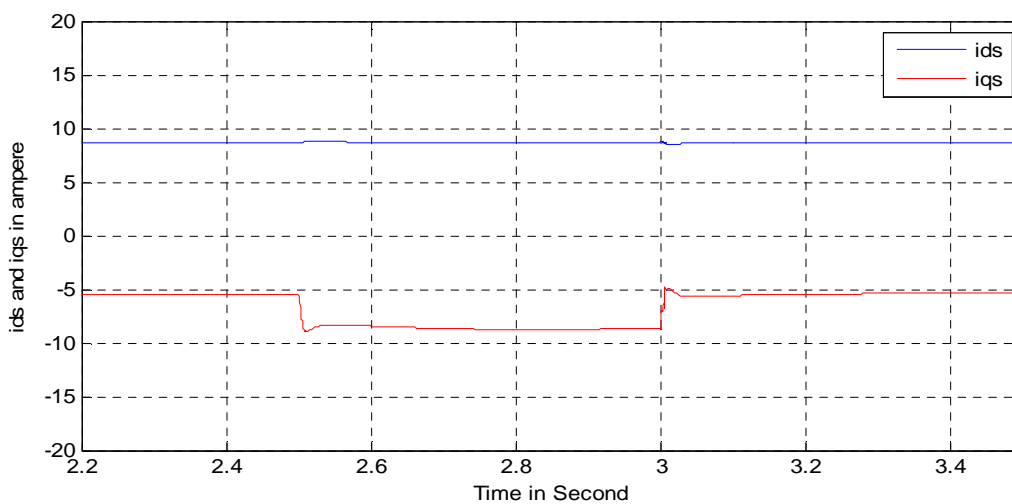


Figure 4.29 *Direct and quadrature axis current response with hybrid controller*

Due to vector control technique the induction machine shows DC machine like performance that is torque and flux component of current are independent of each other. With a variation in i_{ds} there is no variation in i_{qs} and vice versa. From the figures it is clear that when there is variation in turbine torque the torque component of current i_{qs} changes but the flux component of current i_{ds} remains unchanged which gives the induction machine decoupled performance.

4.5.1.5 Power Factor

The power factor of the induction generator with fuzzy controller, self tuned fuzzy controller and hybrid controller are given in Figures 4.30, 4.31 and 4.32, respectively.

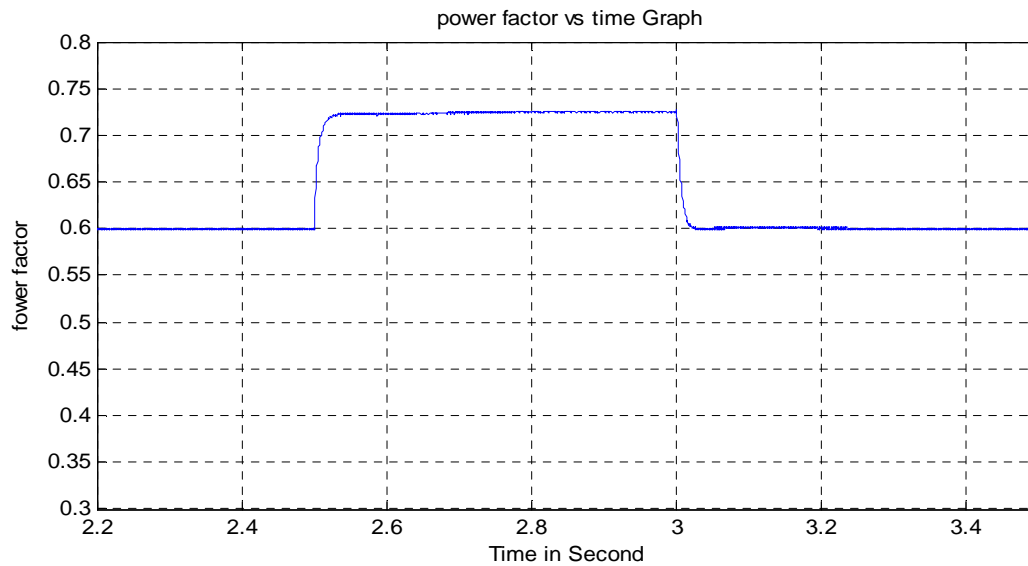


Figure 4.30 Power factor with fuzzy controller

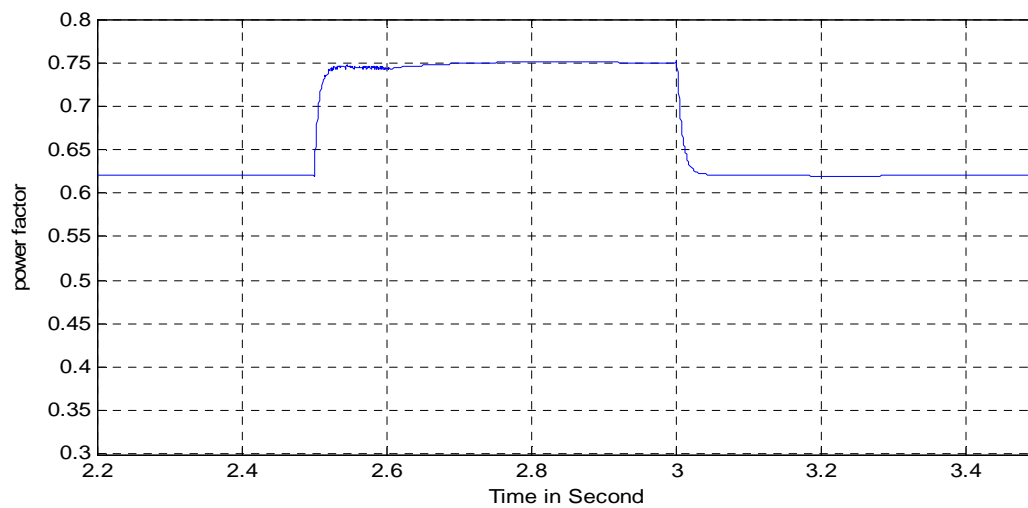


Figure 4.31 Power factor with self tuned fuzzy controller

With turbine torque of 15 Nm the power factor of induction generator is maximum with self tuned fuzzy controller which is 0.75, with fuzzy controller it is 0.726 and with hybrid controller

the power factor is 0.71. This is due to the fact that among the three controllers the reactive power is maximum with hybrid controller, as discussed above. There are large transients at 3s in Fig. 4.26 and Fig. 4.32, with hybrid controller. This is due to (i) step change of turbine torque from 15 N.m to 10 N.m at that instant, and (ii) the switching back and forth between P-I controller and the self tuned fuzzy controller.

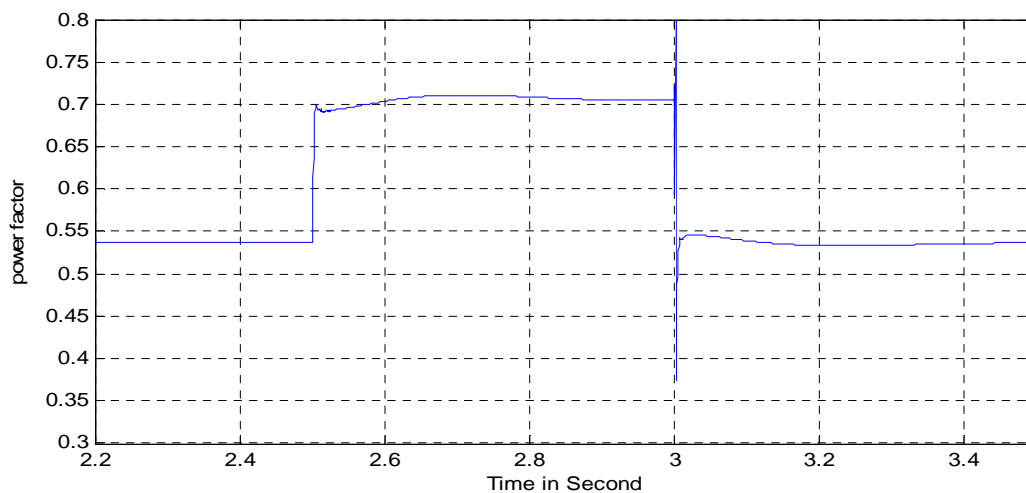


Figure 4.32 Power factor with hybrid controller

4.5.1.6 Phase Current Responses

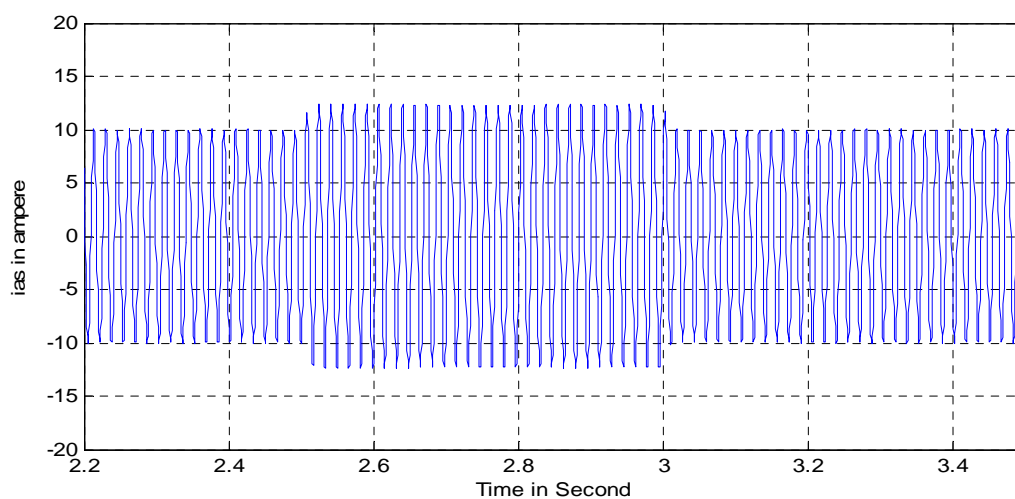


Figure 4.33 Current response with fuzzy controller

Figures 4.33, 4.34 and 4.35 show the phase current response of the induction generator with fuzzy controller, self tuned fuzzy controller and hybrid controller respectively.

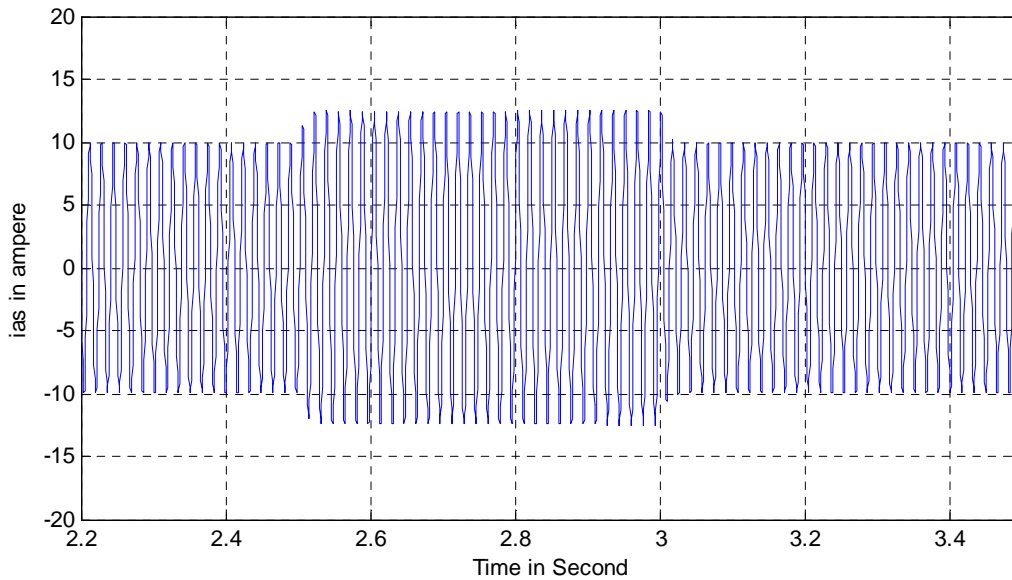


Figure 4.34 *Current response with self tuned fuzzy controller*

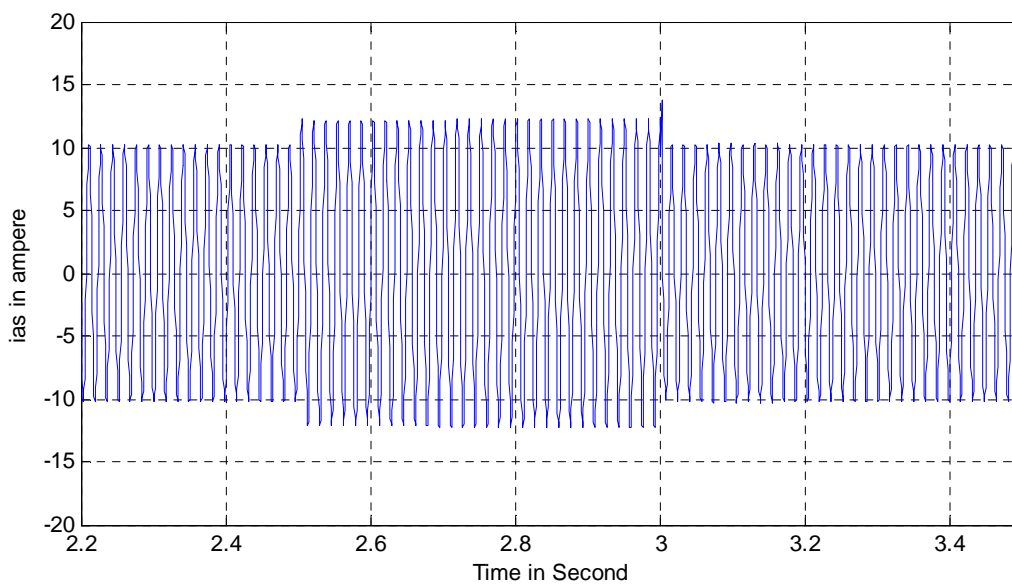


Figure 4.35 *Current response with hybrid controller*

4.5.2 SIMULATIONS WITH A STEP CHANGE IN REFERENCE SPEED

The performance of the induction generator system is again evaluated by subjecting the system to a step change in the reference speed. A step decrease of 200 rpm, i.e. from 1880 rpm to 1680 rpm is given to the reference speed and different responses of the vector controlled induction generator are given below.

4.5.2.1 Speed Responses

Figure 4.36, 4.37 and 4.38 show the speed responses with a step change in reference speed. A step change of 200 rpm is given at 2.5 s which continues for 0.5 s. The speed responses with different controllers shows that the settling time with fuzzy controller is maximum which is 0.12 s and minimum with self tuned fuzzy controller which is 0.045 s, but both the controllers introduce a steady state error in the system as shown in the previous sub section. With hybrid controller the steady state error is zero but the settling time is compromised to a small extent.

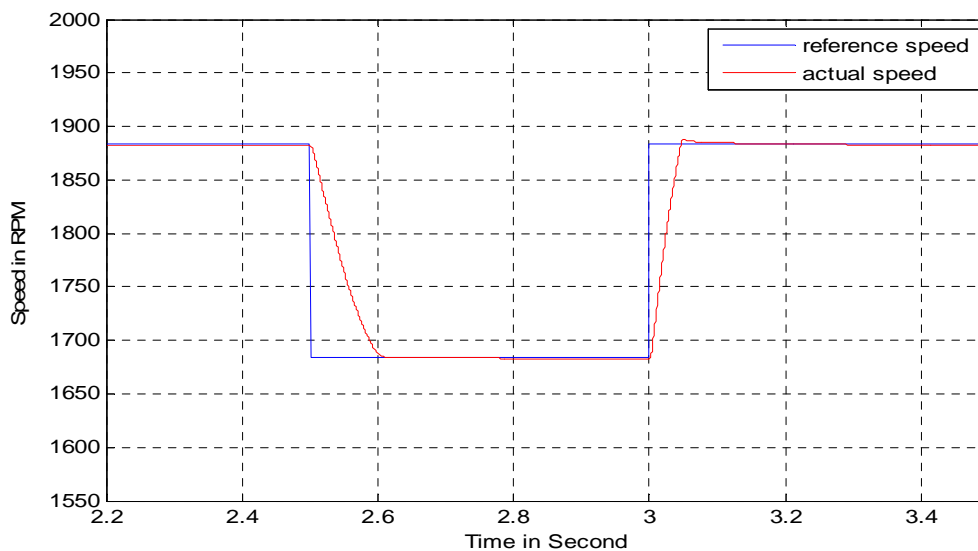


Figure 4.36 Speed response with fuzzy controller

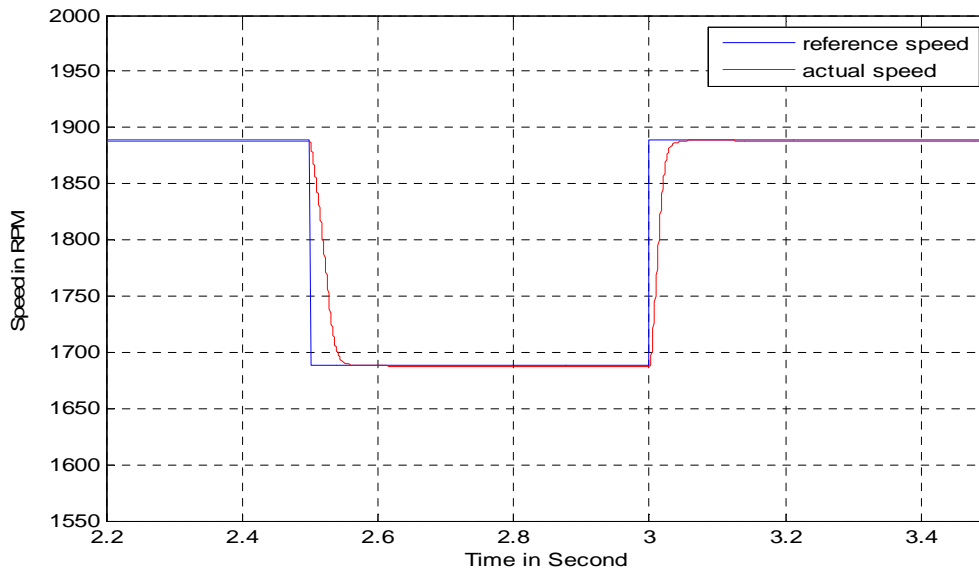


Figure 4.37 Speed response with self tuned fuzzy controller

The settling time with hybrid controller is 0.065 s which is faster than fuzzy controller and a little bit slower than the self tuned fuzzy controller and can be seen from Figure 4.38.

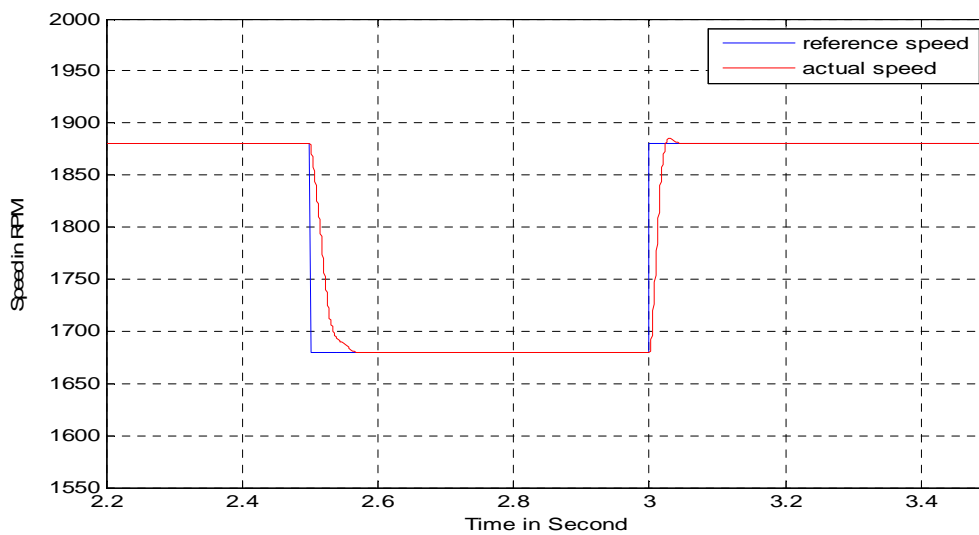


Figure 4.38 Speed response with hybrid controller

4.5.2.2 Torque Responses

The torque responses of the induction generator system with fuzzy, self tuned fuzzy and hybrid controller are given in Figures 4.39, 4.40 and 4.41 respectively.

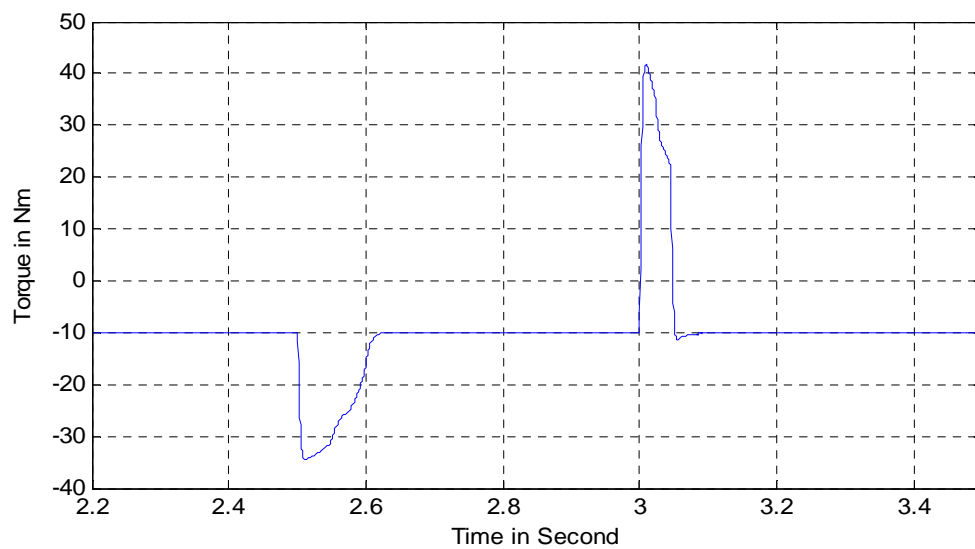


Figure 4.39 *Torque response with fuzzy controller*

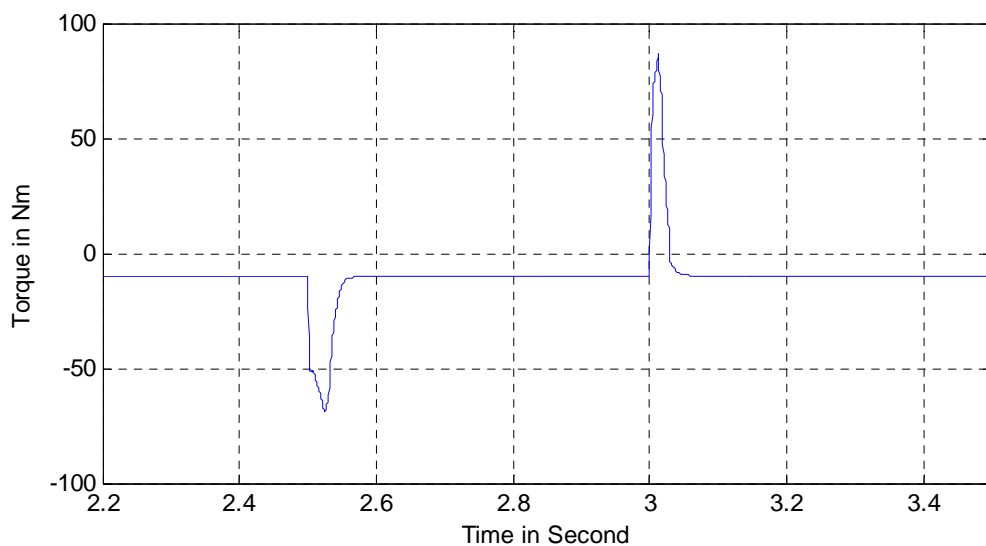


Figure 4.40 *Torque response with self tuned fuzzy controller*

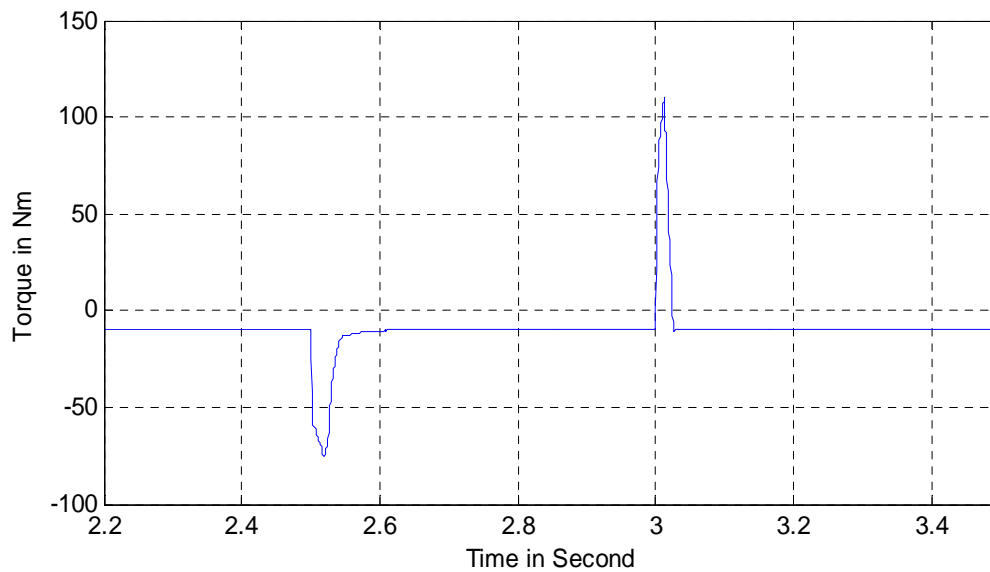


Figure 4.41 *Torque response with hybrid controller*

From the above mentioned figures it can be seen that the settling time is minimum with self tuned fuzzy controller and maximum with fuzzy controller. The settling time of the system with hybrid controller is much less than that with fuzzy controller but is a bit more than that with self tuned fuzzy controller, due to the presence of the PI controller in hybrid controller.

4.5.2.3 Active and Reactive Power Responses

Figure 4.42, 4.43 and 4.44 show the active and reactive power responses of the induction generator system with fuzzy controller, self tuned fuzzy controller and hybrid controller respectively, with a step change in reference speed. As there is a reduction in the input power to the system due to the reduction in machine speed, the active power reduces in the steady state from 1240watts to 1100 watts.

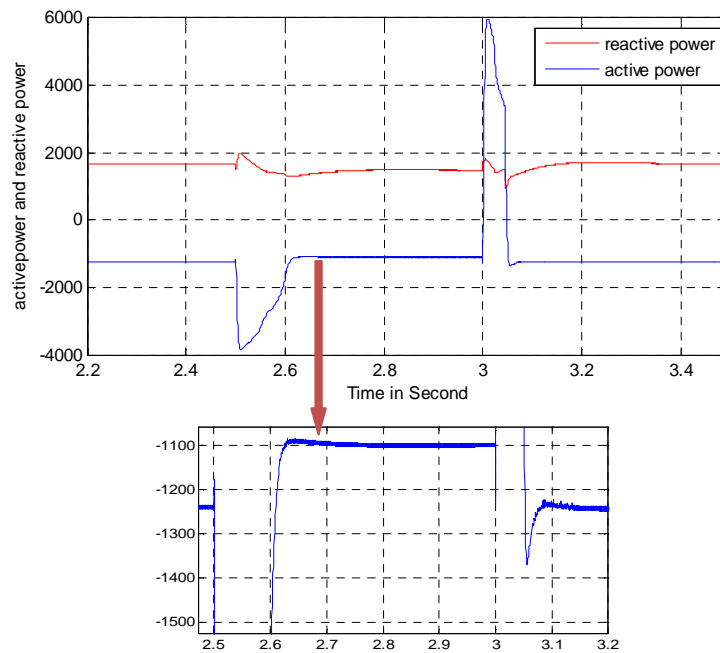


Figure 4.42 Active and reactive power response with fuzzy controller

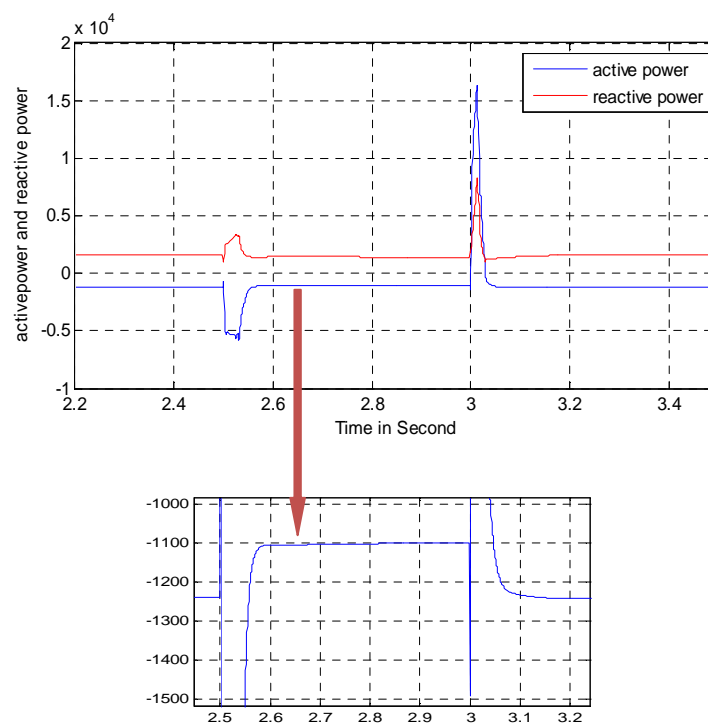


Figure 4.43 Active and reactive power response with self tuned fuzzy controller

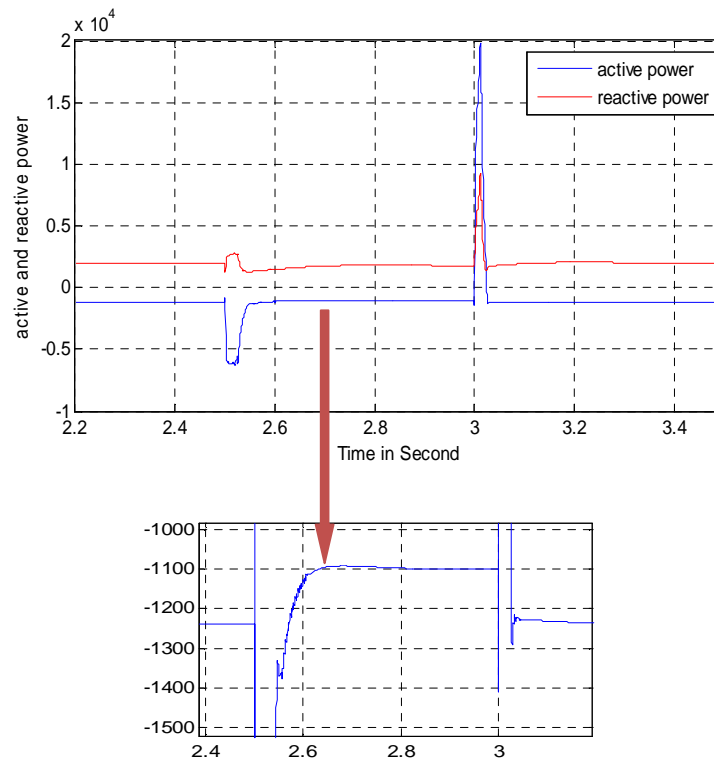


Figure 4.44 Active and reactive power response with hybrid controller

4.5.2.4 Current Responses

Figure 4.45, 4.46 and 4.47 show the direct axis and quadrature axis current responses of the induction generator system with fuzzy controller, self tuned fuzzy controller and hybrid controller respectively, with a step change in reference speed. It can be seen from the figures that except there is a change in quadrature axis current in the transient period, there no change in it during the steady state. But as the reference speed command decreases from 1880rpm to 1680 rpm, the direct axis current value increases from 7.32 amperes to 7.37 amperes.

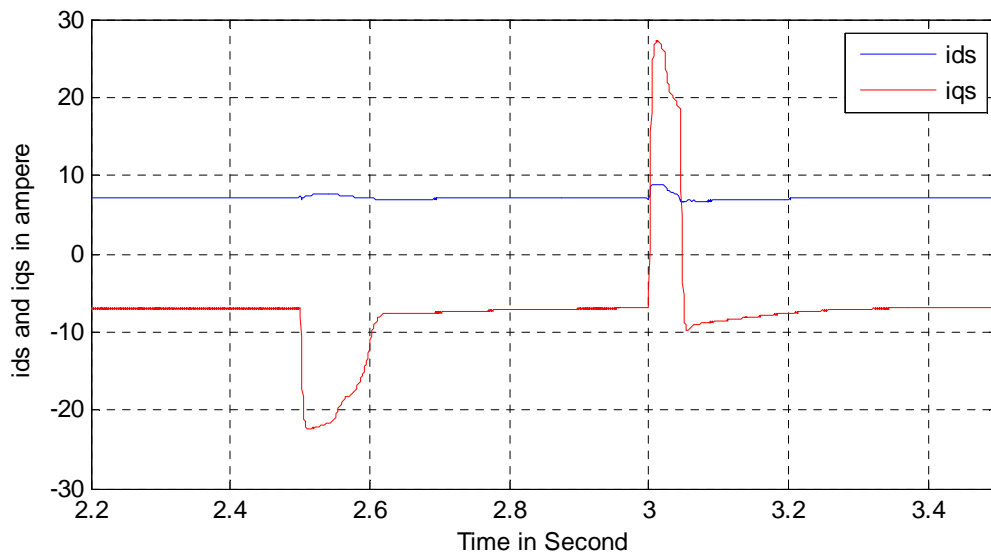


Figure 4.45 Direct and quadrature axis current response with fuzzy controller

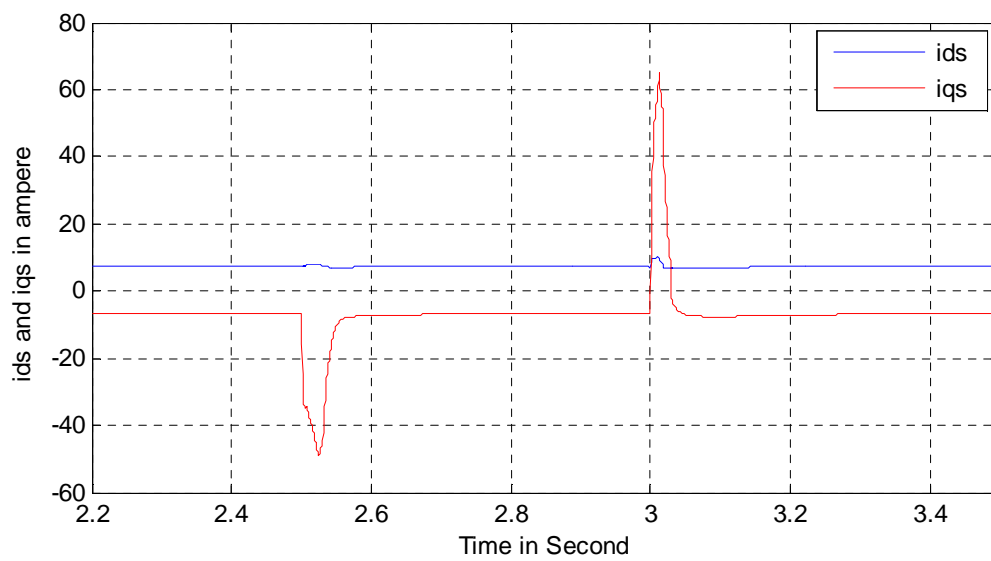


Figure 4.46 Direct and quadrature axis current response with self tuned fuzzy controller

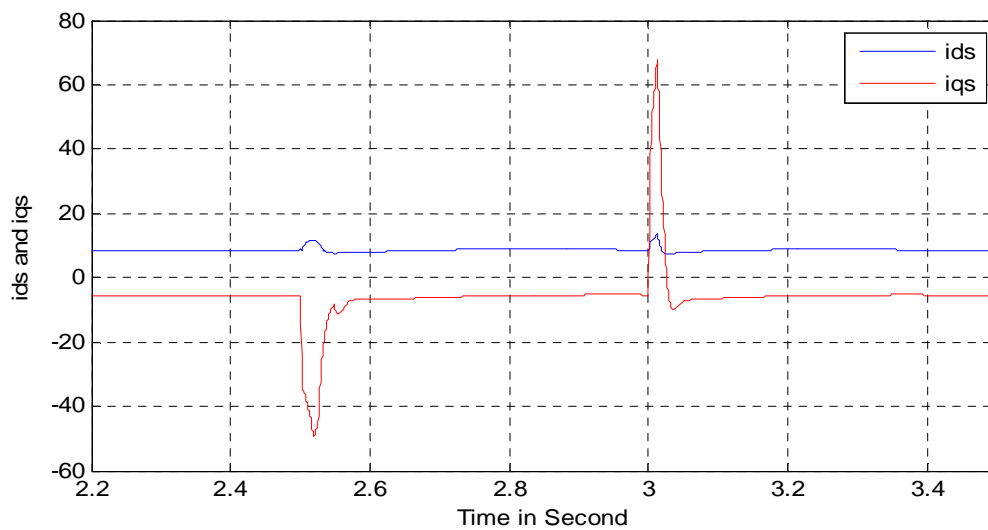


Figure 4.47 *Direct and quadrature axis current response with hybrid controller*

4.6 CONCLUSION

In the above sections three different controllers i.e. fuzzy controller, self tuned fuzzy controller and hybrid controller, are designed and used to improve the performance of an induction generator system. In this chapter the performance of the system is evaluated. we observed that the fuzzy controller gave better transient performance than the PI controller but in steady state the fuzzy controller performance was poorer than the PI controller, as in the steady state the fuzzy controller introduces some error and noise. The self tuned fuzzy controller gives the fastest transient response but it introduces some steady state error and noise in the system which is less than the fuzzy controller, but it remains to be the main drawback of the self tuned fuzzy controller. With hybrid controller the drawbacks in fuzzy and self tuned fuzzy controllers were compensated. The transient response of the hybrid controller is a bit slower than the self tuned fuzzy controller but the hybrid controller gave a superior steady state response than the self tuned fuzzy controller which makes the hybrid controller suitable for high performance control.

Chapter 5

Vector control of grid side PWM converter for power factor improvement

5.1 INTRODUCTION

In the power processor block of Figure 3.8 two VSIs are connected in back to back fashion among which the machine side VSI is used for the vector control of the induction generator. It makes the output voltage of the induction generator of variable magnitude and variable frequency. The line side converter can be made to work as a controlled converter with bidirectional power flow and as a STATCOM capable of working at unity and leading power factors. Besides, the magnitude and frequency of the output voltage can be made constant which allows the system to be grid connected. Two distinctive features in bridge circuit of Figure 3.8 are the inductances L on the ac side and a large capacitance on the dc link. The capacitance is used to ensure fairly constant voltage over a short period of time, irrespective of the transients and the switching the events in the convertor. The phase circuit inductance L is intended to filter out the current ripples and assist in the indirect control process of the current at a chosen power factor.

In this chapter the complete wind power generation system will be discussed which will include two important strategies, which are

- Maximum power point tracking
- Grid side PWM inverter control

5.2 MAXIMUM POWER POINT TRACKING

As shown in chapter-1 the power extracted by a wind turbine for a given wind speed is maximized if C_p is maximized. The optimum value of C_p , always occurs at a definite value of λ i.e. λ_{opt} , this means for varying wind speed, the rotor speed should be adjusted to adhere always to this value of $\lambda = \lambda_{opt}$ for maximum mechanical power output from the turbine. To achieve this condition, a strategy known as maximum power point tracking is used. By using this technique the reference speed command for the induction generator is changed such that the value of λ always remains at λ_{opt} .

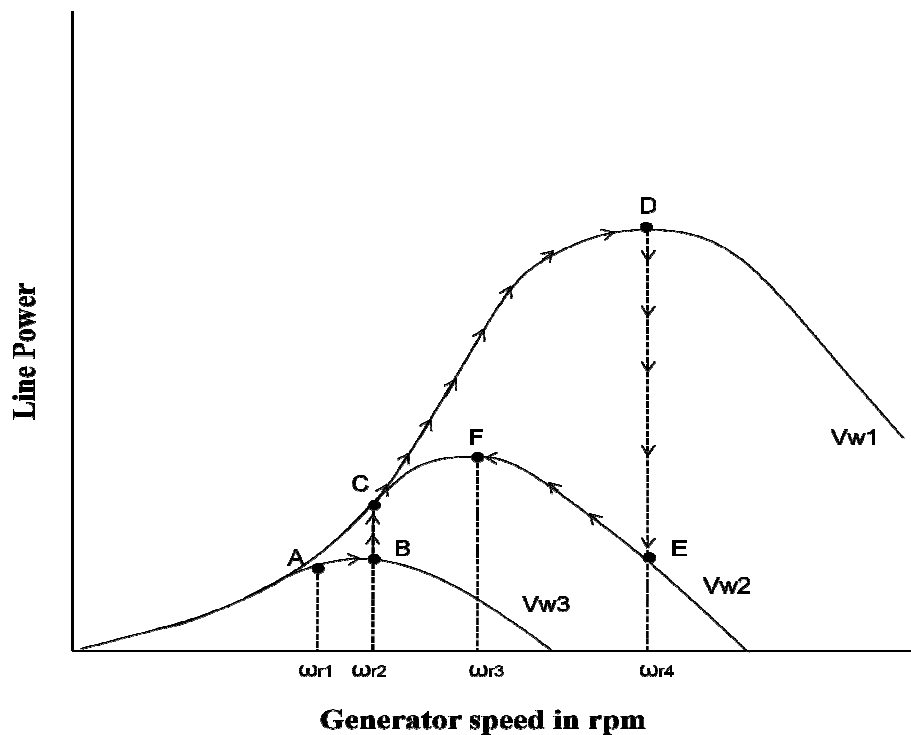


Figure 5.1 Maximum power point tracking strategy

For a particular wind velocity, function of maximum power point tracking algorithm is to search the generator speed until the system settles down at the maximum power output condition. As shown in Figure 5.1, for wind velocity $Vw3$, the output power is at point-A if the generator

speed is ω_{r1} . The maximum power point tracking algorithm alters the speed in steps until it reaches the value ω_{r2} , where the output power is maximum at point-B. If the wind velocity will increase to $Vw1$, the output power will jump to point-C, and then maximum power point tracking algorithm will bring the operating point to D by searching the speed to ω_{r4} . Similarly when the wind speed decreases to $Vw2$, the operating point again jumps to point E. From point E the maximum power point tracking algorithm again drives the operating point to point F which gives the maximum power at wind speed of $Vw2$ for a generator speed of ω_{r3} .

5.3 SUPPLY SIDE CONVERTER CONTROL

With reference to the rectifier convention and considering the fundamental frequency components only, the steady-state ac-side quantities are related in the manner shown in the Figures 5.2, 5.3 and 5.4.

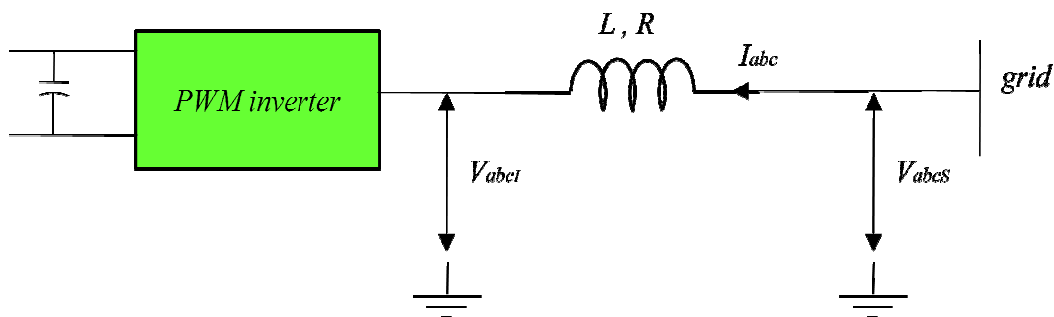


Figure 5.2 Grid side power circuit configurations

For the rectifier mode of operation, shown in Figure 5.3, the fundamental frequency component V_l at the ac input terminals lags behind the source voltage V_s by an angle δ , and I has a component in phase with V_s . In the phasor diagram of Figure 5.4, the voltage V_l leads V_s when the ac supply current I has a component which is in phase opposition to V_s , implying the inverting mode of operation, where the power flow is from the dc side to the ac side. In either

case, neglecting the resistance of the inductor coil, the power flow through the inductor coil is given by

$$P = 3 \frac{V_s V_I}{X_L} \sin \delta \quad (5.1)$$

Where δ is known as the load angle and is supposed to be positive for the lagging phase.

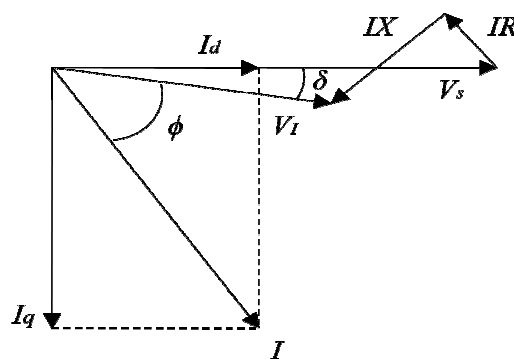


Figure 5.3 Phasor diagram for rectifier mode of operation of PWM inverter

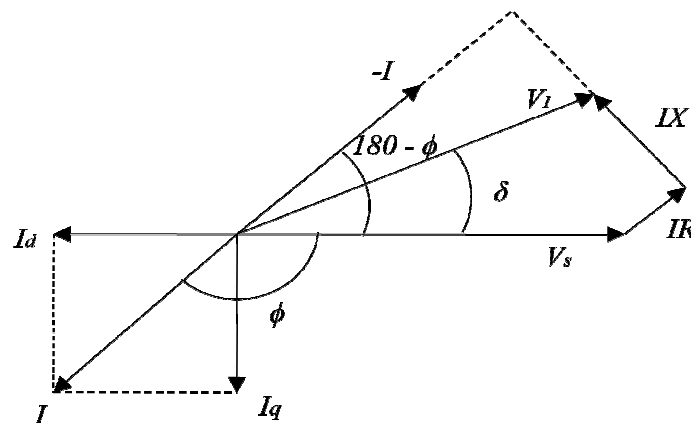


Figure 5.4 Phasor diagram for inverter mode of operation of PWM inverter

Therefore, the current magnitude, power transfer, and the mode of operation (rectifier/inverter) can be controlled by adjusting the magnitude and / or phase (lag or lead) of V_I in relation to the ac supply voltage V_s .

From the phasor diagram in Figure 5.3 the in-phase and the quadrature components of the converter ac terminal voltages are found to be

$$V_I \cos \delta = V_s - RI \cos \phi - XI \sin \phi \quad (5.2)$$

$$V_I \sin \delta = XI \cos \phi - RI \sin \phi \quad (5.3)$$

For the inverting mode, with the current I flowing into the source at a power-factor angle ϕ_I , ϕ in equation (5.2) and equation (5.3) is replaced by $(180^\circ - \phi_I)$.

V_s , R , and X are obtained from direct measurements. To operate the converter at a desired power factor angle ϕ for any demand of the current I , or power, equation (5.2) and (5.3) are used to provide the values of V_I and δ , which decide the magnitude and the phase of the modulating sine waves with reference to the supply voltage.

Inverter terminal voltages v_{aI} , v_{bI} , and v_{cI} can be controlled by a vector controller for their magnitudes and required phases shift from the supply to meet the required active and reactive powers. The voltage equation for the line inductors are

$$v_{abc,s} = Ri_{abc} + L \frac{di_{abc}}{dt} + v_{abc,I} \quad (5.4)$$

In the d^e - q^e reference frame as shown in Figure 5.5, rotating at the supply angular frequency ω_e and the d^e -axis coinciding with the supply voltage vector, the voltage equation 5.4, becomes

$$v_{ds}^e = Ri_{ds}^e + Lp i_{ds}^e - L\omega_e i_{qs}^e + v_{dt}^e, \quad (5.5)$$

$$0 = Ri_{qs}^e + Lp i_{qs}^e + L\omega_e i_{ds}^e + v_{qt}^e, \quad (5.6)$$

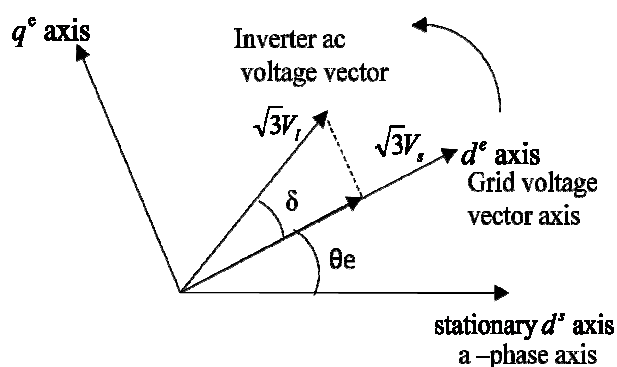


Figure 5.5 Angular relationships

Where v_{di}^e and v_{qi}^e are the components of the inverter ac terminal voltage vector along the d^e and q^e - axis.

Again

$$P = v_{ds}^e i_{ds}^e + v_{qs}^e i_{qs}^e \quad (5.7)$$

$$\text{but, } v_{ds}^e = \sqrt{3}V_s \quad (5.8)$$

$$\text{and } v_{qs}^e = 0$$

From equation (5.7), the active power flow is

$$P = v_{ds}^e i_{ds}^e \quad (5.9)$$

Using equations (5.6) and (5.8) in equation (5.9) for steady state operation, i.e., $p = 0$ and neglecting R .

$$P = -\frac{\sqrt{3}V_s V_{qi}^e}{\omega_e L} \quad (5.10)$$

With reference to the relative positions of the voltage vectors and their components along the d^e - q^e , the power flow given by equation (5.10) becomes

$$P = -\frac{3V_s V_I}{X_L} \sin \delta \quad (5.11)$$

Again the reactive power is given by

$$Q = v_{qs}^e i_{ds}^e - v_{ds}^e i_{qs}^e \quad (5.12)$$

Since $v_{qs}^e = 0$, from equation (5.12), the reactive power flow is

$$Q = -v_{ds}^e i_{qs}^e \quad (5.13)$$

The use of equations (5.5) and (5.8) with voltage vector components along the d^e - q^e axes in figure 5.3 gives

$$Q = \frac{3V_s^2}{X_L} - \frac{3V_s V_I}{X_L} \cos \delta \quad (5.14)$$

The vector control scheme to regulate the power flow is detailed in Figure 5.6. The utility system voltage $v_{abc,s}$ is transformed into stationary d^s - q^s components. As the d^e -axis of the synchronously rotating reference frame is aligned along the supply voltage vector, the angular position of the d^e -axis is computed as

$$\theta_e = \arctan \frac{V_q^s}{V_d^s} \quad (5.15)$$

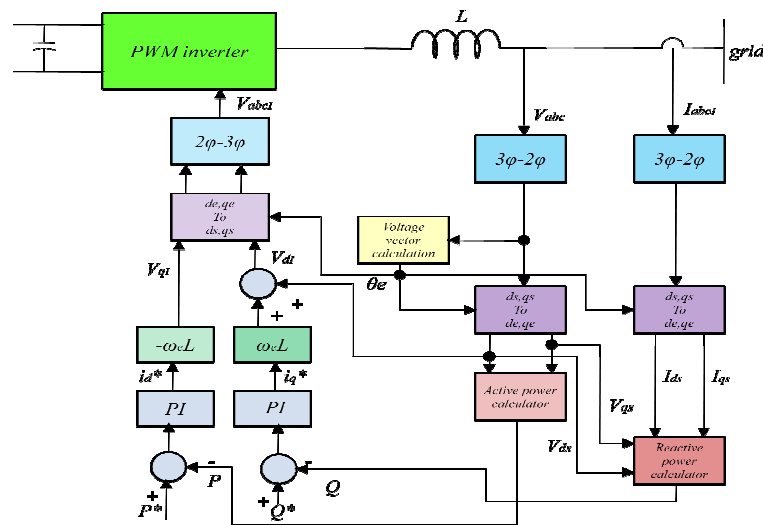


Figure 5.6 Vector control scheme for line side converter

The actual active and reactive powers, computed by equations (5.9) and (5.13), respectively, are compared with the reference values P^* and Q^* to generate the reference values of the inverter terminal voltages v_{dl}^e and v_{ql}^e in accordance with equations (5.5) and (5.6). P^* is the active power generated by the induction generator and the reference reactive power Q^* is taken as zero such that the supply side power factor becomes unity.

Actual power output of the grid side converter will be less than the power output of the induction generator since the losses of the converters are to be supplied. Therefore setting P^* equal to output power of the induction generator will not be able to keep the dc link voltage constant if there are losses taking place in the converters. But for this work the converters are assumed to be lossless so that the power generated from generator becomes equal to the power at the grid side. So, setting P^* equal to the output of the induction generator will not affect the control scheme adversely. Closed loop control of dc link voltage to generate P^* and i_d , and closed loop control of i_q will be interesting future course of research.

5.4 RESULTS AND DISCUSSION

In this section the wind power generation system using induction generator is simulated and the results are presented. The wind power generation system is simulated with varying wind velocities. The maximum power point tracking algorithm decides the reference speed of the induction generator for extraction of the maximum power from the wind. After the reference speed has been decided vector control of the induction generator is done for performance improvement of the induction generator. Then the vector control of the grid side converter is done to make the generated voltage and frequency constant as well as for power factor improvement. The comparison of the generator side and grid side parameters are given below.

5.4.1 Wind velocity Response

Figure 5.7 shows the variation in wind velocity as a function of time. Initially the wind speed reduces from 9m/s to 8m/s then remains constant for 2 s and again increases to 12 m/s and remains constant at that value.

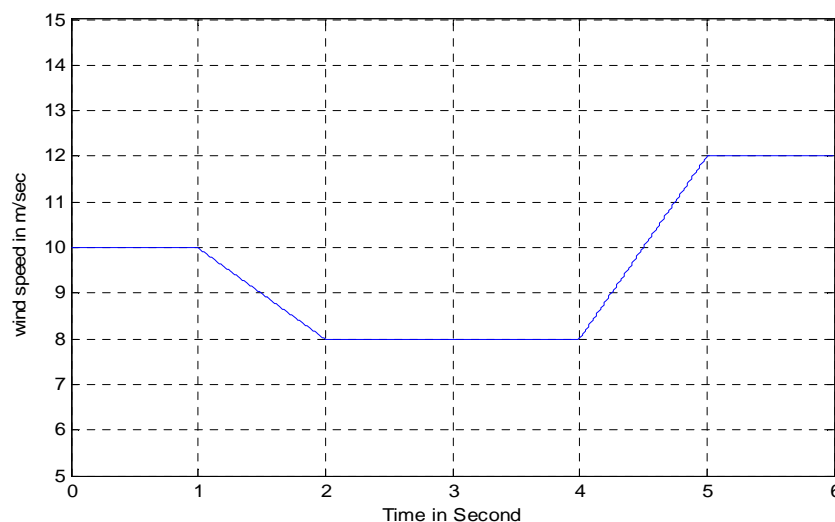


Figure 5.7 Wind velocity as a function of time

5.4.2 Reference speed Response

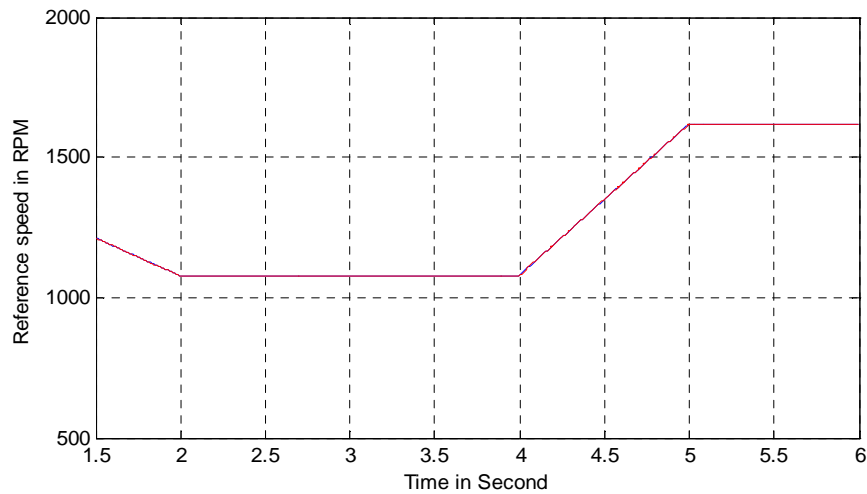


Figure 5.8 Reference speed of the induction generator as given by maximum power point tracking algorithm

As the wind velocity varies, the maximum power point tracking algorithm comes into action and keeps track of the reference speed of the induction generator such that maximum power can be extracted from the wind. The effect of maximum power point tracking technique can be seen from Figure 5.8. The figure shows the change in the reference speed of the induction generator in accordance with the wind velocity to extract the maximum power from the wind.

5.4.3 Turbine torque Response

The mechanical systems of a wind turbine introduce harmonics in the turbine torque which makes the turbine torque pulsating in nature. The oscillatory torque of the wind turbine is more dominant at the first, second and fourth harmonics of the fundamental turbine angular velocity. The oscillatory torque is given as

$$T_{osc} = T_m (A \cos \omega t + B \cos 2\omega t + C \cos 4\omega t) \quad (5.16)$$

The total turbine torque is given as $T_{turbine} = T_m + T_{osc}$ (5.17)

The variation in turbine torque due to the change in wind speed is shown in Figure 5.9. The pulsating nature of the turbine torque due to oscillatory torque can be seen in the figure.

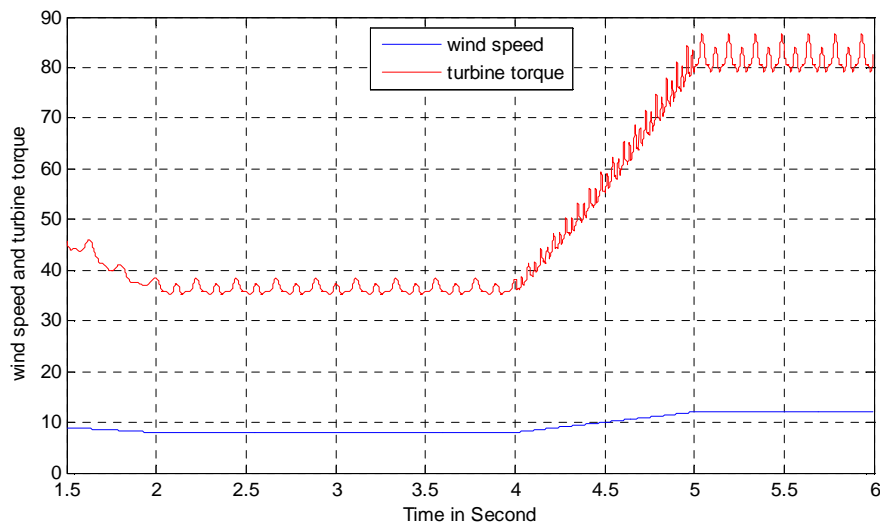


Figure 5.9 Variation in turbine torque

5.4.4 Electromagnetic torque Response of induction generator

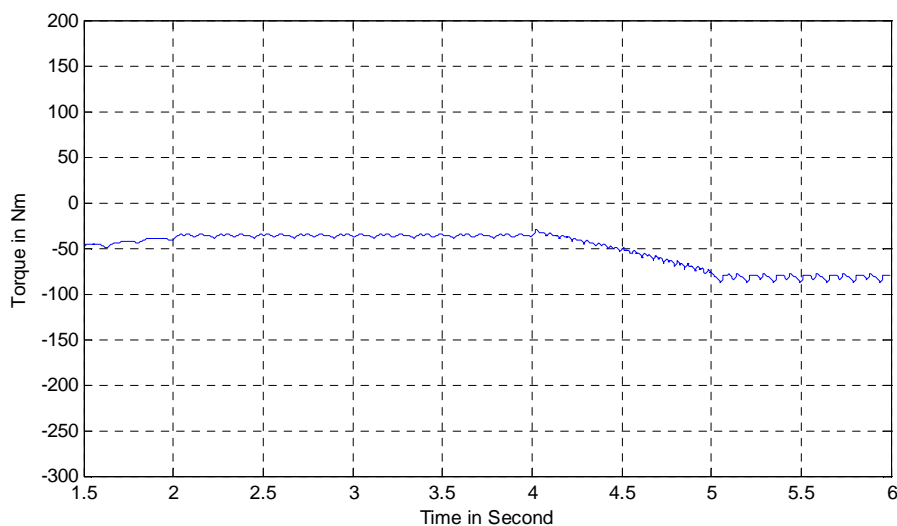


Figure 5.10 Torque response of the induction generator

The electromagnetic torque response of the induction generator is shown in the Figure 5.10.

5.4.5 Direct and quadrature axis current response at generator and grid terminals

Figure 5.11 gives the direct axis and quadrature axis stator currents at the induction generator end.

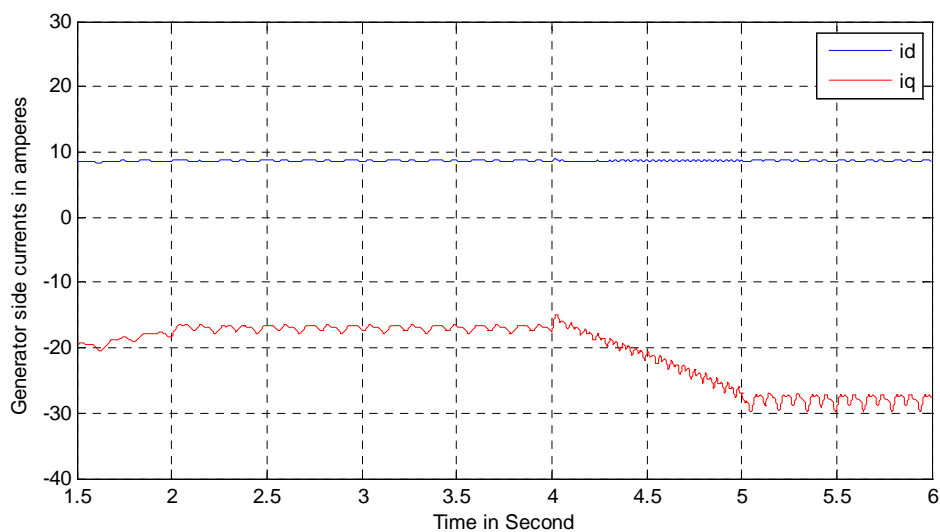


Figure 5.11 Generator side direct and quadrature axis current responses

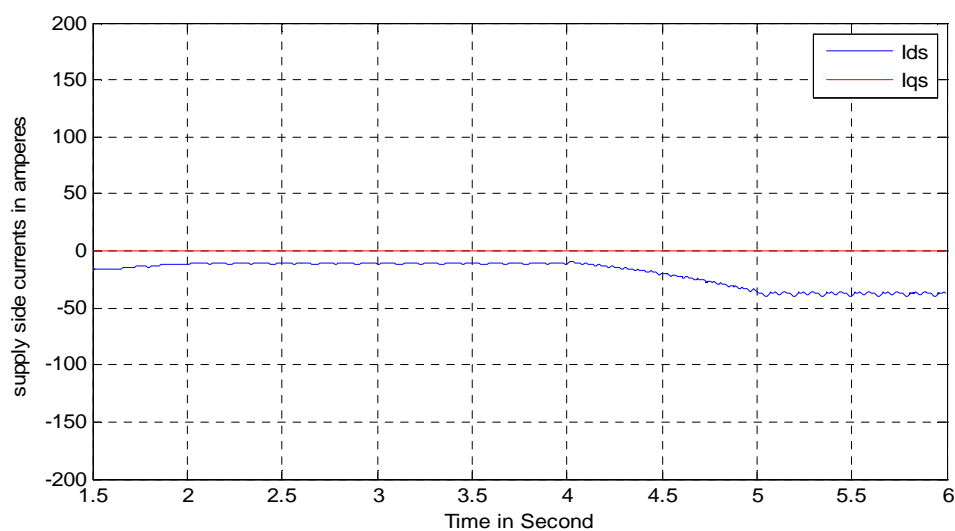


Figure 5.12 Grid side direct and quadrature axis current responses

Due to the effect of indirect vector control technique the direct axis current I_d or the flux component of current remains constant as the torque component of current I_q varies due to the variation of turbine torque. The pulsations in the electromagnetic torque of the induction generator are due to the oscillatory torque of the wind turbine. The responses of the direct and quadrature axis currents at the grid side are given in Figure 5.12.

5.4.6 Active and reactive power responses at generator side and grid side

Figure 5.13 shows the active and reactive power response at the induction generator side. The figure shows that both the active power and reactive power at the generator side vary as the turbine torque varies.

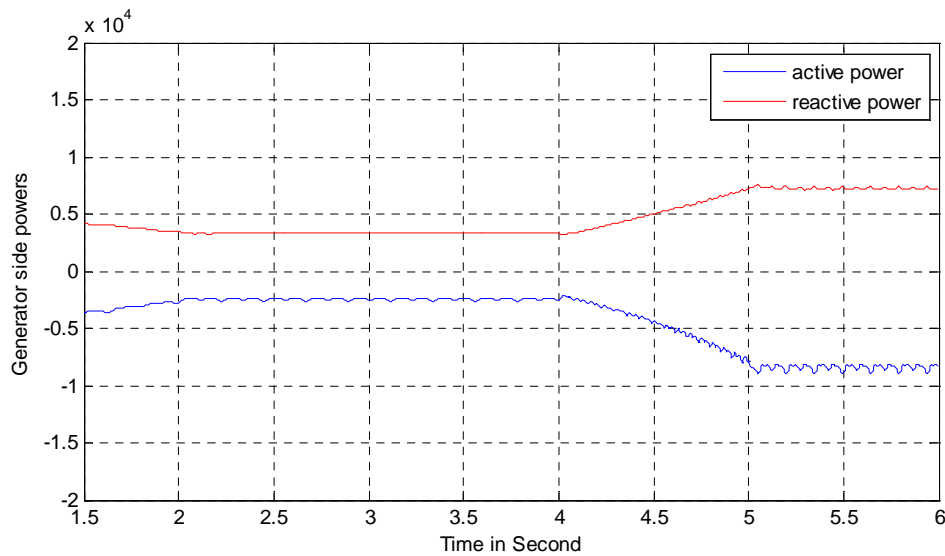
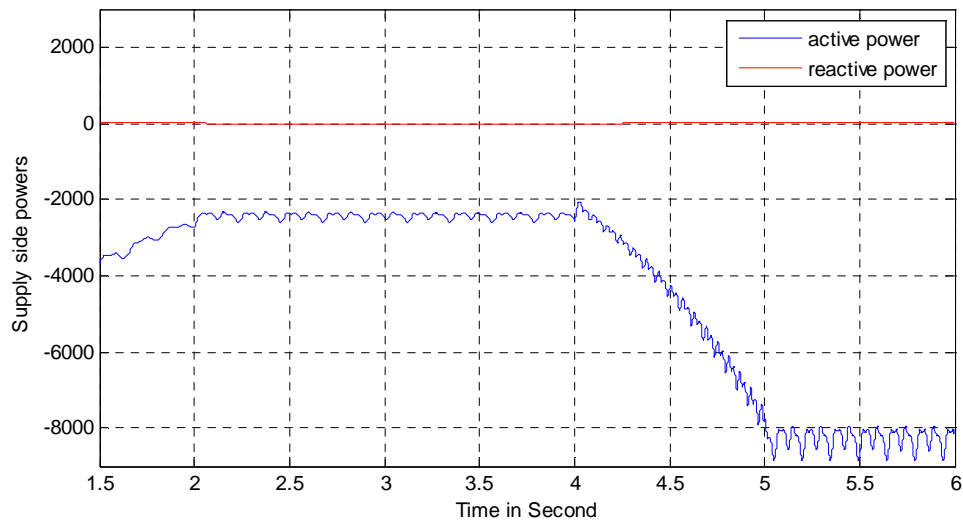
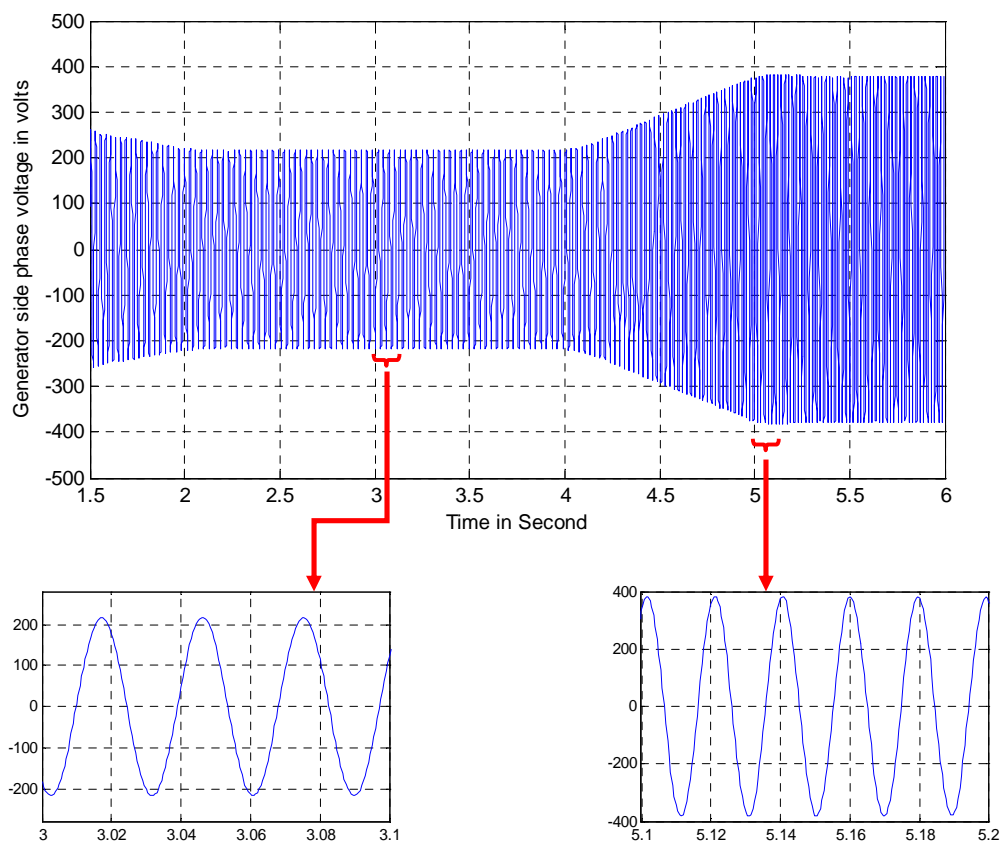


Figure 5.13 Generator side power responses

But due to the vector control of the grid side inverter the reactive power at the grid side becomes zero and only the active power is transferred to the grid which can be seen from Figure 5.14.

Figure 5.14 *Grid side active and reactive power responses*

5.4.7 Phase voltage response at generator side and grid side

Figure 5.15 *Generator side phase voltage response*

The responses for phase voltage at the generator terminals and grid terminals are given in Figure 5.15 and 5.16 respectively. It is clear from the Figure 5.15 that the amplitude and frequency of the generator side phase voltage vary with variation in turbine torque, which makes the induction generator system unsuitable for direct grid connection.

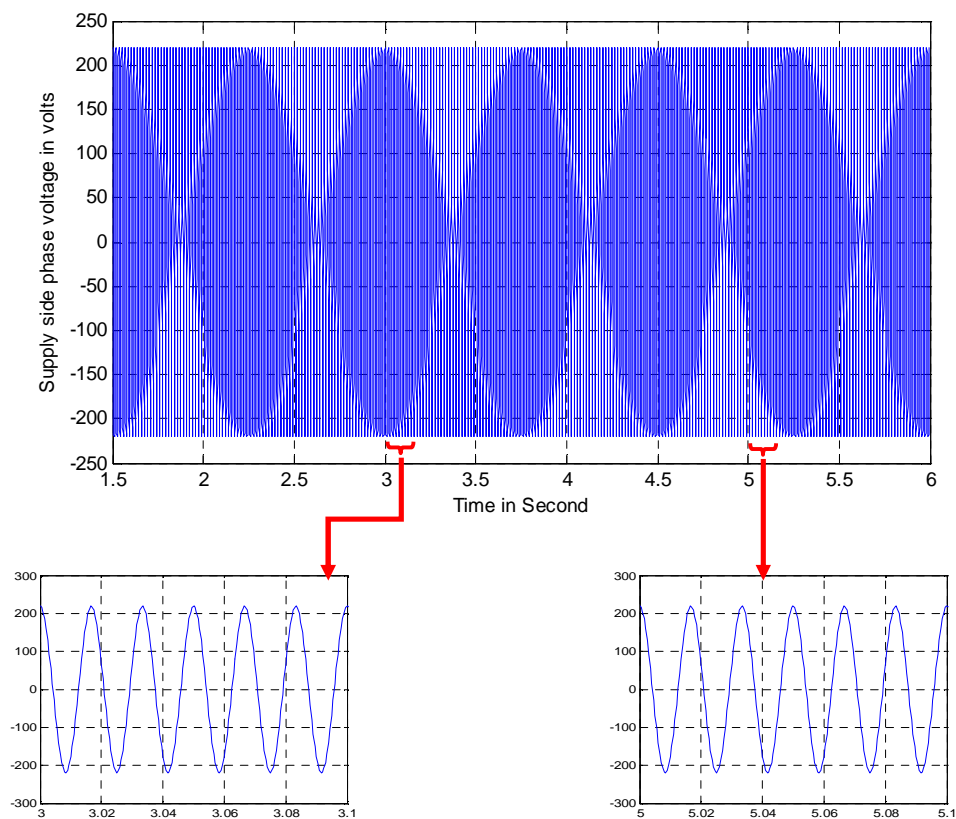


Figure 5.16 *Grid side phase voltage response*

But by vector control of the supply side converter the amplitude and frequency of the grid side phase voltage can be made constant due to which the system becomes suitable for grid connection. Figure 5.16 shows the constant amplitude and constant frequency output phase voltage of the grid side converter.

5.4.8 Phase current response at generator side and grid side

From Figure 5.17 it is evident that the frequency of generator side phase current also varies with the variation in the turbine torque. But from Figure 5.18 it can be seen that due to the vector control of the grid side converter the frequency of the grid side phase current also becomes constant.

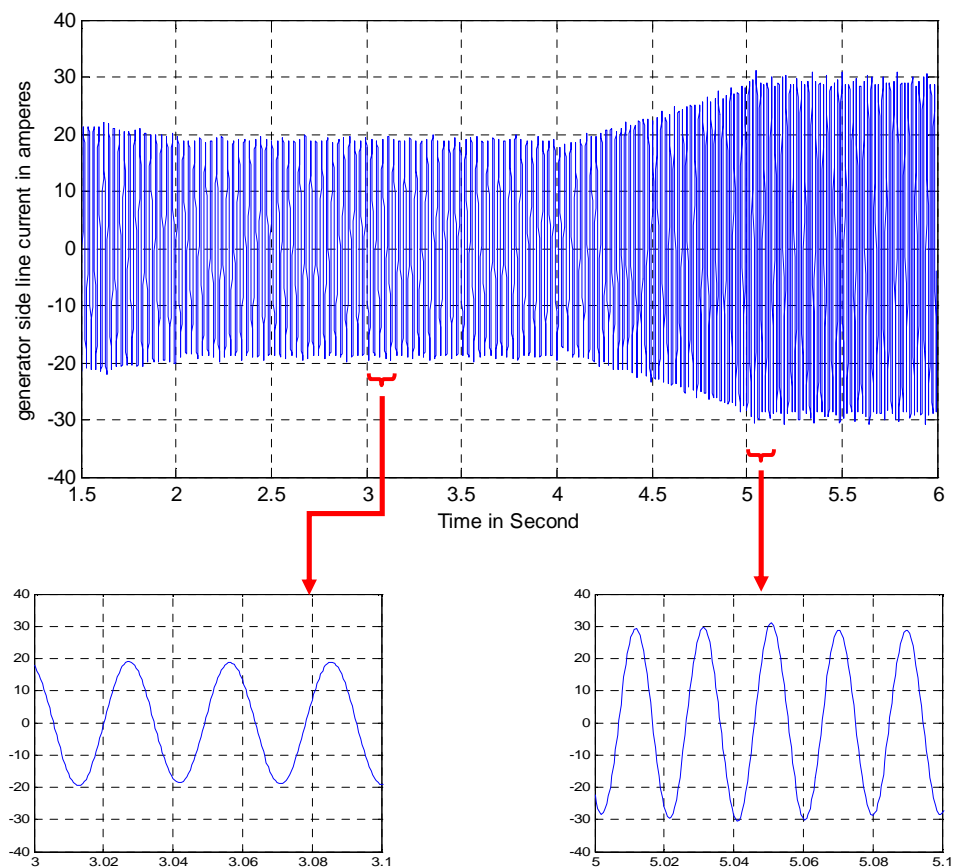


Figure 5.17 Generator side phase current response

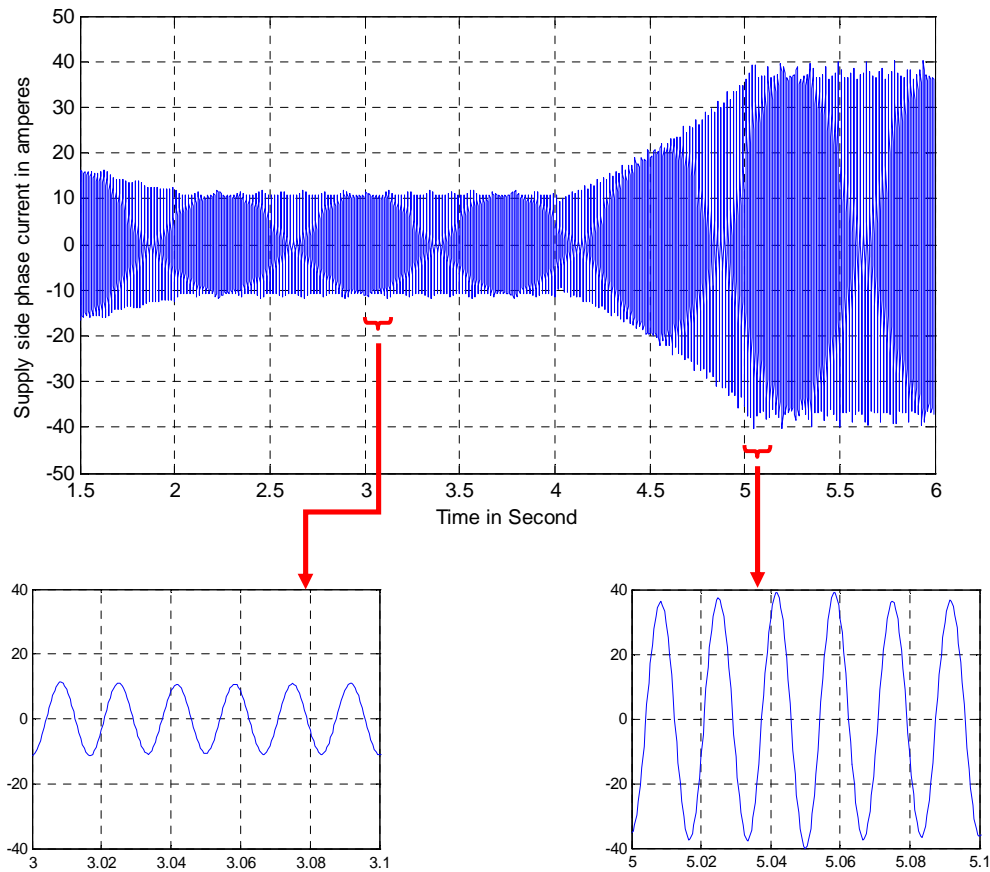


Figure 5.18 *Grid side phase current response*

5.4.9 Power factor response at generator side and grid side

The Figure 5.19 shows the phase relation of the generator side phase voltage and generator side phase current. It is clear from the figure that the phase current lags behind the phase voltage by an angle greater than 90 degrees but less than 180 degrees, due to which the active power becomes negative i.e. active power flows from generator to grid, but the reactive power remains positive and flows from grid to the induction generator. So the power factor at the generator side remains less than unity which can be seen from Figure 5.21.

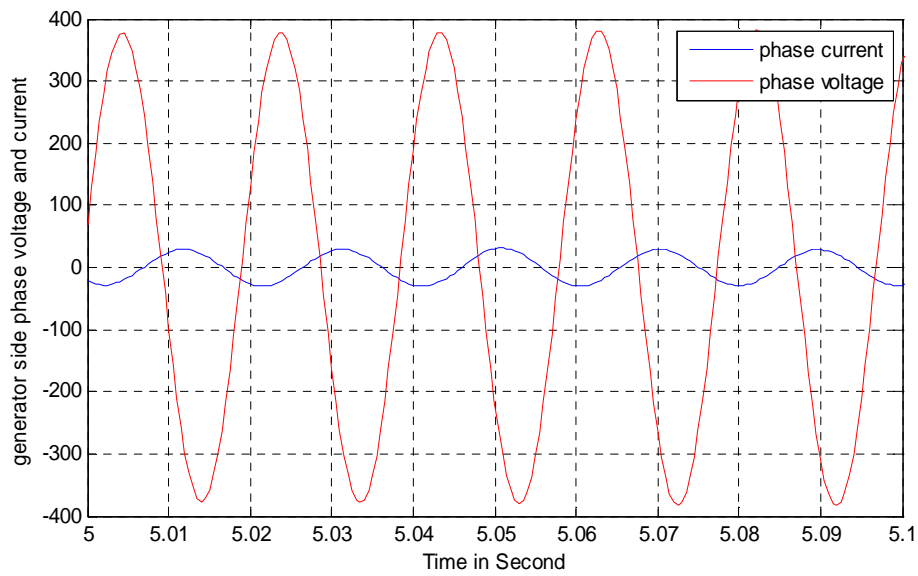


Figure 5.19 *Phase relation between voltage and current of generator side*

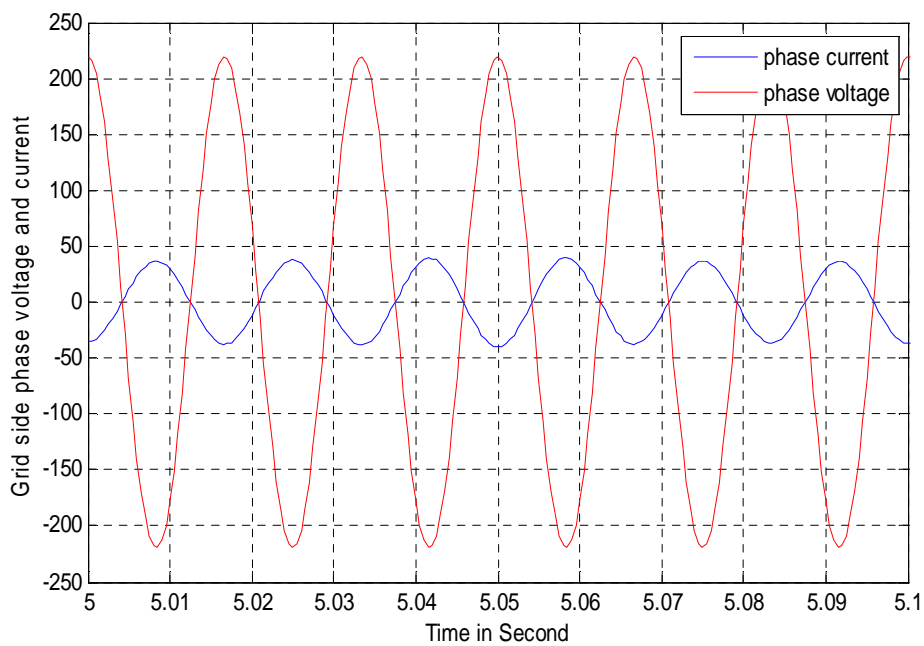


Figure 5.20 *Phase relation between voltage and current of grid side*

The Figure 5.20 shows the phase relation of the grid side phase voltage and grid side phase current. From the figure it can be seen that the phase current and the phase voltage are at a phase difference of exactly 180 degrees, due to which the active power becomes negative i.e. active power flows from generator to grid, and the reactive power becomes zero. So the power factor at the grid side becomes unity which can be seen from Figure 5.21.

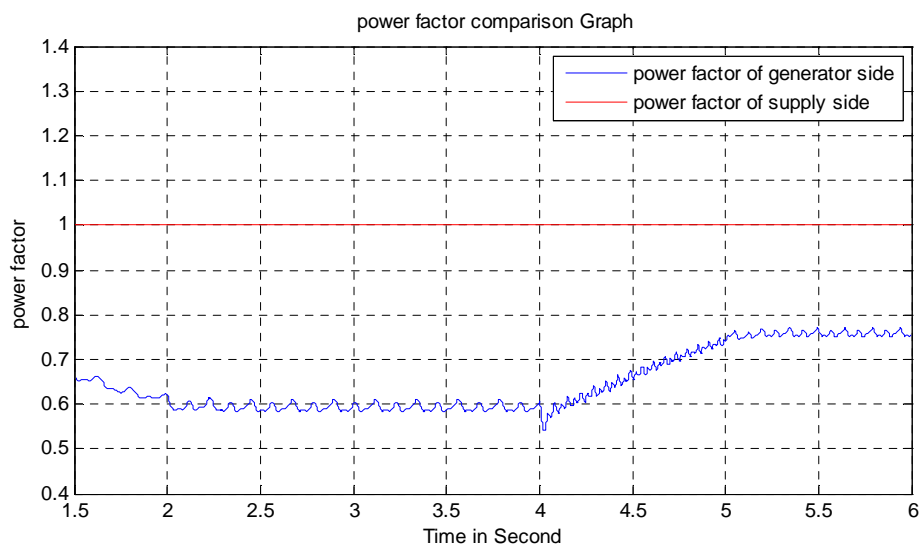


Figure 5.21 *Generator side and grid side power factor*

5.5 CONCLUSION

In this chapter the complete evaluation of the induction generator system is done. By utilizing the maximum power point tracking algorithm maximum power is extracted from the wind. The vector control of the grid side converter made it possible to connect the induction generator system directly with the grid. It also helped in achieving unity power factor at the grid side.

Chapter 6

Fabrication and testing of control circuit for a bidirectional converter inverter set used in line excited induction generator

6.1 INTRODUCTION

The implementation of PI control, fuzzy control or any high performance control requires a complex and fast controller. A microprocessor/microcontroller/ digital signal processor forms an integral part of such a controller. A fast controller provides a faster sampling rate as needed, to ensure stable and successful control. PC- based implementation of the PI control for PWM voltage source inverter-fed induction generator is considered here. The design and fabrication of the control circuit for the bidirectional PWM converter inverter set are described in this section. The test results are presented and discussed later in this section.

A schematic block diagram for the high performance control of induction generator is shown in Figure 6.1. The digital part of the controller involves a Pentium processor-based PC housed with moderately priced add-on cards, such as analog data acquisition card (PCL-208) and analog output card (PCL-726). The different units of the control scheme are:

- The power electronic converters feeding a variable voltage, variable frequency supply to the three phase induction generator.
- The bidirectional PWM converter- inverter control circuits.
- Measurement and Data acquisition modules.

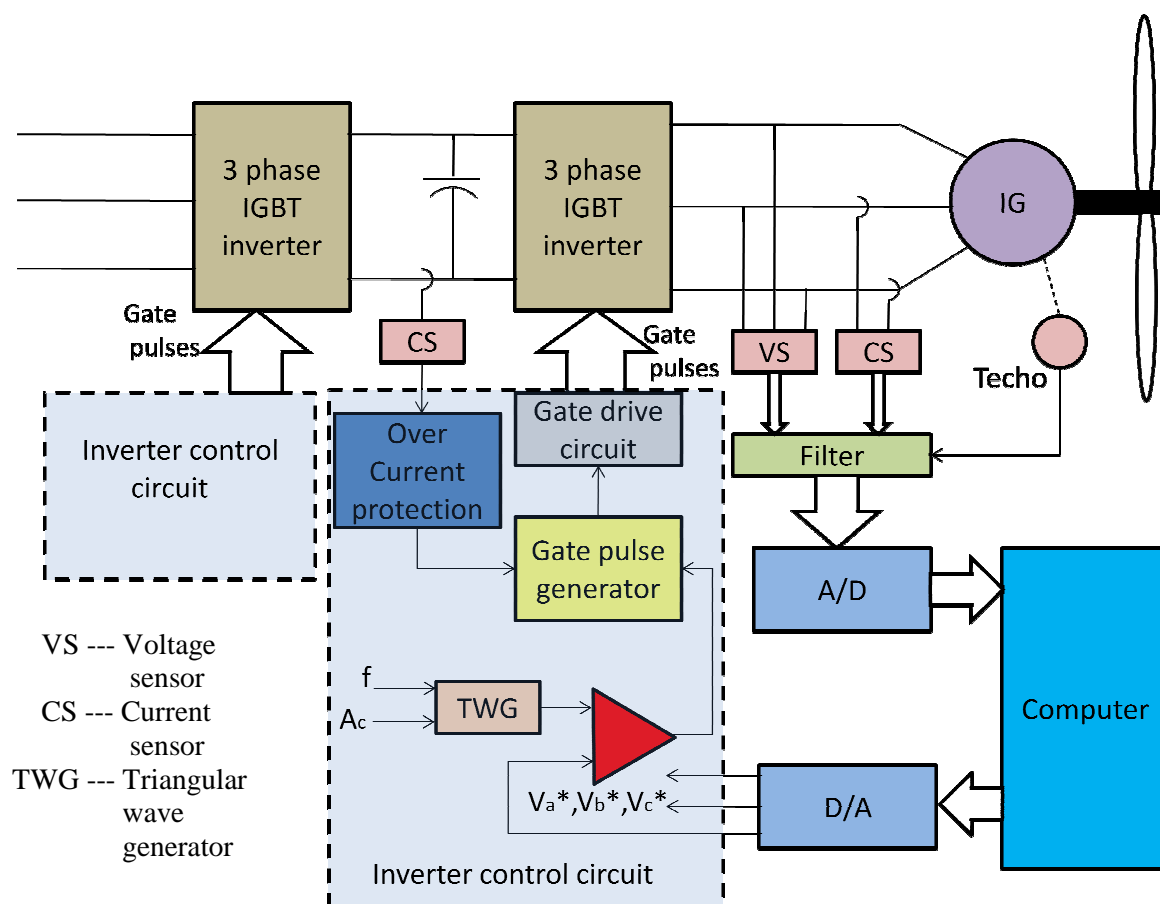


Figure 6.1 Schematic block diagram for induction generator control

6.2 POWER ELECTRONIC CONVERTERS

The power processor for the scheme is a three phase sinusoidal pulse width modulated bidirectional voltage source converter inverter (SPWM-VSI) set to connect variable voltage, variable frequency supply from the induction generator to the grid.

The experimental set up for the drive uses two three phase Pulse Width Modulated (PWM) Voltage Source Converters (VSC) using Insulated Gate Bipolar

Transistors (IGBT). The dc input to the inverter is obtained from the three phase IGBT converter and an auto-transformer combination. The VSI enables the variable voltage, variable frequency operation of the induction generator. Figure 6.2 shows the power circuit diagram of the bidirectional converter inverter set employing IGBTs as the switching devices. Two $1000\ \mu\text{F}$, 500 V electrolytic capacitors are connected across the input of the VSI to filter out the ripples in the dc link voltage.

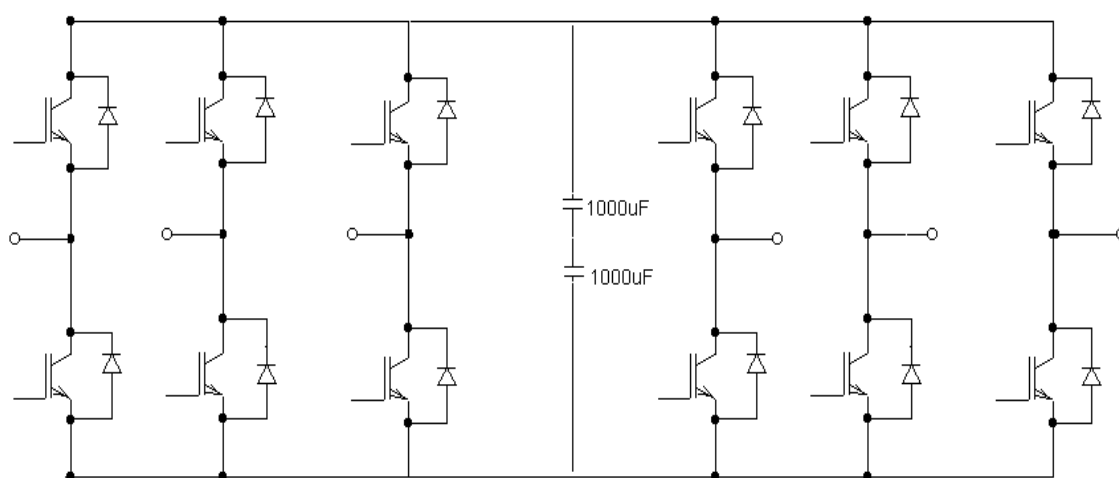


Figure 6.2 *Bidirectional converter inverter set*

6.3 CONTROL CIRCUIT FOR VSI

The block diagram of the control circuit is shown in Figure 6.3. In this modulation scheme, the pulse width is a sinusoidal function of the angular position at which the particular pulse is generated. This type of modulation is realized by comparing a modulating signal termed *control* consisting of a sinusoidal wave of variable amplitude (A) and frequency (f) and a triangular signal termed *carrier* of fixed amplitude (A_c) and frequency (f_c). The frequency, f_c of the triangular wave decides the number of pulses in the output voltage in each half cycle.

The various circuits comprising the control circuit are:

- Triangular wave generator circuit
- Three phase reference sine wave generator
- Comparator circuit
- Lock-out circuit
- Over current protection circuit
- Gate drive circuit

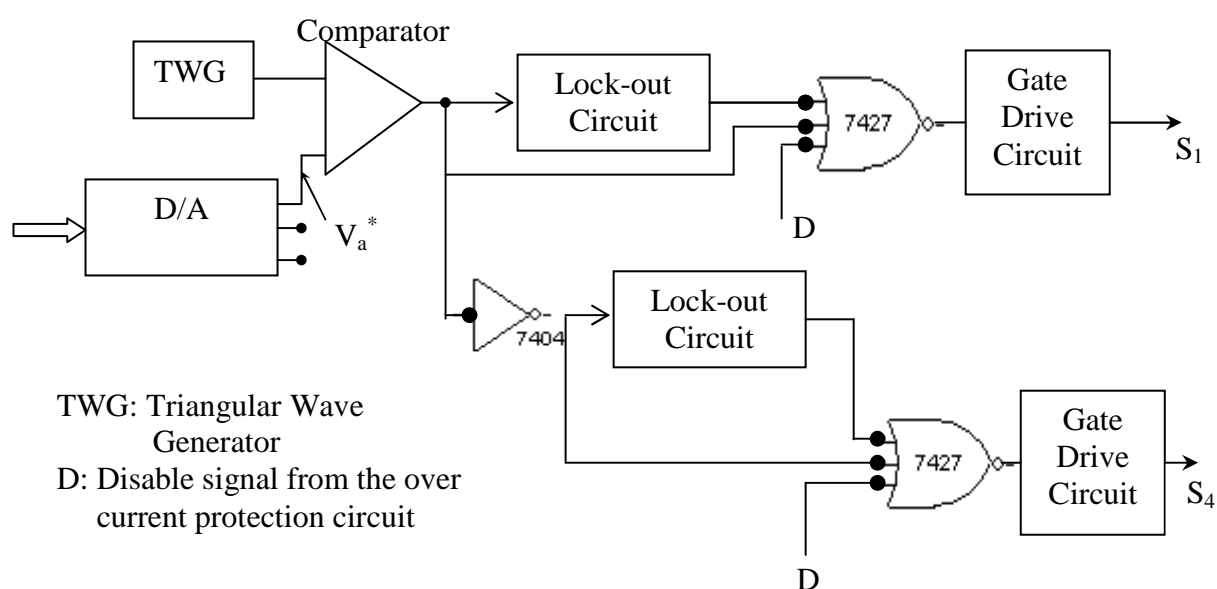


Figure. 6.3 Block diagram of the control circuit

6.3.1 TRIANGULAR WAVE GENERATOR CIRCUIT

A double sided triangular carrier signal is required for modulation. The carrier signal of amplitude, $A_c \geq A$, where A is the peak of the modulating signal; and frequency, f_c is generated using the circuit shown in Figure 6.4. The carrier signal waveform is of nearly triangular shape. The provisions are made to adjust the amplitude

and the frequency of the carrier signal so that the inverter performance is improved. The provision for offset adjustment is also made.

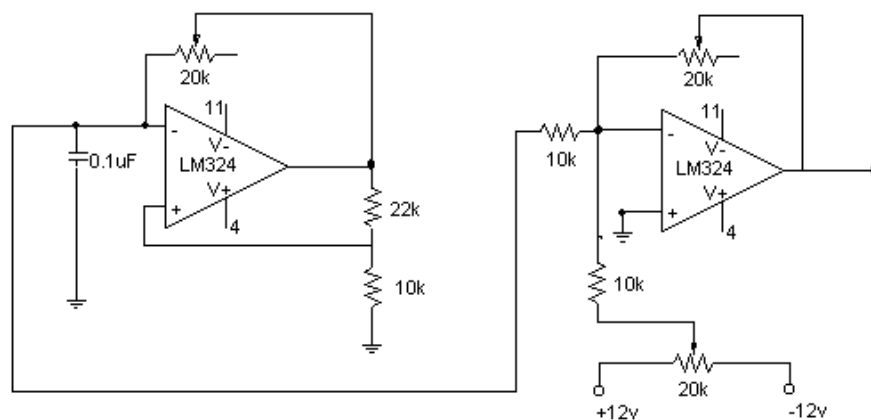


Figure. 6.4 *Triangular wave generator with offset adjustment circuit*

6.3.2 THREE PHASE REFERENCE SINE WAVE GENERATOR

The reference sinusoidal signal is generated by software using a Pentium processor-based PC. The reference signals for phase-a and phase-b are generated with a phase difference of 120° . The reference voltage signal for phase-c is generated using a summing amplifier shown in Figure 6.5, whose inputs are the reference voltage signals for phase-a and phase-b. The potentiometer is provided to adjust the amplitude of the reference voltage signal for phase-c.

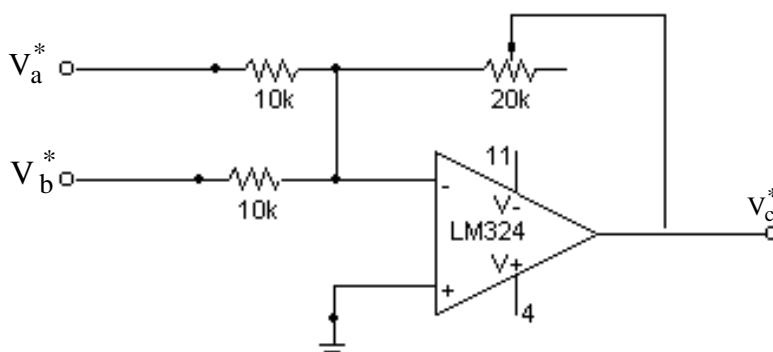


Figure. 6.5 *Summing amplifier circuit*

6.3.3 COMPARATOR CIRCUIT

Figure 6.6 shows the comparator circuit using TL-084. Three reference sinusoidal waves are compared individually with the triangular wave to output the Sinusoidal Pulse Width Modulated (SPWM) signal as required. The negative portion is clipped by the diode and then the output is scaled to +5 V.

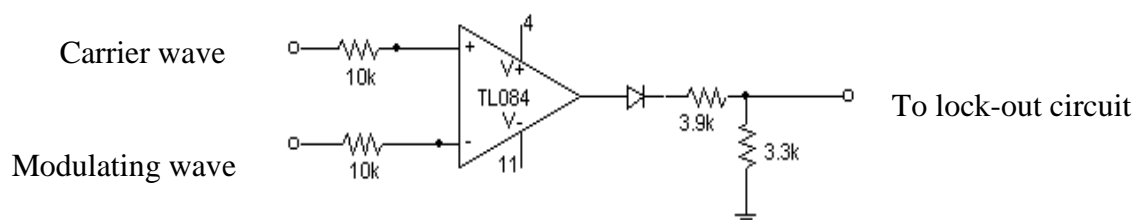


Figure. 6.6 *Comparator, clipping and scaling circuit*

6.3.4 LOCKOUT CIRCUIT

Figure 6.7 shows the lockout circuit. The output of the comparator is passed through a hex inverter gate (7404). The inverted signal and the non-inverted signal are meant for two complementary IGBTs on the same leg of the inverter. These two signals are passed through R-C differentiator and diode circuit, which give a trigger pulse to the monostable multivibrator (555) at the negative edge of the signals. The multivibrator circuit generates a pulse, whose width is constant depending on the values of the resistance and capacitance at the pin numbers 6, 7 of the 555. The width of this pulse (generated by 555) is the interlock delay period. The interlock delay period between a

pair of switching devices (IGBTs) in the same leg is kept at $30\ \mu\text{sec}$. This delay pulse, the signal from the comparator, and the *Enable/Disable* signal from the over current protection circuit are the three inputs to the NOR gate (7427). NOR gates provide the gate pulses to the gate drive circuits of the IGBTs. Three such circuits have been fabricated. The timing diagram of the pulses generated by the lockout circuit are given in Figure 6.8 and Figure 6.9 .

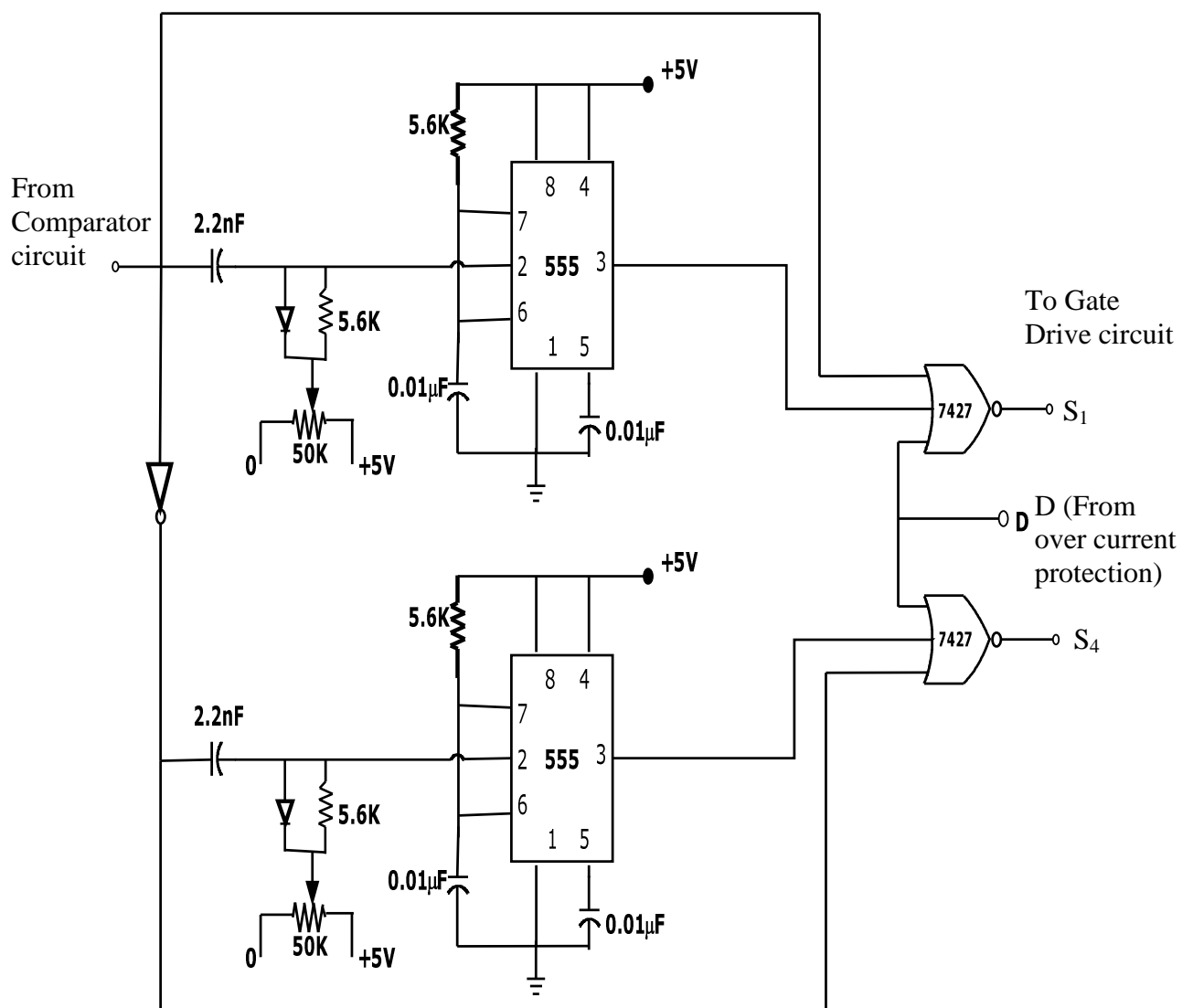


Figure. 6.7 Lockout Circuit

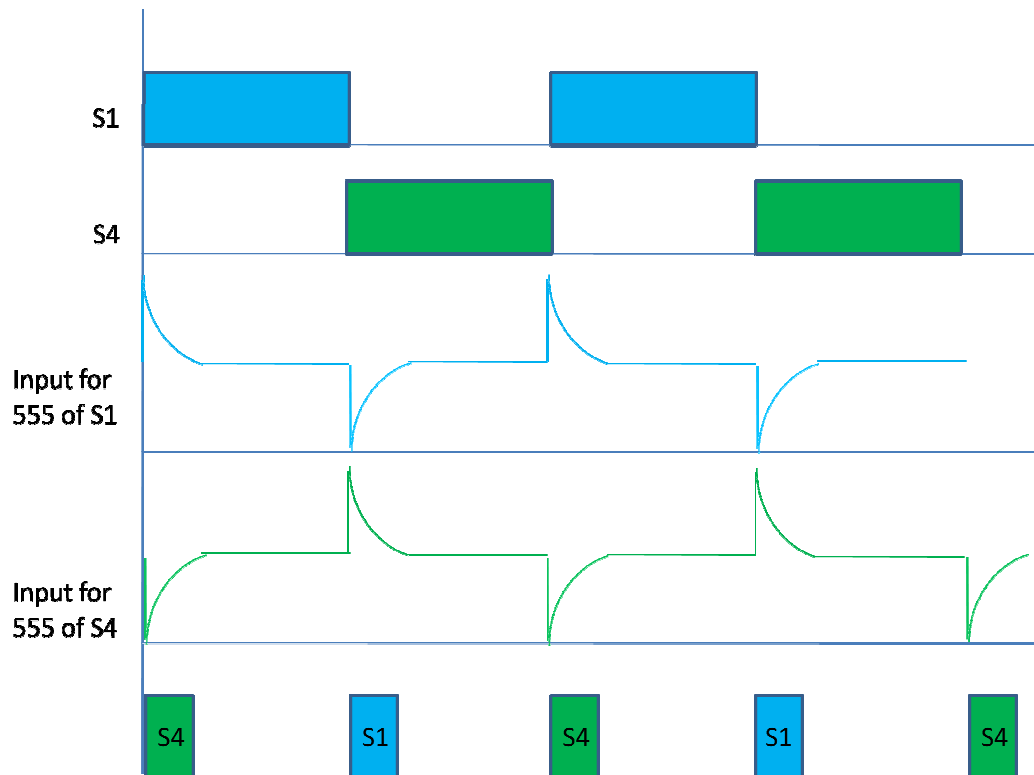


Figure 1.8 Timing diagrams for output pulses of 555

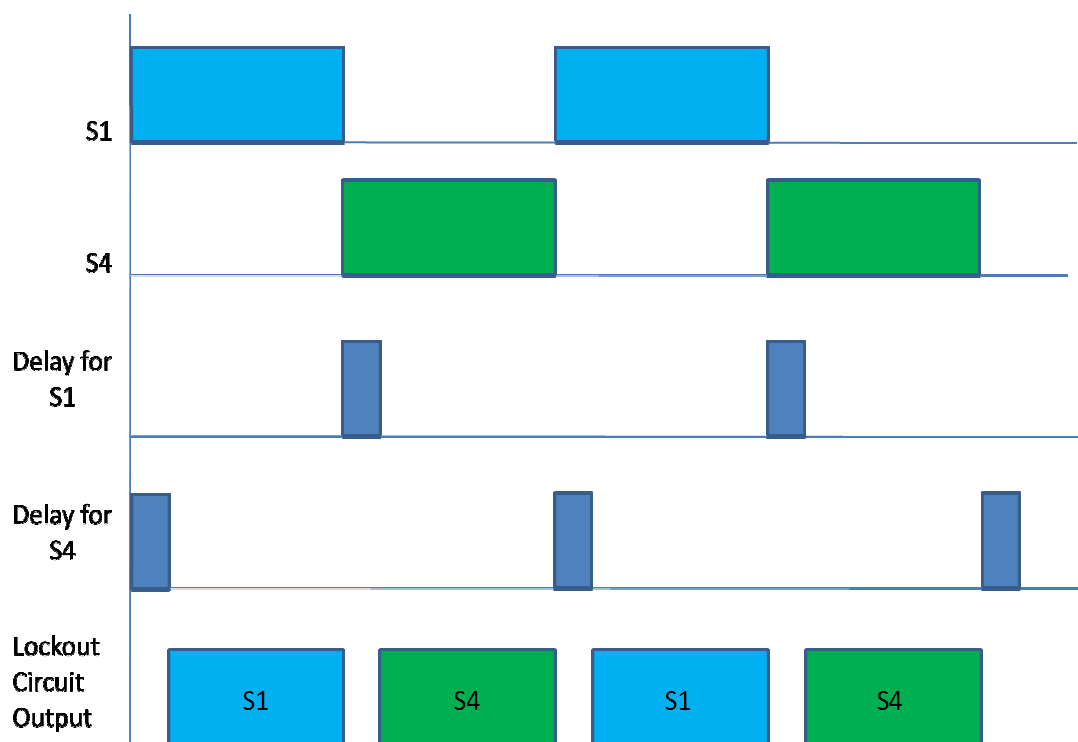


Figure 1.9 Timing diagrams for output pulses of lockout circuit

6.3.5 OVER CURRENT PROTECTION CIRCUIT

Figure 6.10 shows the over current protection circuit. The principle of the circuit is that, when the dc link current exceeds a particular set value, a +5 V output (logic *high*) ($S = 1, R = 0$) is obtained. This logic *high* is NOR-ed with the gate pulse from the comparator circuit, and thus, the gate pulse is disabled ($D = 1$). When the fault is cleared and dc link current is below the set value ($S = 0$); by pressing the *start* Push Button switch ($R = 1$), the gate pulse is enabled ($D = 0$). As long as the fault exists ($S = 1, R = 0$), the gate pulse can never be enabled.

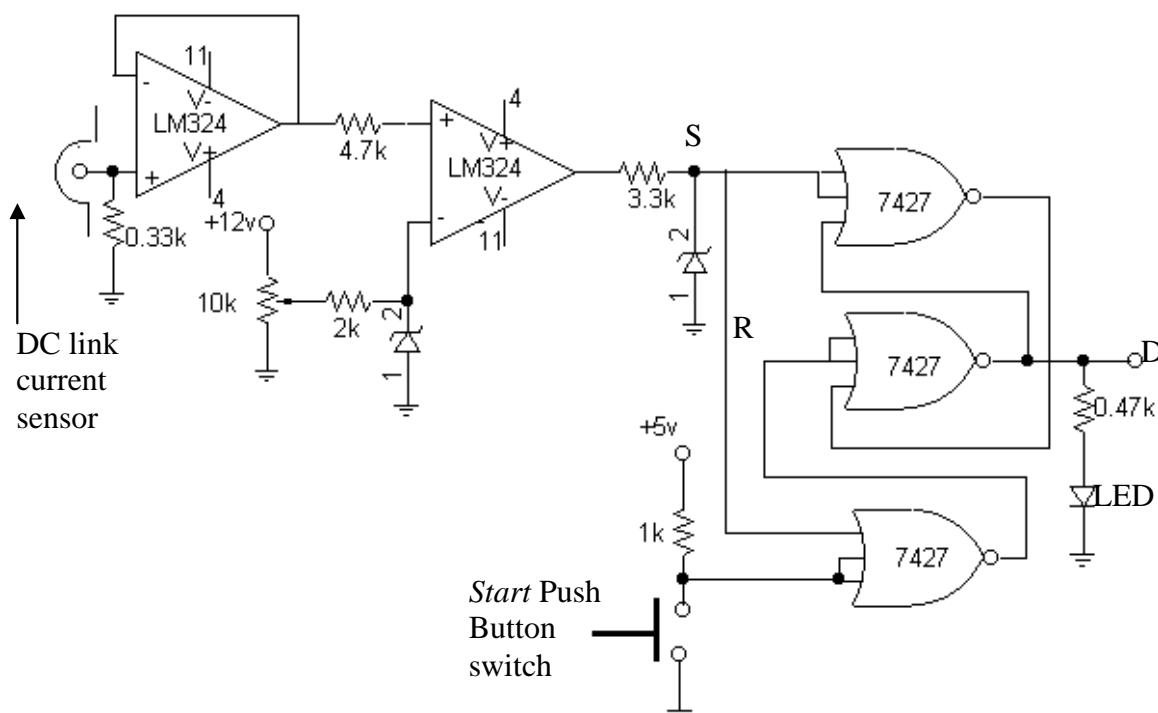


Figure 6.10 Over-current Protection circuit

6.3.6 GATE DRIVE CIRCUIT

The output of the gate pulse generator circuit is fed to the gate drive circuit, shown in Figure 6.11. At the input of the gate drive circuit, there is an opto-isolator, MCT-2E, which isolates the gate drive circuit from the control circuit. The circuit uses a

± 15 V power supply. +15 V is required to turn *on* the IGBT and -15 V is required to turn *off* the IGBT. Gate drive of the IGBT is supplied by the transistor, SL-100. Reverse recovery current of the IGBT is taken by the transistor SK-100. Base drives of both the transistors, SL-100 and SK-100 are supplied by the output transistor of the voltage comparator, LM-311. LM-311 also increases the speed of switching, which otherwise would have been restricted by the switching frequency of the opto-isolator, MCT-2E. The output voltage of the complimentary pair of transistors (SL-100 and SK-100) is clipped at +15 V and -15 V by a pair of zener diode connected back to back. Six such circuits have been fabricated with individual power supplies for driving the IGBTs of the VSI.

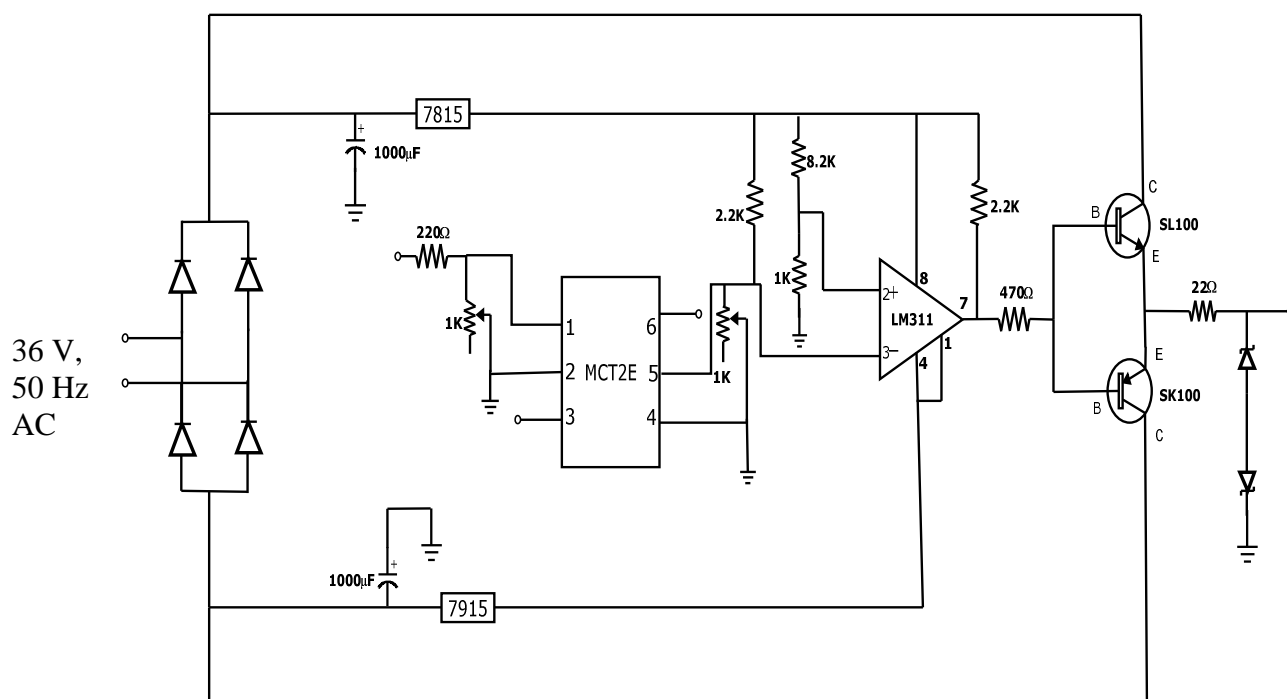


Figure 6.11 IGBT Gate Drive Circuit

6.4 FABRICATED CIRCUITS AND TEST RESULTS

This section includes the photos of the different circuits those have been fabricated and the outputs of each circuit taken from the CRO.

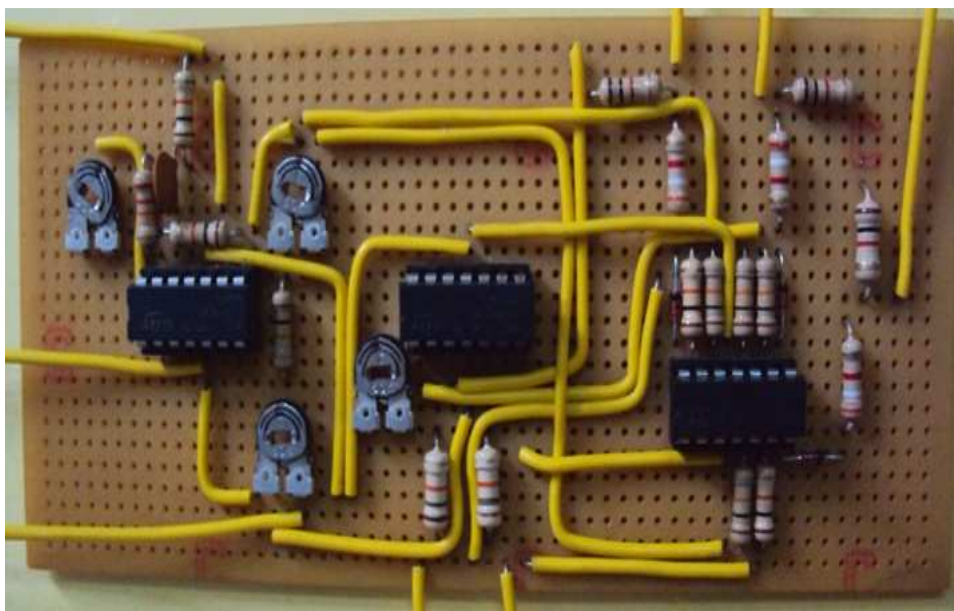


Figure 6.12 *Triangular wave generator, summer and comparator circuit*

Figure 6.12 is the photo of triangular wave generator, summer and comparator circuits fabricated in one board. The input to this circuit is a sinusoidal wave which has been generated from a signal generator. The sinusoidal signal is then compared with a triangular wave which is generated by the triangular wave generator present in the fabricated circuit shown in Figure 6.12. Figure 6.16 shows the wave forms of the triangular as well as the sinusoidal signal. Figure 6.17 shows the PWM signal generated by the comparator due to the comparison of the sinusoidal and the triangular signal. This PWM signal will then be fed to the lock out circuit to create a delay between the gate pulses of the switches in the same leg of the inverter. The fabricated lockout circuit is shown in Figure 6.13 and the output of the lockout circuit

is shown in the Figure 6.18. The outputs of the lockout circuit are pulses having amplitude below 4 volts and the pulses are unipolar having only positive magnitudes.

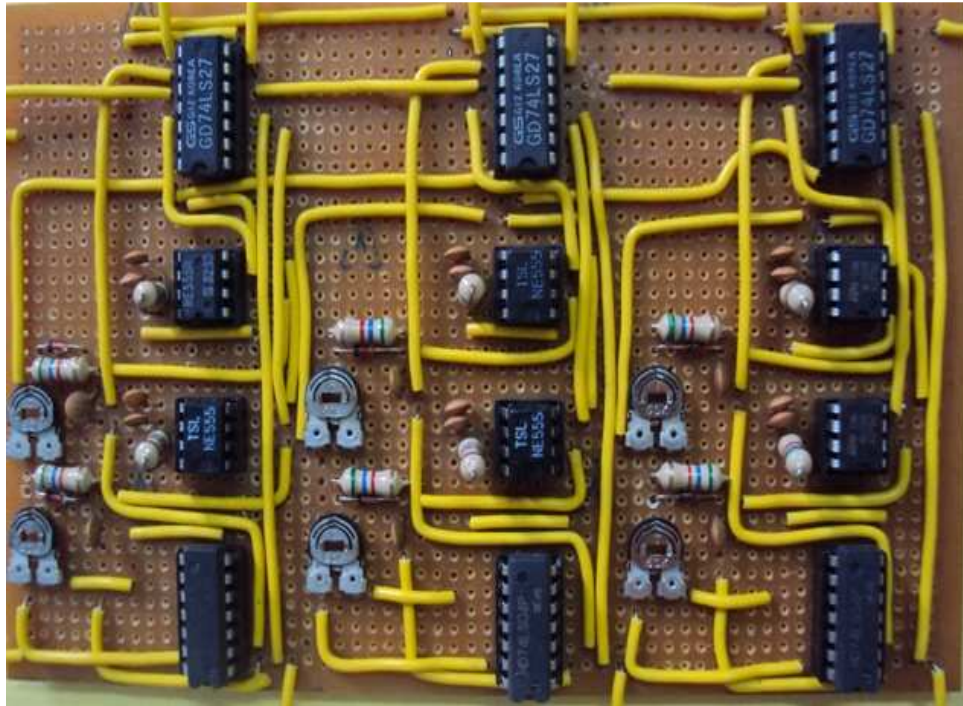


Figure 6.13 *lockout circuit*



Figure 6.14 *Gate drive circuit*

So the output of the lockout circuit is not suitable for being used as gate pulses for the

IGBT's used in the inverter. So the output of the lockout circuit is fed to the gate drive circuit to get appropriate gate pulses for the inverter. Figure 6.14 shows the fabricated gate driver circuit. The gate drive circuit produces bipolar gate pulses and

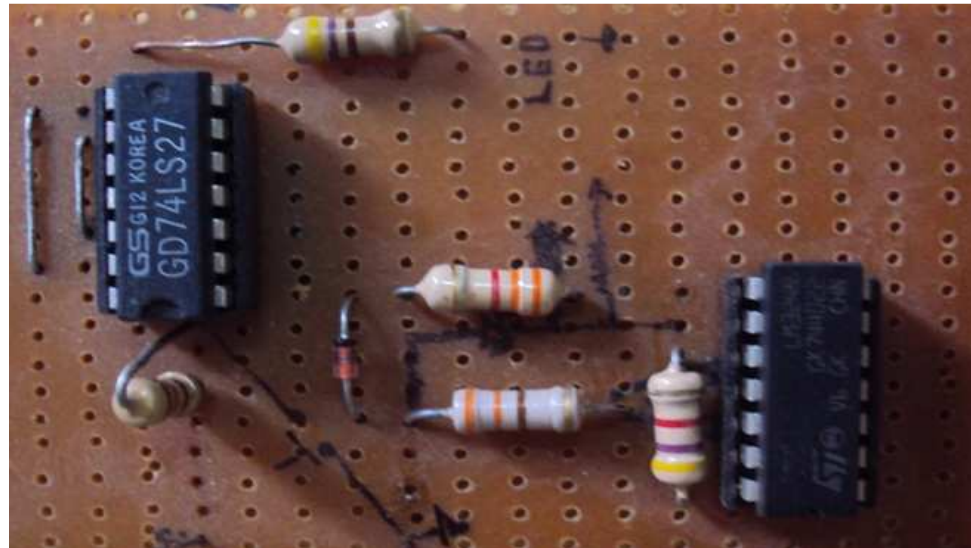


Figure 6.15 *Over current protection circuit*

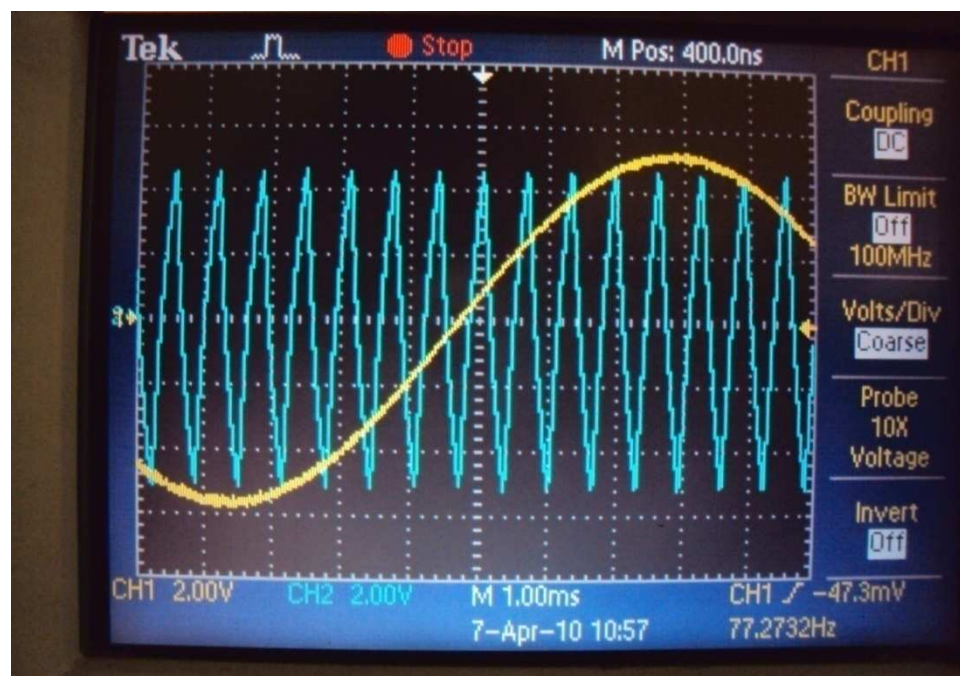


Figure 6.16 *Triangular carrier and sinusoidal control signals*

also provides isolation between the control circuit and the power circuit. The gate pulses at the output of the gate driver circuit are shown in Figure 6.19.

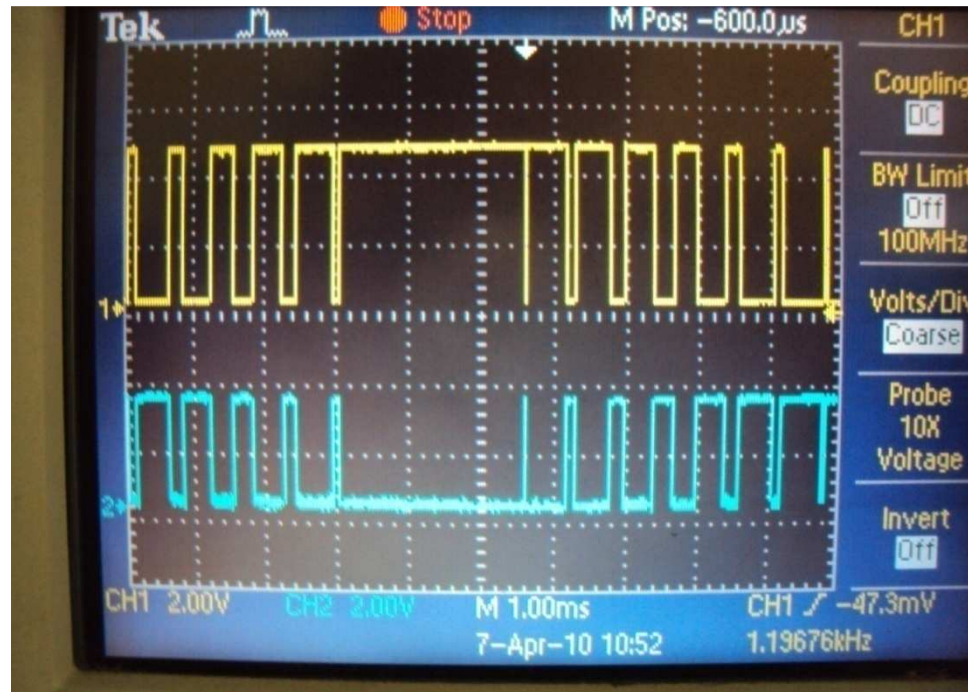


Figure 6.17 *Comparator output and its complement*

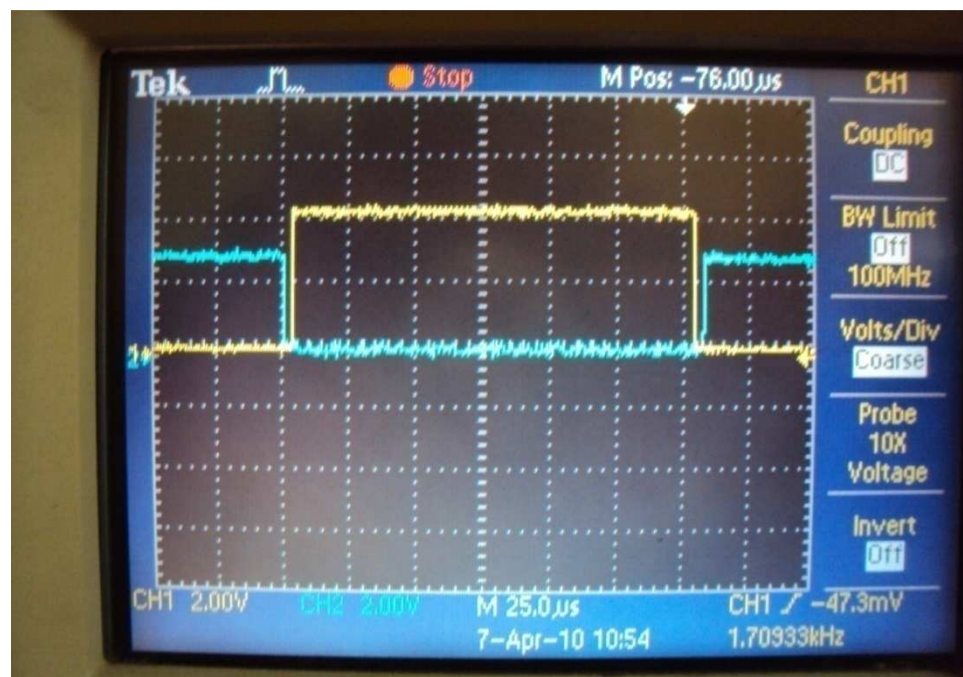


Figure 6.18 *Output of the lockout circuit*

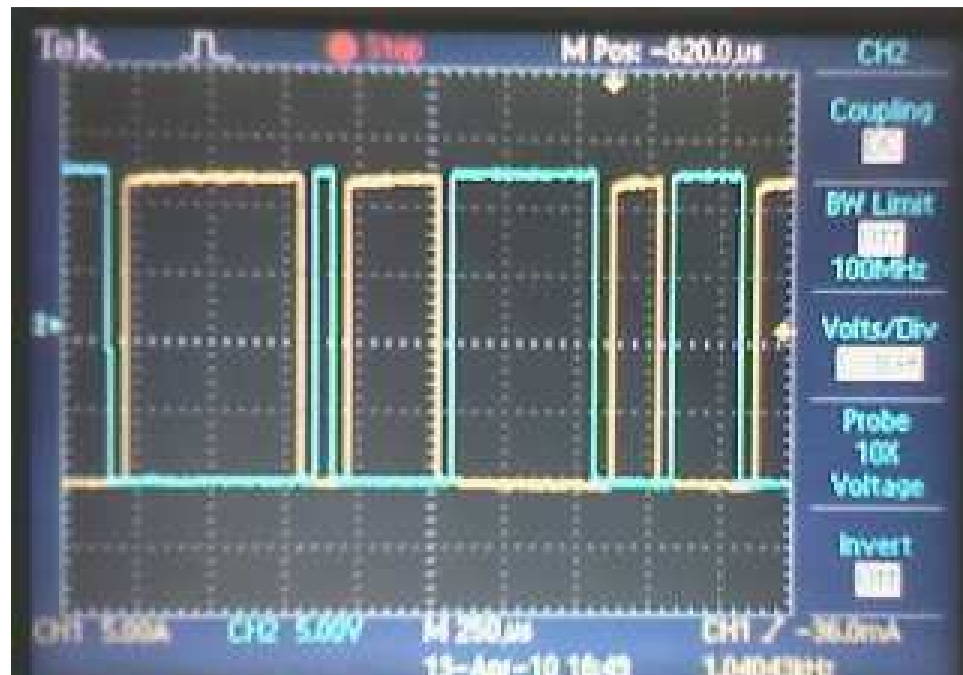


Figure 6.19 Gate pulses for switch S1 and S4

6.5 CONCLUSION

The various components of the control circuit needed for measurement and data acquisition have been fabricated and individually tested before integrating into a complete set-up. The test results of the control circuit were obtained after extensive tests in the laboratory and are satisfactory.

Chapter 7

Conclusion and scope for future work

7.1 CONCLUSION

In this work the d-q modeling of the cage induction generator is successfully done. Then indirect vector control technique is employed to enhance the transient performance of the cage induction generator system by decoupling the active and reactive power of the induction generator. Due to the use of indirect vector control strategy the transient performance of the induction generator system is improved as compared to that with scalar control techniques, but is not optimum. This is due to the fact that the control strategy implemented for the control of induction generator employs conventional PI controllers. So for further improvement in the performance of the induction generator a fuzzy controller is developed and implemented in the same control strategy. The use of fuzzy controller made the transient response faster than that with PI controller but the fuzzy controller introduced some noise in the system. Apart from that the fuzzy controller also introduces some error in the steady state. For further improvements in the overall performance a self tuned fuzzy logic controller is developed. Due to the implementation of the self tuned fuzzy logic controller the noise is greatly reduced and the transient performance of the system became the fastest. But the error in the steady state still remained though its magnitude is reduced. Next to be designed is a hybrid controller, which employed two controllers, the self tuned fuzzy logic controller for faster transient response and better decoupling of active and

reactive power and the conventional PI controller for noise free and error free steady state response. The strengths of the two controllers are added up, to overcome their individual drawbacks. With the hybrid controller the induction generator system gave the best transient as well as steady state performances. The biggest drawback of the wind power generation system employing cage induction generator is poor power factor. This drawback is also overcome by performing vector control of the grid side converter. Due to the vector control of the grid side converter the supply power factor could be made perfectly unity. Thus the overall performance improvement of the wind power generation system was achieved.

The main contributions of the thesis are:-

1. Performance improvement of indirect vector controlled induction generator using:
 - i. Fuzzy logic controller.
 - ii. Self tuned fuzzy logic controller.
 - iii. A novel hybrid controller combining P-I controller and self tuned fuzzy logic controller.
2. Performance comparison with all the controllers in sl. no 2 and 3.
3. Power factor improvement of wind power generation system through control of grid side converter.
4. Fabrication and testing of control circuit for PWM-converter-inverter system.

7.2 SCOPE FOR FUTURE WORK

The author recommends the following topics for future work on the performance improvement of a cage induction generator based wind power generating system.

- Study the control schemes incorporating sensor-less vector control and to compare the performances of different speed sensor less control algorithms.
- Develop robust controllers which would give high performance control even if subjected to machine parameter variation.
- Develop algorithms for accurate estimation of stator and rotor resistances for improvement in flux estimation.
- Improve the total wind power system efficiency by developing control methods for optimization of efficiency.
- Improvements in the control algorithm such that the double sided converter should be able to handle any type of abnormal situations such as fault detection, fault handling, overload control etc.

REFERENCES

- [1] C. V. Nayar, and J. H. Bundell, "Output power controller for a wind driven induction generator," *IEEE Trans. Aerospace Electronic Systems*, vol. 23, pp. 388-401, May 1987.
- [2] L. Holdsworth, X.G. Wu, J.B. Ekanayake, N. Jenkins, "Comparison of fixed speed and doubly-fed induction wind turbines during power system disturbances," *IEE Proc. Gener. Transm. Distrib.*, vol. 150, No. 3, pp 343-352, May 2003.
- [3] Richard Gagnon, Gilbert Sybille, Serge Bernard, Daniel Paré, Silvano Casoria, Christian Larose, "Modeling and Real-Time Simulation of a Doubly-Fed Induction Generator Driven by a Wind Turbine," *International Conference on Power Systems Transients (IPST'05)*, Montreal, Canada, Paper No. IPST05-162, June 2005.
- [4] S. Muller, M. Deicke and Rik W. De Doncker, "Doubly fed induction generator systems for wind turbines," *IEEE industry application magazine*, pp. 26-33, may/june 2002.
- [5] R. Dutta and T. Ranganathan, "Variable speed wind power generation using doubly fed wound rotor induction machine – A comparison with alternative schemes", *IEEE Trans. On energy conversion*, vol. 17, no. 3, September 2002.
- [6] S. N. Bhadra, D. Kastha, and S. Banerjee, *Wind Electrical Systems*, Oxford University Press, New Delhi, 2005.
- [7] C. Chakraborty, S. N. Bhadra, and A. K. Chattopadhyay, "Analysis of parallel operated self excited induction generators," *IEEE Trans. EGY. Conv.*, vol. 14, no. 2, pp. 209-216, Jun 1999.
- [8] R. Cardenas, and R. Pena, "Sensorless vector control of induction machines for variable speed wind energy applications," *IEEE Trans. EGY. Conv.*, vol. 19, no. 1, pp. 196-205, Mar. 2004.
- [9] A. Tapia, G. Tapia, J. Xabier Ostolaza, J. R. Saenz, "Modelling and control of a wind turbine driven doubly fed induction generator" *IEEE Trans. Energy conversion*, vol. 18, No. 2, pp.

REFERENCES

- 194-204, June 2003.
- [10] R.Pena, R.Cardenas, R.Blasco, G.Asher, J.Clare, "A cage induction generator using back to back PWM converters for variable speed grid connected wind energy system," *IEEE 27th annual Conf., IECON 01, Industrial Electronics Society*, pp. 1376-1381, 2001
- [11] R.Pena, J.C.Clare, G.M.Asher, "Doubly fed induction generator using back to back PWM converters and its application to variable speed wind energy generation," *IEE Proc. Electr. Power Appl.*, vol. 143, No. 3, pp. 231-241, May1996.
- [12] M. G. Simoes, B. K. Bose, R. J. Spiegel, "Design and performance evaluation of a fuzzy logic based variable speed wind generation system," *IEEE Trans. Ind. Appl.*, vol. 33, no. 4, pp. 956-965, Aug. 1997.
- [13] M.NasirUddin, Tawfik S. Radwan, M.Azizur Rahman, "Performance of Fuzzy-Logic-Based indirect vector control for induction motor drive," *IEEE Trans. Industry applications*, vol. 38, No. 5, pp. 1219-1225, Oct 2002.
- [14] M.G.Simoes, B.K.Bose, and R.J.Spiegel, "Fuzzy logic based intelligent control of a variable speed cage machine wind generation system," *IEEE Trans. Power Electron.*, vol. 12, pp. 87-95, Jan 1997.
- [15] Chuen Chien Lee, "Fuzzy logic in control systems: Fuzzy logic controller – part1," *IEEE trans. on systems, man, and cybernetics*, vol. 20, no. 2, march / april 1990.
- [16] Zihong Lee, "Methods for improving performance of PI type fuzzy logic controller," *IEEE trans. on fuzzy systems*, vol.1, no. 4, Nov 1993.
- [17] M. Masiala, J.Salmon, "Fuzzy self tuning speed control of an indirect field-oriented control induction motor," *IEEE Trans. industry appl.*, vol. 44, No. 6, Dec 2008.
- [18] R.K. Mudi and N.R. Pal, "A robust self tuning scheme for PI and PD type fuzzy

REFERENCES

- controllers,” *IEEE Trans. fuzzy systems*, vol. 7, no. 1, Feb 1999.
- [19] A. El Dessouky and M. Tarbouchi, “Fuzzy model reference self-tuning controller,” in *Proc. 7th Int. Workshop Advanced Motion Control*, Jul.35,2002, pp. 153–158.
- [20] M. Cheng, Q. Sun, and E. Zhou, “New self-tuning fuzzy PI control of anovel doubly salient permanent-magnet motor drive,” *IEEE Trans. Ind. Electron.*, vol. 53, no. 3, pp. 814–821, Jun. 2006.
- [21] Y. Miloud, A. Miloudi, M. Mostefai, and A. Draou, “Self-tuning fuzzy logic speed controller for inductionmotor drives,” in *Proc. IEEE Int. Conf. Ind. Technol.*, Dec. 8–10, 2004, pp. 454–459.
- [22] L. Mokrani and R. Abdessemed, “A fuzzy self-tuning PI controller for speed control of induction motor drive,” in *Proc. IEEE Conf. Control Appl.*, Jun. 2003, vol. 2, pp. 785–790.
- [23] J. Sun, P. Su, Y. Li, and L. Li, “Application of self-adjusting fuzzy controller in a vector-controlled induction motor drive,” in *Proc. 3rd IEEEInt. Conf. Power Electron. Motion Control*, Aug. 15–18, 2000, vol. 3.
- [24] Sanjiv Kumar, Bhim Singh and J. K. Chatterjee, “Hybrid speed controller for vector controlled cage induction motor drive,” *IEEE conference* 1998.
- [25] Qinghui Wu and Cheng Shao, “Novel hybrid sliding-mode controller for direct torque control induction motor drives,” *Proceedings of the 2006 American Control Conference Minneapolis, Minnesota, USA, June 14-16, 2006*

APPENDIX-1

MACHINE, TURBINE AND SYSTEM PARAMETERS

Induction Generator:

3 ϕ , 4 pole

Power = 10 kW

Voltage = 415V

Current = 36A

Stator Resistance = 0.435 Ω

Rotor Resistance = 0.816 Ω

Stator (rotor) leakage inductance, L_{ls} (L_{lr}) = 1.973 mH

Magnetizing inductance, L_m = 69.347 mH

Inertia = 0.089 Kg-m²

Turbine Parameters:

Gear ratio = 5.7

A= 0.015

B=0.03

C= 0.015

System parameters:

Series inductance = 12 mH

Line resistance = 0.1 Ω

DC link capacitance = 500 μ F

Line side phase voltage = 220 V

DC link voltage = 500 V

APPENDIX-2

LIST OF SYMBOLS

V_{as}, V_{bs}, V_{cs} = Three phase supply voltages

V_{ds}^s, V_{qs}^s = d- q axis voltages in stationary reference frame

V_{ds}, V_{qs} = d-q axis voltages in synchronously rotating reference frame

R_s, R_r = stator and rotor resistances

L_s, L_r = stator and rotor inductances

L_m = magnetizing inductance

$\Psi_{ds}, \Psi_{qs}, \Psi_{dr}, \Psi_{qr}$ = stator and rotor flux linkages

ω_e = synchronous speed(electrical)

ω_r = rotor electrical speed

ω_m^* = reference rotor speed (mechanical)

T_e = electromagnetic torque

T_{turbine} = prime mover torque

J = moment of inertia

B = frictional damping coefficient

ω_{sl} = slip speed

ω_m = rotor mechanical speed

P = pair of poles of the machine

p = active power

q = reactive power

K_p = Proportional gain

K_i = Integral gain

K_o = output gain of fuzzy logic controller

APPENDIX-2

K_e, K_{ce} = Input normalization factors for error and change of error respectively

α = Gain updating factor for self tuned fuzzy logic controller

U = Control input

Y = Output of the system

e = Error

C_p = Power coefficient of wind energy converter

λ = Tip speed ratio

λ_{opt} = Optimum value for tip speed ratio

L = Line inductance

R = Line resistance

V_{abcl} = Converter line side voltages

V_{abcs} = Grid side line voltages

X_L = Inductive reactance of the line

δ = Load angle

P = Grid side active power

Q = Grid side reactive power

V_∞ = Wind velocity without rotor interference

P_0 = Power contained in wind

ρ = Air density

R = Radius of the wind turbine swept area

A = Swept area of the turbine rotor

T_m = Turbine torque

APPENDIX-3

LIST OF COMPONENTS USED

LM 324	---	Quadra opamp
TL084	---	Opamp
LM311	---	Opamp
4148	---	Switching diode
7427	---	NOR gate
7404	---	NOT gate / Inverter
555	---	Multivibrator
N1007	---	Diode
MCT2E	---	Opto-isolator
SL100	---	n-p-n Transistor
SK100	---	p-n-p Transistor
7815	---	Voltage regulator (+15 volt)
7915	---	Voltage regulator (-15 volt)

Dissemination of Work

List of Papers Published

PROCEEDINGS OF CONFERENCES

- Swagat Pati, K.B.Mohanty, Benudhar Sahu, “Performance Improvement with a Robust Self Tuned Fuzzy Logic Controller for Generator Control in Wind Energy System,” in *Proc. IEEE, IECR.*, Dec, 2010..
- Swagat Pati , K.B.Mohanty, “ Power control of induction generator using P-I controllers for wind power applications,” in *Proc. , CERA., FEB*, 2009.
- Swagat Pati, K.B.Mohanty, Benudhar Sahu, “A Comparative Study on Fuzzy and PI Speed Controllers for Field-Oriented Induction Motor Drive,” in *Proc. IEEE, IECR.*, Dec, 2010.

BIO-DATA OF THE CANDIDATE

Name of the candidate : Swagat Pati
Father's Name : Sachidananda Pati
Date of Birth : 27th March 1983
Present Address : M-Tech (Res.)
Department of Electrical Engineering,
National Institute of Technology,
Rourkela-769008
Permanent Address : At/Po :- Singiri,
Via :- Mitrapur,
Dist :-Balasore, Orissa.
Email : swagatiter@gmail.com

ACADEMIC QUALIFICATION:

- (i) **B. Tech.** in (Electrical Engineering), from **Utkal University** with Percentage of 72.8%, Bhubaneswar, Orissa.
- (ii) **+2 Science** from **CHSE Board**, Orissa with percentage of 57% .
- (iii) **10th** from **BSE Board**, Orissa with percentage of 82% .